Landslide Susceptible Zone Mapping in Uttara Kannada, Central Western Ghats

Ramachandra T.V.	**Subash Chandran M.D**	**Joshi N.V.**
Pallav Julka	**Uttam Kumar**	**Bharath H. Aithal**
Prakash Mesta	**Rao G R**	**Vishnu Mukri**

Sahyadri Conservation Series 7

ENVIS Technical Report: 28

February 2012

Environmental Information System [ENVIS]
Centre for Ecological Sciences,
Indian Institute of Science,
Bangalore - 560012, INDIA

Web: http://ces.iisc.ernet.in/energy/
http://ces.iisc.ernet.in/biodiversity
Email: cestvr@ces.iisc.ernet.in,
energy@ces.iisc.ernet.in

CONTENT

Abstract

Large scale landslides involving human casualties and notable losses to property were practically unknown in Uttara Kannada district situated towards the central Western Ghat-west coast region of Indian peninsula. A rethinking has set in, however, following a major disaster in early October, 2009, when following rainfalls of unprecedented intensity for the period, over 20 landslides happened during a single day in Karwar taluk, in which 19 people were buried alive in a single locality itself, and in other places the residents had providential escape due to marginal shifts in the actual locations of slope failures from human habitations. That the threat for future is at large can be deduced from the recurrence of a rockslide hitting a running train during the rains of 2010, killing one person and injuring others. Yet another hillside collapse happened in the outskirts of Kumta taluk, and the ground below being sparsely populated no casualties happened.

In view of the ever increasing developmental pressures in coastal Uttara Kannada, from the establishment of INS Kadamba, India's largest naval base, yet in the process of growth, Kaiga nuclear power plant, Karwar port and Bellikeri port handling specifically iron ore and granites beyond their carrying capacity limits, development of tourism etc. all leading towards increased deforestation of coastal hills and pediment cutting the risk proneness from slope failures appears to be looming large in the future years. The risk enhancement factor needs to be analyzed in view of the erratic rainfalls, and increased intensities in October, when otherwise the season of rains should have been tapering off. The specter of climatic change necessitates greater focus on slope failures, identification of hillsides prone to slope failures, study of causative and triggering factors , depiction of vulnerable areas on GIS based and locality specific maps and on evolving innovative technologies for future management.

1. INTRODUCTION

The Earth consists of atmosphere, hydrosphere, and lithosphere. These layers are subject to different processes due to mutual interaction or self-interaction. Interactions can lead to various phenomenon, weathering, erosion, floods, hurricanes, landslides, earth quakes, volcanoes, tectonic movements, etc., which can lead to natural hazard. Natural hazards are an integral component of life on Earth. Natural disasters are grouped as:

- Hydro-meteorological disasters: avalanches/landslides, droughts/famines, extreme temperatures, floods, forest/scrub fires, windstorms and other disasters, such as insect infestations and wave surges
- Geophysical disasters: earthquakes, tsunamis and volcanic eruptions.

The number of recorded natural hazards has increased in the last 50 years with the greatest increase in frequency attributed to hydro-meteorological disasters, with a lesser increase attributed to biological disasters and a slightly lesser increase attributed to geological disasters. The pressure for infrastructure development to meet the need of rapid urbanisation and global competition has led to expansion of construction activities even in hilly terrains and has catapulted frequency of landslides to dramatic proportions in recent decades. Landslide refers to the movement of a mass of rock, debris, or earth down a slope or any down slope movement of soil and rock under the direct influence of gravity. This includes various types of slope failures, like, earth and debris flows, slumps, slides, and soil and rock fall. Landslide is a phenomenon of a mass movement of landform and which is characterized by moderately rapid to rapid (> 30 cm per year) down-slope transport, by means of gravitational stresses, of a mass of rock and regolith that may or may not be water saturated. Landslides are one of the normal landscape building processes in undulating terrain and are common in Himalayas and Western Ghats regions in India. It includes any detached mass of soil, rock, or debris that moves down a slope or a stream channel. They are classified according to the type and rate of movement and the type of materials that are transported. Two types of forces are at work:

(1) driving forces combine to cause a slope to move, and

(2) friction forces and strength of materials act to stabilise the slope.

When driving forces exceed resisting forces, landslides occur. It is one of the common natural hazards with devastating effects. They become a problem when they interfere with human activity resulting in damage to property and loss of life, evident from recent episodes in Ooty (Tamil Nadu) and Kerala. In order to minimise the losses due to landslide, it is necessary to identify and analyse the most important determining factors leading to slope failures. They occur as “on-site” hazards and “off-site” hazards, and should be distinguished to effectively plan for future hazard situations.

- On-site hazards occur on or near the development site and are typically the slower moving landslides that cause most of the property damage in urban areas. They include features called slumps, earth flows and block slides.
- Off-site hazards typically begin on steep slopes at a distance from homes or developments, and are often rapidly moving.

Landslide occurs when force that is pulling the slope downward exceeds the shear strength of the earth materials that compose the slope or when sliding factor (Fs) <1

$Fs=F_f / F_d$ Where, F_f= frictional force

$F_f=\mu N$ F_d= driving force

$N= mg.\cos(\theta)$ μ= coefficient of friction

$F_d= mg.\sin(\theta)$ N= normal component

When dams are constructed along a river's course they drastically change the river's hydrology, causing severe impacts on its ecosystems (up and downstream of the dam). One of the most significant immediate impacts is the drastic change that can occur in the groundwater table. In the case of the Sharavathi River Basin, the Linganamakki reservoir submerged 375 km^2 of land increasing the water table level by over 40 m to designate a new shoreline. In response to this action, anthropogenic activity, including the creation of roads, houses and development had to be pushed higher up the valleys into the terrain of higher elevation than had previously been used. The purpose of this study is to see the parameters that are likely to have a decisive role in the slope failures. Figure 1.1 depicts a typical landslide that has occurred in the Sharavathi river basin due to slope failure.

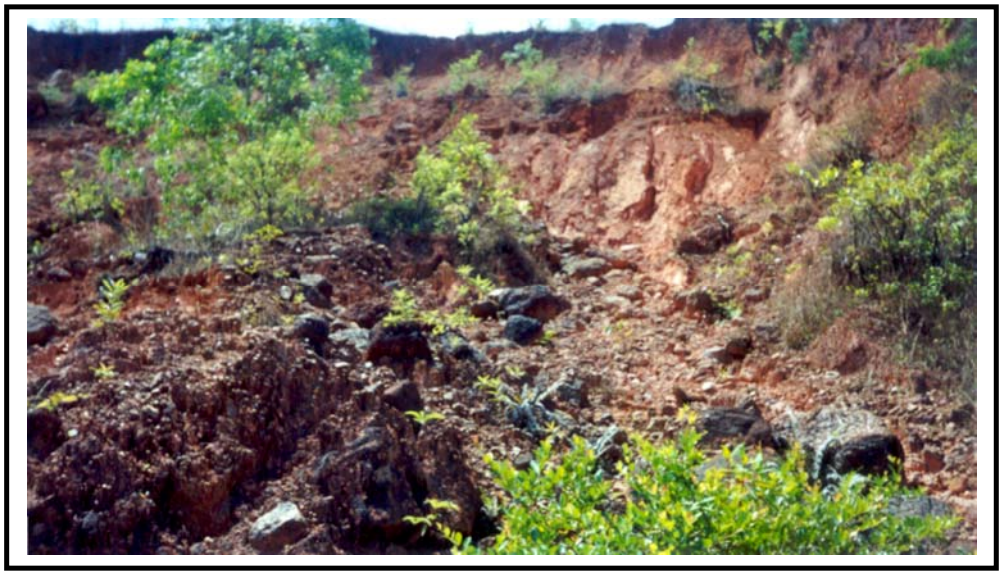

Figure 1.1: A view of a landslide in the study area

1.1 Different Types of Landslides

Landslides are classified and described on the basis material and types of movement (Varnes, 1978) are listed in Table 1. Materials wise classification is on based on the size of predominant material present in the slide i.e., is it rock, debris and earth. The movement based classification is divided into six types as falls, topples, slide, spread, flow, complex. These types of landslides are resultant of the temporal conjunction of several factors.

Landslides are classified by causal factors and conditions, and include falls, slides and flows, which are described below. There are many attributes used as criteria for identification and classification including rate of movement, type of material and nature of movement. A combination of characteristics can also contribute to an increased risk of landslide hazards.

a. **Falls**: Falls are abrupt movements of rocks and boulders i.e., masses of geologic materials that become detached from steep slopes or cliffs. Movement occurs by free-fall, bouncing, and rolling on separation along discontinuities such as fractures, joints, and bedding planes. Gravity, mechanical weathering, and the presence of interstitial water strongly influence falls.In falls, material is detached from a steep slope or cliff and descends through the air by free fall or by bouncing or rolling down the slope. Rock fall, the most common type, is a fall of detached rocks from an area of intact bedrock.

b. **Topples: The end-over-end motion of rock down a slope.** Under the actions of gravity and forces exerted by adjacent units or by fluids in cracks toppling occurs. Toppling failures are distinguished by the forward rotation of a unit or units about some pivotal point, below or low in the unit.

c. **Slides:** Even though the term slide used in general for any landslide it has more restrictive use of the term refers only to mass movements, where there is a distinct zone of weakness that separates the slide material from more stable underlying material. Slides include rockslides – the down slope movement of a rock mass along a plane surface; and slumps – the sliding of material along a curved (rotational slide) or flat (translational slide) surface. Slow-moving landslides can occur on relatively gentle slopes, and can cause significant property damage, but they are far less likely to result in serious human casualties.

d. **Flows**: Flows are plastic or liquid movements in which mass (e.g., soil and rock) breaks up and flows during movement. Flows are typically rapidly moving and also tend to increase in volume as they scour out the channel.

   a. ***Debris flow***: A debris flow is a form of rapid mass movement in which a combination of loose soil, rock, organic matter, air, and water mobilize as a slurry that flows downslope. Debris flows include <50% fines. Debris

flows are commonly caused by intense surface-water flow, due to heavy precipitation or rapid snowmelt that erodes and mobilizes loose soil or rock on steep slopes. Debris flows also commonly mobilize from other types of landslides that occur on steep slopes, are nearly saturated, and consist of a large proportion of silt- and sand-sized material. Debris-flow source areas are often associated with steep gullies, and debris-flow deposits are usually indicated by the presence of debris fans at the mouths of gullies. Fires that denude slopes of vegetation intensify the susceptibility of slopes to debris flows.

b. ***Earth flow***: Earthflows have a characteristic "hourglass" shape. The slope material liquefies and runs out, forming a bowl or depression at the head. The flow itself is elongate and usually occurs in fine-grained materials or clay-bearing rocks on moderate slopes and under saturated conditions. However, dry flows of granular material are also possible.
c. ***Mud flow***: A mudflow is an earthflow consisting of material that is wet enough to flow rapidly and that contains at least 50 percent sand-, silt-, and clay-sized particles. In some instances, for example in many newspaper reports, mudflows and debris flows are commonly referred to as "mudslides."
d. ***Creep***: Creep is the unnoticeably slow, steady, downward movement of slope-forming soil or rock. Movement is caused by shear stress sufficient to produce permanent deformation, but too small to produce shear failure. There are generally three types of creep: (1) seasonal, where movement is within the depth of soil affected by seasonal changes in soil moisture and soil temperature; (2) continuous, where shear stress continuously exceeds the strength of the material; and (3) progressive, where slopes are reaching the point of failure as other types of mass movements. Creep is indicated by curved tree trunks, bent fences or retaining walls, tilted poles or fences, and small soil ripples or ridges.
e. ***Lateral spread***: Lateral spreads are distinctive from other slides. They usually occur on very gentle slopes or flat terrain. The dominant mode of movement is lateral extension accompanied by shear or tensile fractures. The failure is caused by liquefaction, the process whereby saturated, loose, cohesionless sediments (usually sands and silts) are transformed from a solid into a liquefied state. Failure is usually triggered by rapid ground motion, such as that experienced during an earthquake, but can also be artificially induced due to human activity like mining, or even micro seismic waves from construction activities and vehicular movement. When coherent material, either bedrock or soil, rests on materials that liquefy, the upper units may undergo fracturing and extension and may then subside, translate, rotate, disintegrate, or liquefy and flow. Lateral spreading in fine-grained materials on shallow slopes is usually progressive. The failure

starts suddenly in a small area and spreads rapidly. Often the initial failure is a slide, but in some materials movement occurs for no apparent reason. Combination of two or more of the above types is known as a complex landslide.

Slides due to cut-and-fill failures during roadway and building excavations, river bluff failures, lateral spreading landslides, collapse of mine-waste piles (especially coal), and in wide variety of slope failures are associated and open-pit mines or quarries in low-relief areas. It might be a slide in hilly terrain or in a low relief area landslides are resultant of the temporal conjunction of several factors or variables.

Table 1: Types of landslides. Abbreviated version of Varnes' classification of slope movements (Varnes, 1978).

<table>
<tr><td colspan="2" rowspan="3">Type of Movement</td><td colspan="3">Type of Material</td></tr>
<tr><td rowspan="2">Bedrock</td><td colspan="2">Engineering Soils</td></tr>
<tr><td>Predominantly Coarse</td><td>Predominantly Fine</td></tr>
<tr><td rowspan="2"></td><td>FALLS</td><td>Rock fall</td><td>Debris fall</td><td>Earth fall</td></tr>
<tr><td>TOPPLES</td><td>Rock topple</td><td>Debris slide</td><td>Earth slide</td></tr>
<tr><td rowspan="2">SLIDES</td><td>ROTATIONAL</td><td rowspan="2">Rock slide</td><td rowspan="2">Debris slide</td><td rowspan="2">Earth slide</td></tr>
<tr><td>TRANSLATIONAL</td></tr>
<tr><td rowspan="3"></td><td>LATERAL SPREADS</td><td>Rock spread</td><td>Debris spread</td><td>Earth spread</td></tr>
<tr><td rowspan="2">FLOWS</td><td rowspan="2">Rock flow (deep creep)</td><td>Debris flow</td><td>Earth flow</td></tr>
<tr><td colspan="2">(soil creep)</td></tr>
<tr><td>COMPLEX</td><td colspan="3">Combination of two or more principal types of movement</td></tr>
</table>

1.2 Causes of Landslides

Causes of landslides can be broadly distinguished as intrinsic and extrinsic factor, where the probability of landslide occurrence depends on both the intrinsic and extrinsic variables.

a. **Internal factors or Intrinsic variables:** Geology, slope gradient; slope aspect, elevation, soil geotechnical properties, vegetation cover, and long-term drainage patterns are intrinsic variables that contribute to landslide susceptibility. The steeping of the slope, water content of the stratum and mineralogical composition and structural features, which tend to reduce the shearing strength of the rocks, are also vital factors for causing landslides.

b. **External factors or Extrinsic variables:** A slight vibration or jerk to the mass would greatly add up against the frictional resistance and the mass would become unstable. The heavy traffic in a hilly terrain could be a contributing factor towards causing the imbalance of masses. The extrinsic variables may change over a very short time span, and are thus very difficult to estimate. If extrinsic variables are not taken into account, the term susceptibility could be employed to define the likelihood of occurrence of a landslide event. Variables which determine the probability of landslide for a particular slope or an area (Dai et al., 2002; 2001) may be grouped into two categories:
    a) **Triggering variables or dynamic variables** or extrinsic properties like heavy rainfall, glacier outburst, seismic activity, etc which often caused slope movements i.e., they shift the slope from a marginally stable to an unstable state and thereby initiating failure in an area of given susceptibility
    b) **Preparatory variables or quasi static variables** or intrinsic properties, which make the slope inherently susceptible to failure due to many existent concomitant properties which make the slope susceptible to failure without triggering it, such as geology, slope gradient, and aspect, elevation, soil, vegetation cover and long-term drainage patterns and weathering; and (Wu and Sidle, 1995, Atkinson and Massari, 1998).

Hydrology: The water in the region plays an important role as can be seen from classification of landslides. Heavy rainfall is a critical factor in triggering landslides because it generates rapid increases in pore pressure in the vadose zone and groundwater flow in the saturated area (Jiu J. Jiao, 2005).The percolating water through soil and sandstone wet the clay layer adding to the weight that reduces the slope strength. In addition to this water swells the clay and also decreases friction between grains, contributing to a loss cohesion intern decreasing resistance to landslide.

Geology: Geology comprised of structure and lithology. Lithology also influences landslide occurrences. Lithology, conditions both the shear strength of the rock mass and the permeability, and, consequently the possibility of there being increase in the increase pressure in the subsoil (L. Donati, and M.C. Turrini, 2002). Landslide occurs in loose and poorly consolidated slope material than in bedrock. The erodibility or the response to rocks to the process of weathering and erosion are the cause for formation of regolith. The rocks like quartz, limestone and igneous are generally hard, and resistant to erosion, forming steep slopes. In comparison, sedimentary rocks are vulnerable to erosion and form more easily landslide. Phyllites and schists are characterized by flaky minerals which weather quickly and promote instability (Giacomo D'Amato Avanzi et al, 2004). A sequence of strata having thin, soft and weak beds lying in between hard and thick beds provide a congenial set-up for landslide occurrence (Terzaghi and Peck, 1967). The instability is shown by joints,

folds and faults or generally by lineaments which are the expressions of earths moulding and remoulding process. The presences of folds with anticline, with flanks mainly dipping towards the slope free face are more prone for landslide. The presence of lineaments is highly correlated with lithology (Pachauri et al, 1992; Atkinson et al, 1998A sequence of strata having thin, soft and weak beds lying in between hard and thick beds provide a congenial set-up for landslide occurrence (Terzaghi and Peck, 1967).

Structure: The structural weakness like inclined lineaments, bedding planes, joints, faults or shear zones increase the chance of landslide occurrence. Lineaments are defined as "mappable simple or composite linear features of a surface, whose parts are aligned in rectilinear or slightly curvilinear relationship and which differ distinctly from the patterns of adjacent features and presumably reflects a sub surface phenomenon" (O'Leary et al., 1976). Investigations have shown that the probability of landslide occurrence is notably increased at those sites closer to lineaments (Greenbaum et al., 1995). When the dip coincides with that of the surface slope they create conditions of instability (Kesavulu, 1997). Faults and joints provide scope for easy percolation of rainwater enhancing the instability.

Topography: Slope angle is another cause for landslides. Slope angle is formed between any part of surface of the earth and the horizontal datum. It is a means by which gravity induces stress in the slope rocks, flux of the water or other material; therefore, it is of great significance in hydrology and geomorphology. As the slope angle increases, then the shear stress in the soil or other unconsolidated material generally increases. Not only stress on the rock increases but slopes even affect the velocity of both surface and subsurface flow and hence soil water content, soil formation, erosion potential and other important geomorphic process. Places where the slope angle is near to 00 are considered to be safer in terms of failure initiation (Gomez H and Kavzogul T, 2005). Gentle slopes are expected to have a low frequency of landslides because of the generally lower shear stresses associated with low gradients. Steep natural slopes resulting from outcropping bedrock, however, may not be susceptible to shallow landslides (Saro Lee and Touch Sambath). Slope failure tends to increase with slope angle but when the slope becomes near the vertical, landsliding is scare or absent altogether as there is lack of soil development and debris accumulation in such topographic conditions (Selby, 1993; Derruau, 1983). But under such circumstance the rock fall increases. Still it noticed that frequency of landslide is more on steeper slope (McDermid and Franklin, 1995; Cooke and Doornkamp, 1990). Apart from the slope aspect and curvature also play an important role. The curvature is a morphological measure of the topography. A positive curvature indicates that the surface is upwardly convex at that cell, and a negative curvature indicates that the surface is upwardly concave at that cell. A value of zero indicates that the surface is flat.

Soil: The one of the most sensitive parameters is soil thickness (Van Westen et.al, 2006). Page et al. (1994) correlate sediment thickness with landslide events. Landslide is triggered as a decrease in shear strength of the soil due to an increase in pore-water pressure on the failure surface. An increase in pore-water pressure can be caused directly by percolating rainfall or indirectly by an accumulation of water at a certain depth due to changes in permeability within the soil cover (perched water tables) or by an accumulation of water at the soil-bedrock contact (Terlien, 1998). In soils, pore water pressures may be due to: (i) the hydrostatic head, (ii) pressures exerted by water flowing through a soil mass whose volume remains constant, and (iii) pressures associated with stress changes in the soil, which initiate changes in volume of the soil mass (consolidation or swelling) (Parcher, 1968). The pore water pressure build-up, prior to failure, accelerating the volume decrease of the soil, with water expelled from the voids contributing to an increase in pore pressure. An immediate consequence of the volume decrease during the pre-failure stage could be a debrisflow mobilization (Se´rgio et al, 2006). Several pore water pressure measurement conducted in the field have recorded that pore water pressure drops due to crack development or preferential pathway formation (Harp et al., 1990).

In addition to soil saturation, there always exists subsurface flow that may tend to concentrate at shallow depths. Shallow sub-surface flow can occur soon after an intense rainfall as pore-water suction in the layer closest to the ground surface is depleted. Subsurface flows are confined within the pore systems of the soil mass (R. Bhasin et al., 2002). As for the case of surface run-off, subsurface flow can be blocked, e.g., by an impermeable layer. Cases in which decrease in hydraulic conductivity downslope has impeded subsurface flow and generated pore-water pressures have been reported by Hudson and Hencher (1984) and Au (1998).

Land use/land cover: Land-use/land-cover changes, whether of natural origin or man-made, can influence the susceptibility of slopes to landslides (Diaz et al, 2005). The vegetation cover influences directly the susceptibility to landslides through various factors including (i) protection of the surface, (ii) consolidation of the soil and (iii) agriculture resulting in bare soil for long periods (Atkinson et al, 1998).

The mechanical properties of slope materials can be altered through agricultural activities involving ploughing or other modifications of the existing cover, as well as through conversion, i.e. changes of the cover from one type class to another (e.g. deforestation for cropland, timber, reservoirs, etc). The root system of the vegetation helps in binding the soil particles together and thereby increasing the shear strength. The influence of root reinforcement on landslides has been well established through mechanistic and empirical studies, few studies have also examined how local vegetative patterns influence slope stability (Roering, et al, 2003). Because root networks spread outward from trees, the species, size, and spacing of trees should influence the spatial distribution of root strength. Although many factors may

influence the morphology of root networks (including slope angle, soil and bedrock types, soil moisture, species, hillslope aspect, and interaction with other trees) the lateral extent of root systems can be predicted from observations of tree species and stem diameter (Smith 1964).

The different type of vegetation has different interaction with the soil or the regolith i.e., depending on the root system. Studies for more than a century associations between forest cutting and landslides have been interpreted as evidence that forest clearing accelerates erosion in mountainous terrain (Lyell, 1853). The shear strength which is a property of the soil type related and vegetation in the context of landslide Hastie 1990). Remote sensing in forest management has led to many studies that concluded that forest clearing dramatically accelerates rates of landslides over rates in undisturbed forest (Sidle et al., 1985, Montgomery et al, 2000).

Forest and hill miss management: Forest logging, fire and cultivation on hill slopes are considered the most important in triggering shallow landslides (Garcı´a-Ruiz et al., 1988; Cannon, 2000; Squier and Harvey, 2000).

1.3 Causal Factors: The causal factors that contribute to landslides in an area are (i) preparatory and (ii) triggering factors. These mainly consist of:

- **Fissured Materials**- Loose soil, rock and fragmented materials.
- **Mass discontinuities**- Adversely oriented slip control, bedding lineaments, faults, etc.
- **Water and soil erosion of the slope toe**- Due to streams or human anthropogenic activities.
- **Intense short period rainfall**- Heavy rainfall for a shorter duration on a weak plane.
- **Prolonged high precipitation**- High rainfall, dam construction and alteration in river course.
- **Loading of the slope at its crest**- Construction on the top of slope, heavy earthmoving equipments, etc.
- **Shrink and swell of expansive clay**- Soil of clayey or clay loamy with high permeability and porosity.
- **Water leakage**- Seepage of water from any construction or natural resources.

Understanding of these factors in a region helps in adopting at stabilisation approaches. Landslide can be triggered by various factors. The relationship of them can be expressed as:

Landslide = f (hydrology, geology, land use and land cover, slope morphometry, anthropogenic activity, natural hazards).

Application of GIS and Remote sensing Landslide hazard zonation

Landslides often cause damage for property and people. To reduce the losses due to landslides over the long term identification of unstable slopes to aid in mitigation of landslide hazards is the integral part of land management. Landslide hazard zonation is a process of ranking different parts of an area according to the degrees of actual or potential hazard from landslides (Varnes, 1984). The evaluation of landslides is a complex task as the occurrence of the landslide is dependent on many factors. The process of zonation of landslides comprises of preparation of maps showing the status of causality factors in the study area with the help of aerial photographs, satellite imagery, topographic maps and geographical maps.

The geological data of lithology and structure can be extracted from the remote sensing data or by the digitizing the map. The lithological units can be mapped by a panchromatic or multispectral or radar data. Over the same lithology, the spectral response may be quite variable, being a function of several factors. The factors that have to be accounted for deducing the lithological information are a) general geological setting, b) weathering and landform, c) drainage, d) structural features, e) soil, f) vegetation and g) spectral characteristics. These parameters are also interdependent, and interpretation is generally based on multiple convergence of evidence; however, even single parameter could be diagnostic in a certain case. The structural units like folds, faults, lineaments and bedding can be identification depends on resolution and dimension of the discontinuities.

1.4 Mapping and Monitoring Landslide Susceptible Regions

Monitoring, mapping and modelling, are based upon a few, widely accepted principles or assumptions (Varnes et al., 1984; Carrara et al., 1991; Hutchinson and Chandler, 1991; Hutchinson,. 1995; Turner and Schuster, 1995) such as

- Landslides are controlled by mechanical laws that can be determined empirically, statistically or in deterministic fashion. Conditions that cause landslides instability factors directly or indirectly linked to slope failure, can be collected and used to build predictive models of landslide occurrence (Dietrich. et al., 1995) .
- The past and present are keys to the future (Varnes et al., 1984; Carrara et al., 1991; Hutchinson, 1995) as slope failures in the future will be more likely to occur under the conditions which led to past and present instability. Hence, the understanding of past failures is essential in the assessment of landslide hazard.
- Landslide occurrence, in space or time, can be inferred from heuristic investigations, computed through the analysis of environmental information,

or inferred from physical models. Therefore, a territory can be zoned into hazard classes ranked according to different probabilities.

Monitoring is defined as the comparison of landslide conditions like areal extent, speed of movement, surface topography, and soil humidity from different periods in order to assess landslide activity (Mantovani et al., 1996). The monitoring of landslide phenomena has acquired great importance for the scientific community since the use of adequate monitoring systems is a powerful tool for understanding kinematic aspects of mass movements and permits their correct analysis and interpretation; in addition, it is an essential aid in identifying and checking alarm situations (Bogaard T.A, 2000). A wide range of field monitoring techniques has been and remote sensing techniques are used for monitoring. Table 2 lists the methods adopted in monitoring landslide (Gunzburger et al, 2005).

Table 2: Quantitative monitoring methods for surface movements

	Provided data	Typical range	Typical precision	Spatial continuity	Temporal continuity	Physical contact with slope
Conventional geotechnics						
Micrometer screw-level, clinometer	Angular displacement	Angle changes<10^{o}	10^{-4} rad	No	Yes	Yes (for installation, maintenance and eventually downloading of data)
Fissurometer, levelling vernier pole, short-base extensomete	Crack opening	Aperture = 1–10 cm	0.1mm			
Precision tape, fixed wire extensometer	Distance changes between two targets	Distance = 10–100m	0.5mm			
Conventional topography						
Electro-optic distance-meter (EDM)	Changes in distances between landmarks and station	Distance = 10–10 km	0.1mm+1–5ppm	No	Yes	No (except for installation of the reflectors)
Theodolite	Changes in horizontal and vertical angles of landmarks with respect to the station	Distance = 0.01–10 km	10^{-6} rad			

Tacheometer	Displacement of moving landmarks with respect to the station	Distance = 0.01–10 km	Distances: 3mm+1–5ppm, angles:10^{-6} rad			
Full-automated total station (TS)	Displacement of moving landmarks with respect to the station	Distance = 0.01–10 km	Distance: 0,1 mm, angles: angles:10^{-6} rad			
Satellite positioning						
GPS (global positioning system)	Relative and absolute displacement of moving benchmarks	Distance = 0.01–100 km	Horizontal: 2-3mm, vertical: 5–10mm^2	No	Yes	Yes (for installation and eventually displacement of the antennas from point to point)
France's DORIS system	Relative and absolute displacement of moving benchmarks	Distance = 0.01–100 km	2mm			
Passive remote sensing (conventional photography) and resulting digital elevation models (DEM)						
Terrestrial stereo-photogrammetry	Relative displacement of points	Size = 10–100m	1–10 cm	Yes	No	No
Aerial stereo-photogrammetry (with eventual ortho-rectification)	Relative displacement of points					
Active remote sensing						
InSAR (interferometric combination of pairs of terrestrial, aerial or spatial SAR images)	Changes in distances between points of the slope and station	Variable	3–5mm	Yes	No (due to revisiting time)	No
Laser scan (still under development)	Changes in distances between points of the slope and station	Distance = 100–700m	0.5–2.5mm	Yes	Yes	No

Mapping: Evaluation of landslide hazard requires the preliminary selection of a suitable mapping unit. The term refers to a portion of the land surface which contains a set of ground conditions which differ from the adjacent units across definable boundaries (Hansen, 1984). At the scale of the analysis, a mapping unit represents

domain that maximises internal homogeneity and between-units heterogeneity. Various methods have been proposed to partition the landscape for landslide hazard assessment and mapping (Meijerink, 1988; Carrara et al., 1995). All methods fall into one of the following five groups: grid-cells; terrain units; unique-condition units; slope-units; and topographic units.

Terrain units, traditionally favored by geo-morphologists, are based on the observation that in natural environments the interrelations between materials, forms and processes result in boundaries which frequently reflect geomorphological and ecological differences. Terrain units are the base of the land-system classification approach which has found application in many land resources investigations (Cooke and Doornkamp, 1974; Speight, 1977; Verstappen, 1983; Burnett et al., 1985; Meijerink, 1988; Hansen et al., 1995).

Unique-condition units (Bonham-Carter, 1994;. Chung et al., 1995) imply the classification of each slope-instability factor into a few significant classes which are stored into a single map, or layer. By sequentially overlying all the layers, homogeneous domains unique conditions are singled out whose number, size and nature depend on the criteria used in classifying the input factors.

Slope-units, automatically derived from high-quality DTMs, partition the territory into hydrological regions between drainage and divide lines (Carrara, 1988; Carrara et al., 1991). Depending on the type of instability to be investigated deep-seated vs shallow slides or complex slides vs. debris flows the mapping unit may correspond either to the sub-basin or to the main slope-unit right or left side of the sub-basin. Slope-units can be further subdivided into topographic units defined by the intersections of contours and flow tube boundaries orthogonal to contours (O'Loughlin, 1986). For each topographic unit, local morphometric variables and the cumulative drainage area of all up-slope elements are computed.
Selection of an appropriate mapping unit depends on a number of factors, namely: the type of landslide phenomena to be studied; the scale of the investigation; the quality, resolution, scale and type of the thematic information required; and the availability of the adequate information management and analysis tools. Each technique for tesselling the territory has advantages and limitations that can be enhanced or reduced choosing the appropriate hazard evaluation method.

Landslide hazard modeling: Methods for ranking slope instability factors and assigning the different hazard levels can be qualitative or quantitative and direct or indirect. Qualitative methods are subjective and portray the hazard zoning in descriptive qualitative terms. Quantitative methods produce numerical estimates probabilities of the occurrence of landslide phenomena in any hazard zone. Direct methods consist of the geomorphological mapping of landslide hazard (Verstappen,

1983). Indirect methods for landslide hazard assessment are essentially stepwise. They require first the recognition and mapping of landslides over a target region or a subset of it (training area). It follows the identification and mapping of a group of physical factors which are directly or indirectly correlated with slope instability (instability factors). They then involve an estimate of the relative contribution of the instability factors in generating slope-failures, and the classification of the land surface into domains of different hazard degree hazard zoning. These are grouped into few main categories (Carrara et al., 1992; van Westen, 1993; Carrara et al.,. 1995; Hutchinson, 1995) as geomorphological hazard mapping; analysis of landslide inventories; heuristic or index based methods; functional, statistically based models; geotechnical or physically based models.

Geomorphological mapping of landslide hazard is a direct, qualitative method that relies on the ability of the investigator to estimate actual and potential slope failures (Humbert, 1977; Godefroy and Humbert, 1983; Kienholz et al., 1983, 1984; Bosi et al., 1985; Zimmerman et al., 1986; Seeley and West, 1990; Hansen et al., 1995). The heuristic approach, based on the a priori knowledge of all causes and instability factors of landslides in the area under investigation, is an indirect, mostly qualitative method, that depends on how well and how much the investigator understands the geomorphological processes acting upon the terrain. Instability factors are ranked and weighted according to their assumed or expected importance in causing mass movements (Nilsen and Brabb, 1977; Amadesi and Vianello, 1978; Hollingsworth and Kovacs, 1981; Neeley and Rice, 1990; Montgomery et al., 1991; Mejıa-Navarro et al., 1994).

All other approaches are indirect and quantitative. The analysis of landslide inventories attempts to predict future patterns of instability from the past and present distribution of landslide deposits. This is accomplished by preparing landslide density (‘‘*isopleth*’’) maps, i.e., maps showing the number or percent of area covered by landslide deposits over a region (Campbell, 1973; Wright, 1974; Wright and Nilsen, 1974; Wright et al., 1974; DeGraff, 1985, Guzzetti et al., 1994). Statistical, ‘‘black-box’’ approaches are based on the analysis of the functional relationships between instability factors and the past and present distribution of landslides. Various multivariate statistical techniques have been applied on various mapping units. The discriminant analysis like, linear and logistic regression, and neural networks has been applied by many (Neuland, 1976; Carrara, 1983; Carrara et al., 1991; Carrara et al., 1995; Roth, 1983; Yin and Yan, 1988; Neeley and Rice, 1990; Mark, 1992; van Westen, 1993, 1994; Chung et al., 1995, Lee,2004) and fuzzy approaches (Juang et al. 1992; Binaghi et al. 1998; Ercanoglu and Gokceoglu 2002, Lee, 2006). A statistical model of slope instability is built on the assumption that the factors which caused slope-failure in a region are the same as those which will generate landslides in the future. Process-based geotechnical models rely upon the understanding of few

physical laws controlling slope instability (Okimura and Kawatani, 1987; Dunne, 1991; Montgomery and Dietrich, 1994; Dietrich et al., 1995; Terlien et al., 1995). These models couple shallow subsurface flow i.e., the pore pressure spatial distribution, predicted soil thickness and landslides of the soil mantle (Dietrich et al., 1995). Stability conditions are generally evaluated by means of a static model, such as the ‘‘infinite slope model’’, where the local equilibrium along a potential slip surface is considered.

Hazard models and mapping units are conceptually and operationally interrelated (Carrara et al., 1995). In the direct hazard mapping the geomorphological unit of reference is implicitly defined by the interpreter that maps those portions of the territory that are subject to different geomorphological hazards Hansen, 1984. In all other cases i.e., grid-based modelling, unique-condition units, slope-units, topographic units, the mapping unit is explicitly defined by the operator. In general, grid-cells are preferred for heuristic (Pike, 1988; Mejıa-Navarro et al., 1994), statistical (Carrara, 1983; van Westen, 1994) and physical or simulation (Mark, 1992; Terlien et al., 1995) modelling. Unique-condition units have been applied to both heuristic (van Westen, 1993) and statistical methods (Carrara et al., 1995; Chung et al, 1995). Slope-units and topographic units have been used in statistical (Carrara et al., 1991; 1995) and physically based (Montgomery and Dietrich, 1994) models. The information provided by the hazard maps helps to minimize losses caused by existing and future landslides by means of prevention, mitigation and avoidance.

Landslide mitigation is carried out in order to stop or reduce the landslide movement so that the resulting damages can be minimized. The landslide mitigation works are broadly classified into two categories: i) control works or soft solution; and ii) restraint works or hard solutions. The control works involve modifications of the natural conditions of landslides such as topography, geology, ground water, and other conditions that indirectly control portions of the entire landslide movement. Restraint works include avoiding landslide hazard areas by proper zoning and land-use regulations. Long-term hazard reduction and avoidance can likely be achieved most efficiently by implementing soft solutions to landslide hazards. Also, zoning and land-use regulations are more cost-effective measures over the long-term than constructing debris dams and retaining walls. The restraint works rely directly on the construction of structural elements like debris dams, retaining walls, and drainage systems in landslide-prone areas.

Mitigation measures: Typical stabilization measures are selected according to local conditions and construction practice (Kwong A.K.L, 2004), which include trimming and cutting the rock bedding; hand-dug lateral resistance piles with or without pre-stressed ground anchors; reinforced concrete wall between lateral resistance piles; pre-stressed or passive ground anchors; gravity masonry retaining wall and slope

surface protection including hydro seeding, sprayed concrete and reinforced concrete grids. retaining wall with or without tie-back; re-compaction of fill slopes; soil nailing; mini-piles; scaling and trimming; bolting and dowelling; meshing; buttressing and anchoring (occasional).

Jayakumar et al.(1989), worked on landslides in Wynad region of western ghats, peninsular India. In the study direct and indirect methods was adopted assess the susceptibility of landslide in the region. Ramana et al (1990) presents the case histories of two catastrophic landslips in hard rock terrains with varied climatic and geological environments. Nagarajan, et.al., (2000) highlights the utility of temporal remotely-sensed data and knowledge based Geographical Information Systems for collection, integration and analysis of spatially-oriented data, as well as in finding out the inherent relation between various factors in parts of Western Ghats.

1.5 Prediction of Landslide using Remote Sensing and GIS

In order to minimise the damage due to landslides, it is required to identify the regions, which are susceptible to landslides. This requires spatial and temporal data related to the region. Geospatial technologies such as Geographic Information System (GIS) and Remote Sensing (RS) help in the analysis of spatial and temporal data. Remote sensing provides the spatial data at regular intervals, while GIS helps in the analysis. GIS is the ideal tool for the analysis of parameters with a high degree of spatial variability.

Landslide susceptibility is defined as the proneness of a terrain to produce slope failures and susceptibility is usually expressed in a cartographic way. A landslide susceptibility map depicts areas likely to have landslides in the future by correlating some of the principal factors that contribute to landslides with the past distribution of slope failures.

Landslide hazard zonation map can be derived through interpretation of satellite imagery and by using the factors leading to the occurrence of the potentially damaging phenomenon. With the increasing availability of high-resolution spatial datasets along with GIS, it is possible to partially automate the landslide hazard mapping process that eliminates the need of longer time expenditure in fieldwork and extensive expert input. GIS is used combined with remote sensing to determine the relationship between various influencing parameters and predict areas that may be highly susceptible to landslides. Validation of this exercise is done by considering the historical data of past slope failures, and causal factors that resulted in unstable conditions. The essential steps followed in landslide susceptibility zoning are:

- A landslide distribution mapping, differentiated according to type, activity, dimensions, etc., and based on information covering, when possible, a time span as large as possible.

- Spatial mapping of the relevant terrain parameters related to the occurrence of landslides.
- The analysis of the terrain conditions, which are responsible for the occurrence of the different types of landslides.
- The assignment of weights to the causal factors, depending on their role in landslides.
- Formulation of decision rules and designation of susceptibility classes.

In order to predict the landslide prone regions, the data required are gathered in the field using GPS and for the high-resolution spatial data analysis the remote sensing data is used. The landslide map is prepared using remote sensing as well as ground-based maps and statistical data. Base map layers required for terrain analyses were derived from the toposheets. Collateral data (soil, lithology, rainfall, etc.) with the interpreted remote sensing data in GIS helped in mapping. After collecting the information needed it was organised into a database that could be presented graphically and in the GIS form. GIS is suitable to meet the requirements of synthesising the available information. The strength of GIS lies in its capability of storing interpreted and available information as maps and linked attributes. Mapped areas and attributes are retrieved, and cross-calculated. Landslide monitoring involves field data collection for meteorological, hydrological, topographical and geophysical data. The influencing factors that determine the occurrence of landslide hazards are topography (slope angle and aspect), soil, geology, underground water, rainfall intensity, land-use, the distribution of road and various geological features like lineaments, faults, etc. The recent development of automatic sampling, recording, and transmitting devices has helped immensely in landscape monitoring for predicting landslides.

Case Study: Sharavathi River Basin

2. OBJECTIVE

The aim of the study is to map landslide prone zones in the Sharavathi river basin (Uttara Kannada and Shimoga districts, Karnataka State) using the remote sensing data and GIS techniques. Specific objectives are:

- Identification of causal factors of landslides using information collected from fieldwork, government agencies and remote sensing.
- Spatial mapping of landslide prone zones, and
- Assessment of the extent of damage due to landslide hazards.

Remote sensing data with better spectral and spatial resolutions along with data of soil, land use, climate, etc. and GIS would help in preparing the landslide distribution map. This involves:

1) Generating a spatial database identifying the base layers that play a role in landslide susceptibility pertaining to the study area.
2) Creating a landslide database to identify the causative factors of landslide slumps and creeps in the study area, through mapping, gathering information in the field and remote sensing approaches.
3) Evaluating the direct relationship between the causative factors of hill slope instability and the combination of landslide susceptibility from contributing base layers.
4) Creation of a landslide hazard map using statistical data generated to create landslide susceptible polygons.
5) Evaluating human hazards and suggesting corrective measures to minimise future risks towards areas of human habitation, infrastructure and transportation.

3. METHOD

The aim of this study is to identify the causal factors of landslides, using information collected from fieldwork, GIS and remote sensing sources and to identify slide prone zones and assess human hazard in the Sharavathi River Basin. Methods as outlined in Figure 3.1 involved to achieve the objectives are:

(a) Pre Fieldwork: Review of literature; Collection of secondary data; Collection of topo-sheets on 1:50,000 scales.

(b) Field investigation: Identification of landslides in the study area and collection of their coordinates using GPS; Collection of attribute data; Collection of training data (GCP's) for supervised classification of remote sensing data; Documentation of sensitive areas with the feedback from local people; Identification of environmentally unsound anthropogenic activities such as diversion of streams, road cuts, etc.

(c) Post Fieldwork: Creation of Digital database of secondary data and toposheets, etc.; Geo-referencing of maps and images; Digitisation of cadastral maps; supervised classification of remote sensing data; generating Digital elevation model (DEM), slope and aspect maps of study area; Preparation of final map tables and diagrams.

3.1 Data Used

- IRS 1C/1D LISS III MSS data (temporal data) IRS 1C/1D PAN data
  $\rightarrow$ to see the spatial and temporal changes.
- Survey of India Toposheets on 1:50000 scales to create GIS base layers.
- Geological map with attribute data from Karnataka State Remote Sensing Applications Centre (KSRSAC).
- Soil map along with attribute data from National Bureau of Soil survey and Landuse Planning.
- Meteorological data from India Meteorological Department, Pune.
- Rainfall data of Sub-basins from Karnataka Power Corporation Limited (KPCL), Agriculture Departments (Honnavar, Kumta, Siddapur, Sagar and Hosanagara).
- Literature that provide an understanding of the concept and advancement in this area of research.

3.2 Software Used

IDRISI 3 for D.E.M, fusion of PAN & LISS-III, images raster analysis and image analysis and Arc View 3.2, MAPINFO 6.0 for vector analysis.

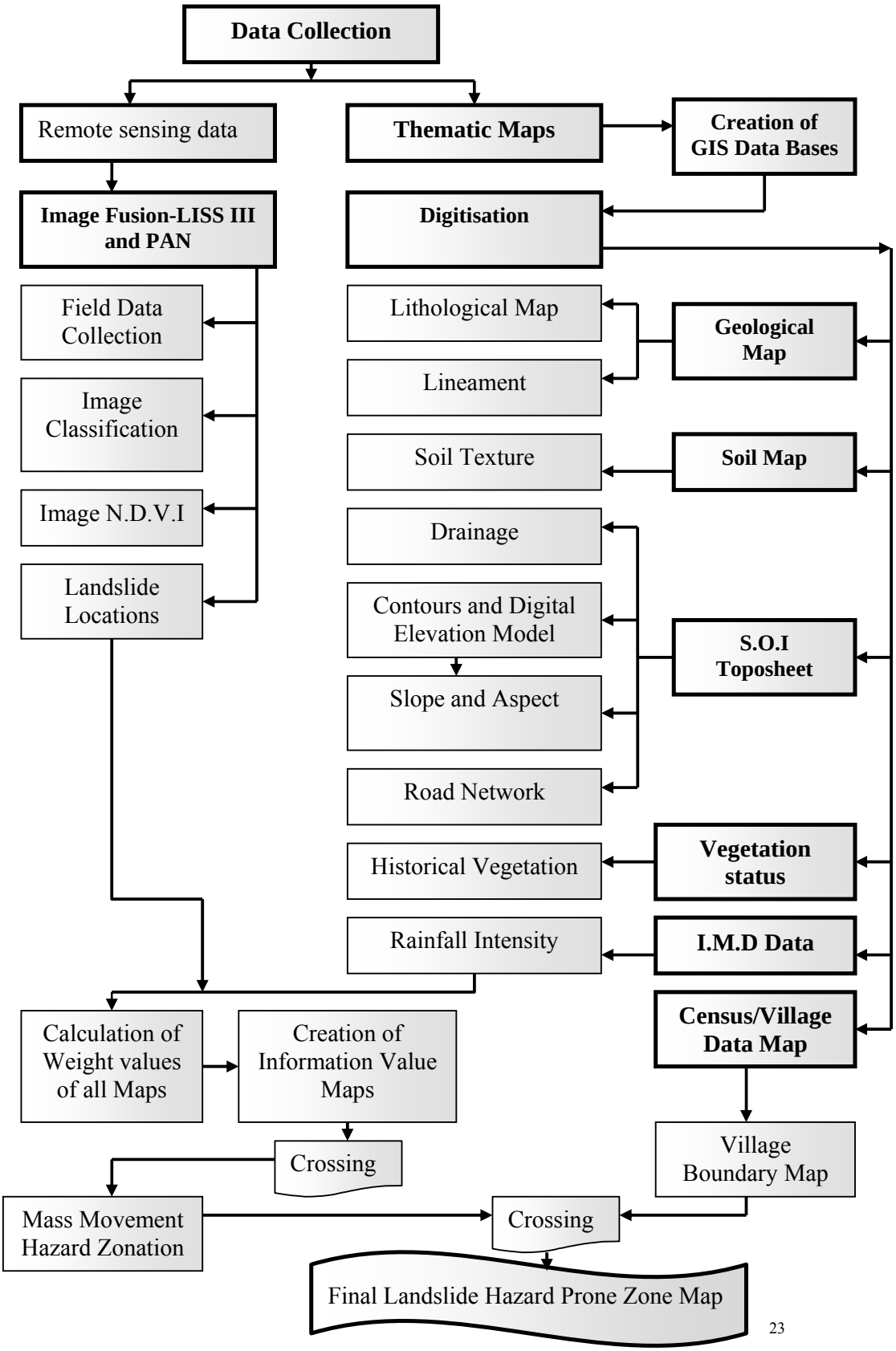

Fig 3.1: Method- flowchart

4. STUDY AREA

This study was carried out in the Sharavathi river basin, one of the west flowing rivers of Karnataka (figure 4.2). This river has been utilised for power generation through two reservoirs (at Linganamakki and at Gerusoppa). It is located at Shimoga and Uttara Kannada Districts of Karnataka State. Shimoga district is situated roughly in the mid-south-western part of the state. Sharavathi River Basin, is situated in the north part of the Western Ghats, a continuous range of hills that act as a drainage divide, separating the South Deccan Plateau from the Coastal Plain. The district is situated between 13°27' and 14°39' north latitude and 74°38' and 76°04' east longitude, bestowed with abundant natural resources. The general elevation along the Sharavathi River Basin is about 640 metres above sea level in the west, falling to about 529 meters in the east. The important rivers that flow in the district are Tunga, Bhadra, Sharavathi, Kumudwathi and Vardha. The Sharavathi River discharges into the sea at Honnavar in North Kannara. The Karnataka Power Corporation Limited (KPCL) has constructed a dam across the river near Linganamakki, one of the oldest hydroelectric power projects in India. The entire study area falls in mid region of Western Ghats having steep and undulating terrain. The area under study is the Sharavathi river basin with catchment area of 2924 km^2. Figure 4.1 illustrates that Sharavathi basin as a hydrological unit comprising of geographical, ecological and cultural diversities.

Fig 4.1: A view of Sharavathi river basin study area

STUDY AREA: Sharavathi River Basin, Karnataka

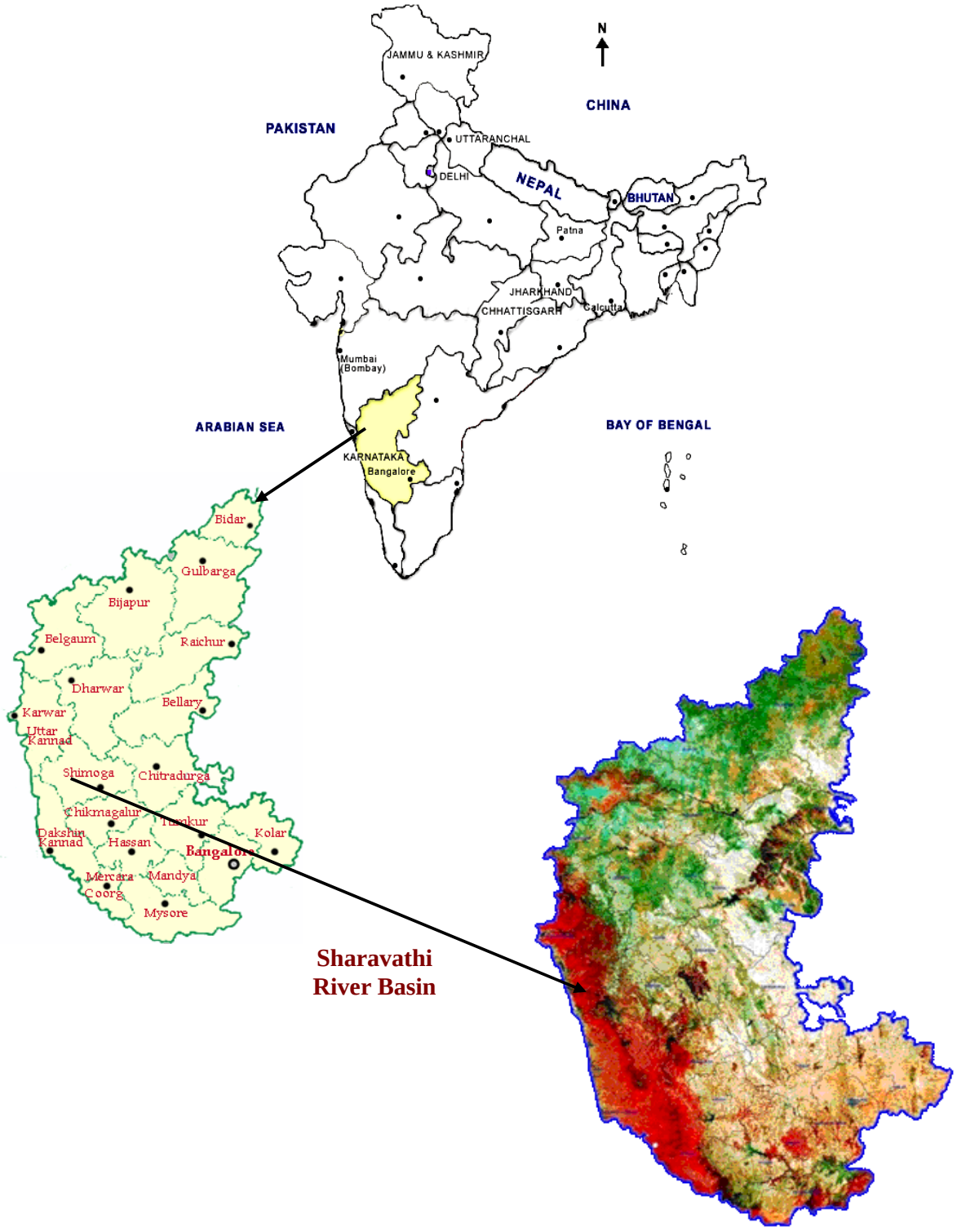

Fig 4.2: Sharavathi river basin, Karnataka, India

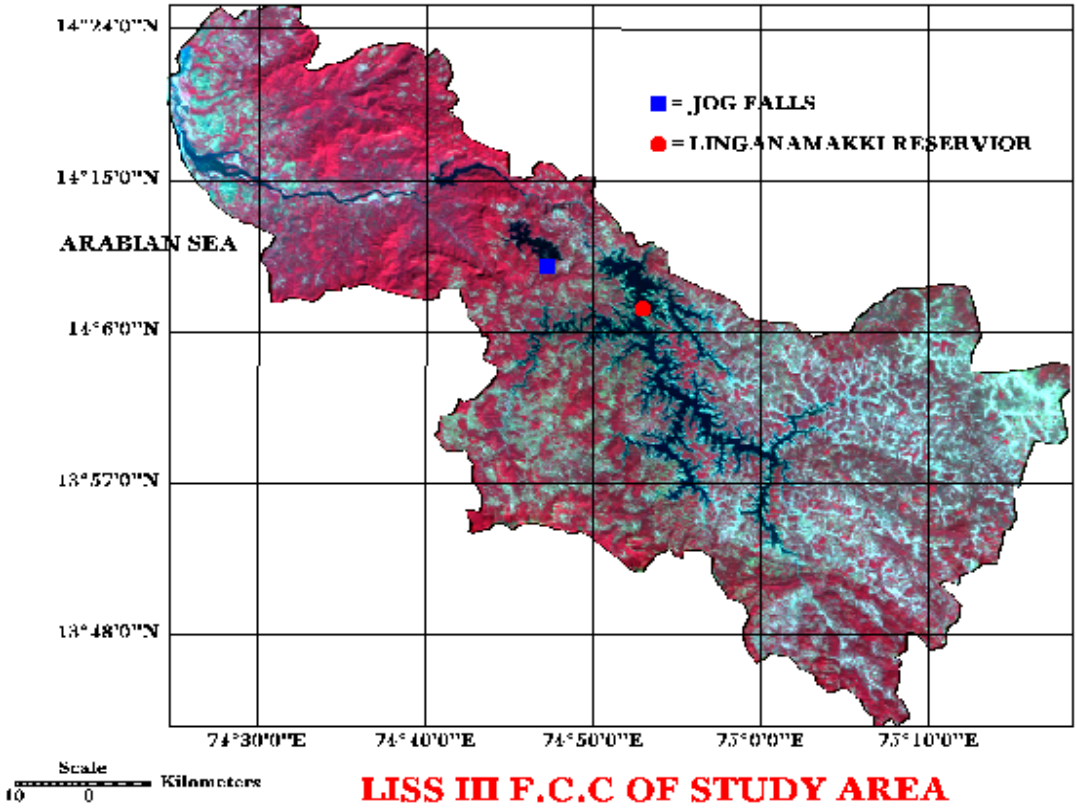

4.1 **Accessibility:** This study area is well connected by road and rail to several major cities of Karnataka and neighbouring states and an important railhead of the newly constructed Konkan railway connects this coastline; the newly built bridge across the Sharavathi river, dominates the landscape. The study area is about 350 km from Bangalore, 200 km from Goa and is less than 60 km from Shimoga. Except some hilly areas, almost the entire area is well connected by the metalled roads and water ferry. Some villages inside the forest area are well connected with ordinary roads. The Bangalore-Goa highway passes through the study area. Rest of the hilly areas are well connected with non-metalled or metalled roads. Many foot tracks and water ferries are also present in the hilly terrain.

4.2 **Physiography:** Physiographically, the study area encompasses low-lying flat terrain to highly undulating hilly ranges. The lowest elevation observed in the study area is around 20 m above sea level that is near the Arabian Sea and the highest relief is around 1340 m in the southern part of upstream area and northern part of downstream area. The study area is part of the rugged terrain of Western Ghats of southwest Shimoga and southeast Uttar Kannada. This region, by virtue of its geographical location in the central Western Ghats, and heterogeneity in the terrain and micro-climatic variations support a rich diversity of flora and fauna.

The Karnataka Power Corporation Limited has constructed a dam across the river in 1964 near Linganamakki, which is at present one of the oldest hydroelectric power projects in India. The dam is located at about 14°41'24" N latitude and 74° 50’54’’ E longitudes with an altitude of 512 m. The water from Linganamakki dam flows to Talakalale Balancing Reservoir through a trapezoidal canal with a discharge capacity of 175.56 cu m. The length of this channel is about 4318.40 m with a submersion of 7.77 sq. km. It has a catchment area of about 46.60 sq.km. The gross capacity of the reservoir is 129.60 cu m. Sharavathi River alone, in its fullest potential, accounts for an estimated electricity generation of about 6,000 million units (kWh) per annum. Due to the hilly terrain, the submergence and consequent increase in water-spread area due to the dam and Sharavathi River has resulted in the creation of several islands distributed throughout the reservoir. There are about around 125 islands with sizes ranging from 2-3 sq. km to less than 25 sq. km. In most of the submerged areas the highlands and hilltops protrude out of the water-filled surroundings as islands.

4.3 **Climate and Rainfall:** The area has well-marked seasons of monsoon from May-June to October, winter from November to January and summer from February to May. The temperature ranges from 10°C in winter nights to 32°C in summer. The weather is humid throughout the year with a variation of average rainfall from 1200 mm to 2600 mm in different parts of the catchment. Relative humidity is generally high at around 75% during southwest monsoon season and moderate during the rest of the year. Humidity during summer afternoons is relatively low. Average minimum and maximum temperature are about 15ºC and 38ºC respectively. Wind is generally moderate with some increase in strength during monsoon months and is mainly South-westerly in the mornings and between Northeast and Southeast in the afternoons. There is rapid increase of temperatures after January. April is usually the hottest month with the mean daily maximum temperature at 35.8°C and the mean daily minimum temperature at 22.2°C. In December, the mean daily maximum temperature is 29.2°C and the mean daily minimum temperature is 14.9°C.

The climate of the area is dominated by the southwest monsoons during June to August that bring "incessant rainfall" depositing 5000 to 8000 mm per annum in the Sharavathi catchment basin. The annual normal rainfall in the area is 1526 mm and some station locations even experience an annual rainfall of 2875 mm. Southwest monsoon starts normally from the second week of June and peaks during July and August. During monsoon, the water level reaches its peak leaving the top of the hills and hillocks on which the vegetation thrives. However, summer season interconnects the Islands as the water level recedes. As a result of this heavy rainfall the Western Coast drainage basin is home to one of the major tropical evergreen forest regions in India, which provide much of the timber to the economies of Sagar and Hosanagara taluks.

4.4 **Drainage:** The Sharavathi river originating in the central Western Ghats runs through the districts of Shimoga and Uttara Kannada. The river has a catchment area of about 3600 sq. km. Sharavathi River Basin lies entirely in the Western Coast drainage basin bordered by the eastern drainage divide to the east and the west escarpment to the west, which is most visibly pronounced at Jog Falls where the river drops precipitously from a height of 255 m into a deep gorge and it is characterised by very steep "V" shaped sub parallel ravines formed by steep, fast, west flowing streams. It is one of the most spectacular scenic places of the Western Ghats. The river water is stored in three major reservoirs, namely, at Linganamakki (14º10'24" N, 74º50'54" E), Talakalale (14º11'10" N, 74º46'55" E) and Gerusoppa (14º15'N, 74º39' E). The areas submerged for these reservoirs are 326.34, 7.77 and 5.96 km^2 respectively. The river, and its tributaries and numerous streams run through the rugged terrain of the Ghats. The river, which takes birth at Ambuthirtha in Thirthahalli taluk, flows northwesterly for 130 km to join the Arabian Sea at Honnavar, in Uttara Kannada district. The major tributaries of the river are, Nandiholé, Haridravathi, Sharmanavathi, Hilkunjiholé, Nagodiholé, Hurliholé, Yenneholé, Mavinaholé, Gundabalaholé, Kalkatteholé, and Kandodiholé.

4.5 **Soil Texture:** Soils in the region are mainly lateritic in origin and tend to be predominantly acidic and reddish in colour. In Sagar taluk, soils are 94% acidic while in Hosanagara taluk the percentage drops slightly to 76%. Nitrogen and phosphorous concentrations range from moderate to very low for Sagar and Hosanagara taluks respectively, while in both the taluks, soils are deficient in phosphorous (Karnataka State Gazetteer, 1975). Soils are rich in organic matter and low in phosphate, nitrate and sulphate concentration, while pH ranges from 5.5 - 6.8. The sediments have low sulphate (0.191 - 0.68 mg/gm), nitrate (0.0 - 0.0007 mg/gm) and phosphate (0.00024 - 0.001 mg/gm) concentrations, indicating close correlation between sediment and catchment soil. The sediment samples are rich in organic carbon and the elements like Na, K, Ca, and Mg are found well within the prescribed standards. Bulk density of sediments in streams of the western region indicates their porous condition (0.783 - 0.983 gm/cm^3) while in the eastern side they are less porous (1.23 - 1.475 gm/cm^3).

4.6 **Geological Parameters:** The Karnataka Carton, similar to other shield areas in the world, consisting of geologically stable rocks of Achaean age mainly dominates the geology of the region. Geological units include the Dharwar Schist Belt and the Older Gneiss Complex. Due to the humid climate of the region substantial intense in-situ weathering has taken place, leading to extensive creation of laterite over much of the terrain, making it the third major geological unit in the study area. The ghat area extending for a longer length lies parallel to the west coast, forming one of the most magnificent escarpments of tertiary age. Sediments of Palaeocene and younger ages are deposited in the graben area (Figure 4.3), developed at the west of the present day west coast of India. As the

area is having a prominence of hilly terrain, it encompasses lots of lineament cracks, which play a vital role in the creation of loose slopes for the failure.

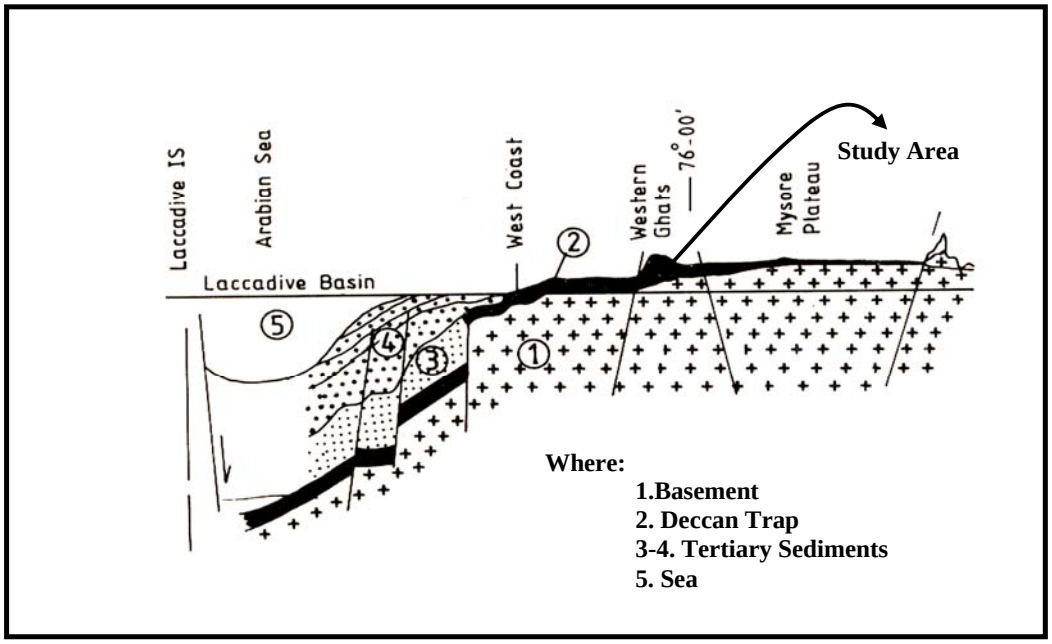

Source: B. P. Radhakrishna, R. Vidyanadhan. Geology of Karnataka, GSI (1994)

Fig 4.3: Western Ghats - study area, the faulted margin of the west coast and Arabian sea filling up the graben

Figure 4.4 below shows a topographical undulation in the terrain with higher mountainous area along with geological unconformities of folds and faults.

Fig 4.4: Topographical and geological view of Western Ghats - study area

4.7 Vegetation - Flora and Fauna

Sharavathi river upper and lower catchment areas have a variety of natural vegetation ranging from the climax tropical evergreen to semi-evergreen forests with around 16% of them along the high rainfall areas of the main hill ranges of the Western Ghats to the moist deciduous forests, and around 25% of them in the undulating plains and low hills along the eastern drier tracts of the river basin. The landscape everywhere is in fact a mosaic of a variety of elements caused by human impacts through historical times to the current period. Around 21% of all vegetation consists of grassland, scrub, and cultivable waste. River Basin is also rich in animal diversity as it covers a large part of Sharavathi Wildlife Sanctuary. The region is also adjacent to Mookambika Wildlife Sanctuary of Udupi District and Shettihalli Wildlife Sanctuary of Shimoga District. Due to rising human pressures including creation of numerous monoculture plantations, many of the migratory paths of the animals are disrupted.

5. REMOTE SENSING, DIGITAL IMAGE PROCESSING AND GIS

5.1 Remote Sensing data:

The data used for the study area to analyse the Landslide Prone Zone Mapping using Remote Sensing and GIS Technique is mainly IRS-1C: LISS-III and PAN images were acquired from NRSA (National Remote Sensing Agency). Table 5.1 lists the spectral and spatial resolutions along with other details.

Table 5.1: Technical specification of LISS III and PAN imagery

IRS 1-C		
Specifications	**LISS-III**	**PAN**
Spatial resolution (m)	B2 B3 — 23.5 B4 B5 -- 70.5	5.8
Spectral bands	B2- 0.52 to 0.59 B3- 0.62 to 0.68 B4- 0.77 to 0.86 B5- 1.55 to 1.70	0.5-0.75
Swath (km)	140	70
Repetivity	24 days	24 days
Revisit	5 days	5 days

5.2 **Digital Image Processing:** Digital image processing encompasses four major areas of spatial data analysis (Figure 5.1), which are:

- **Image Restoration or Pre-processing-** Computer routines correct a degraded digital Image to its intended form, which is usually a precursor to the following steps.
- **Image Enhancement-** Computer routines improve the detestability of objects or patterns in a digital image for visual interpretation.
- **Image Classification-** Quantitatively classifying or identifying objects or patterns on the basis of their multi spectral radiance values.
- **Data-Set Merging-** Computer routines integrate multiple sets of data from the same location such that appropriate measurements can be made.

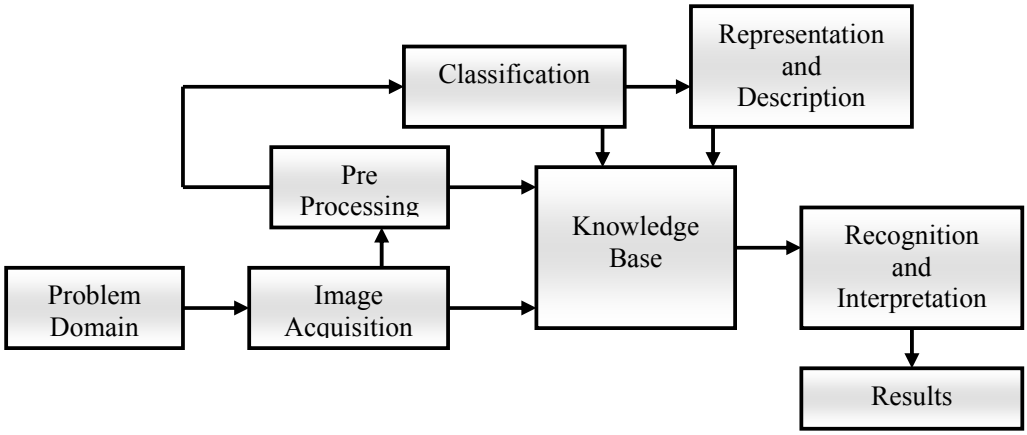

Fig 5.1: Fundamental steps in digital image processing

5.3 Geographical Information System (GIS)

These information systems aid to create, manipulate, store and use spatial data much faster compared to conventional methods. The factors, which are included in determining the occurrence of landslide hazard, are topography (slope angle and aspect), geology, geological-structures, soil texture and rainfall intensity. Along with these, other factors that can determine the degree of disaster include nature conditions, land-use, and anthropogenic activities i.e. the distribution of buildings and roads. GIS along with terrain analysis can be used for setting up a database.

6. TERRAIN ANALYSIS AND GIS DATA GENERATIONS

6.1 **Terrain Analysis:** The topographic data required a more extensive treatment. From the Survey of India toposheet (1:50000 scale) the contours are digitised at 20-metre intervals. Digital elevation model (DEM) "which is a digital cartographic representation of the elevation of the terrain at regularly spaced intervals in X and Y directions using Z values referenced to a common vertical datum i.e. Height" was developed to get the 3-D visualisation of the whole terrain. The DEM can be generally as Triangular Irregular Network (TIN), which is based on an irregular array of points, forming a sheet of non-overlapping contiguous triangle facets or Gridded Surfaces (DEMs, DTMs) as a rectangular array of cells storing the elevation value for the centroid of the cell. The study area is having diverse topographic features from sea level (0 m) to 1340 m height in extreme hilly terrain areas and Gridded surface DEM is used for model generation. Slope is a calculation of the maximum rate of change across the surface either from cell to cell in a gridded surface or of a triangle in a TIN. Aspect identifies the steepest downslope across the surface, always considered to be a significant determinant of landslide hazard. Higher the slope, there is a greater chance of occurrence of landslide. The digital elevation model developed using the topographic data is used to derive a corresponding slope and aspect model. These groups are generalisations about slopes in the study area, creating classes that are termed flatter due to lower slope value and steeper resulting from higher slope value in the slope zone legend. Slope is either calculated as percent of slope or degree of slope. An aspect map is also derived from elevation values in DEM. The aspect value assigned to each cell in an aspect map helps in identifying the direction (north, south, etc.) to which the side cell is oriented and landslide occurred. The topographic data contours are shown in the Figure 6.1 below, which helped in DEM, 3-D perspective (as shown in Figure 6.1 a and 6.1 b in the annexure), slope and Aspect Map creation.

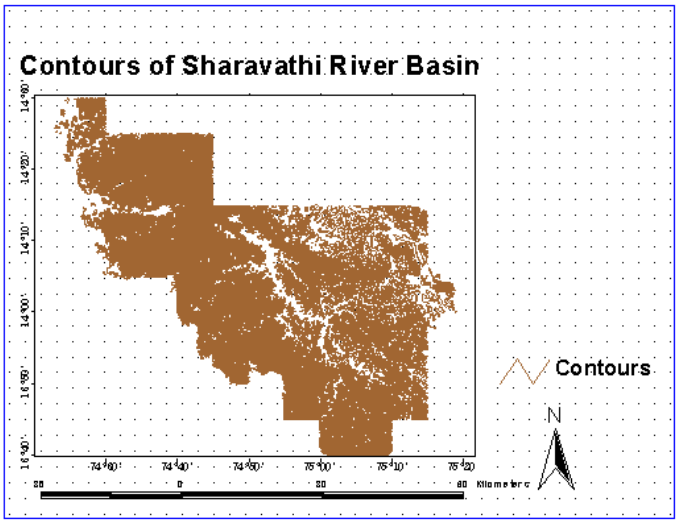

Fig 6.1: Contours of Sharavathi river basin

Existing Landslide: Field visit to existing landslide points helped in collection of GPS readings for areas under landslide, determination of soil bulk density of the landslide site, area affected due to the landslide and sample for soil texture and lithology. These details are used in determination of various aspects, which can be used in calculating the weights that helps in preparing the map of susceptible landslide areas. The existing landslide map is prepared on the basis of observations collected in the field to know the exact location of landslide. This is overlaid on the geo-referenced remote sensing data, which helped in identifying the parameters responsible on the basis of tone and texture in the image. With this information, probable area of landslide can be mapped. The existing landslide map of the study area is shown below in Figure 6.2. The location details (geo co-ordinates) of the landslide locations are given in Table 6.1.

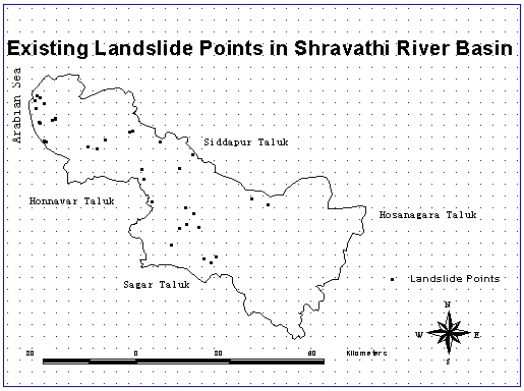

Fig 6.2: Existing landslide points in Sharavathi river basin

6.2 Base Layers - Road Network

Mass wasting and landslides can also occur in response to modification of hill slope conditions and hydrology. Road density, road network and road location can set the stage for mass wasting to occur especially when the site has an inherent propensity for sliding. Often there is a combination of causes for failures that involve increased water in the slide mass itself, which adds weight and reduces the soil strength by increased pore pressure. This in combination with the loss of support due to a road cut at the toe of a slide can result in mass wasting. In some cases, simply the loss of support at a road cut can cause a slide where increased water may not be a factor. Roads have been built across the toe of slides, which have removed this support giving or an otherwise stable hill slope into a chronic source of sediment and a site for mass wasting (Figure 6.3). Experimental studies showed that landslides, especially from poorly designed roads during major storms, pulsed large amounts of sediment in brief episodes, while surface erosion from roads and clear cuts was more chronic.

Table 6.1: Landslide location details

Sr. No	NORTHING	EASTING	Length*Width*Height (m)
1	14° 12′ 31.76	74° 51′ 4.14	250* 50* 50
2	14° 8′ 36.70	74° 43′ 19.67	200* 200*100
3	14° 14′ 33.54	74° 27′ 13.94	200*50*100
4	14° 13′ 30.18	74° 35′ 42.58	50*100*100
5	14° 13′ 42.78	74° 34′ 16.68	100*100*100
6	14° 14′ 51.03	74° 37′ 1.09	200*25*25
7	14° 3′ 1.08	74° 51′ 13.6	200*100*100
8	14° 3′ 57.20	74° 49′ 54.08	100*50*50
9	14° 0′ 37.51	74° 48′ 58.78	200*50*75
10	13° 55′ 43.53	74° 52′ 48.82	150*50*50
11	13° 55′ 8.94	74° 53′ 56.4	50*50*100
12	13° 56′ 1.79	74°54′ 46.8	150*50*100
13	13° 57′ 55.15	74° 47′ 42.21	100*50*100
14	14° 1′ 11.74	74° 50′ 5.78	100*25*50
15	14° 0′ 46.98	74° 51′ 59.43	250*100*150
16	14° 0′ 48.31	74° 52′ 7.96	150*75*100
17	14° 10′ 17.25	74° 48′ 59.04	50*50*100
18	14° 4′ 52.96	74° 44′ 32.60	50*50*50
19	14° 4′ 52.53	74 44′ 37.10	200*50*100
20	14° 4′ 22	75° 3′ 3.85	100*100*50
21	14° 5′ 20.5	75° 0′ 34.2	500*100*100
22	14° 15′ 30	74° 45′ 55	50*25*100
23	14° 16′ 15.88	74° 41′ 28.45	100*25*25
24	14° 16′ 11	74° 41′ 3	150*25*50
25	14° 18′ 20	74° 29′ 10	250*25*50
26	14° 18′ 14	74° 29′ 3	250*25*50
27	14° 14′ 46.24	74° 27′ 22	250*50*50
28	14° 14′ 36.63	74° 27′ 41.50	300*100*200
29	14° 17′ 38.68	74° 26′ 33.75	500*500*100
30	14° 17′ 36.85	74° 26′ 42.82	500*500*100

31	14° 18′ 1.62	74° 28′ 34	200*50*100
32	14° 21′ 14.32	74° 25′ 55.3	300*50*100
33	14°21′ 43.2	74°26′ 34.51	300*50*100
34	14°21′ 57.45	74°26′ 13.38	200*50*100
35	14°20′ 48.08	74°27′ 14.25	200*50*50
36	14°19′ 53.04	74°25′ 58.58	200*100*200
37	14° 10′ 7.5	74° 42′ 55.26	500*100*50

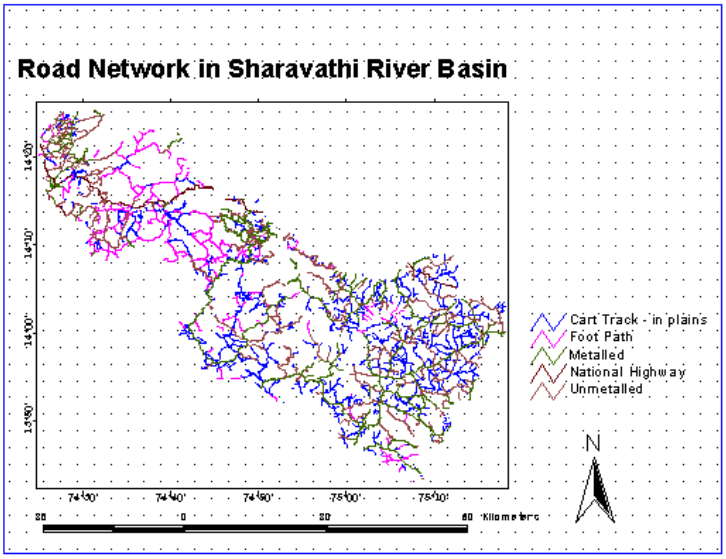

Fig 6.3: Road network in Sharavathi river basin

6.3 Village Boundary, Settlement Location and Population

The village boundary, settlements and population map in the study area are also prepared using the village taluk maps, toposheets and census data (1991). This helps in identifying the socio-economic status of the region and the extent of damage in case of hazards (people affected, etc.). This also would aid in quantifying the extent of damage due to natural disaster and remedial measures to be undertaken. The village boundary map and settlement location map of the study area are shown below in Figures 6.4 and 6.5.

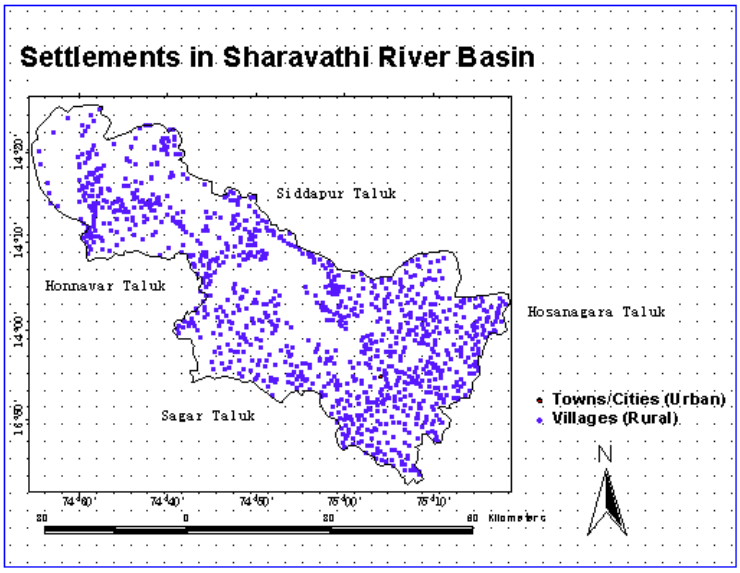

Fig 6.4: Settlements in Sharavathi river basin

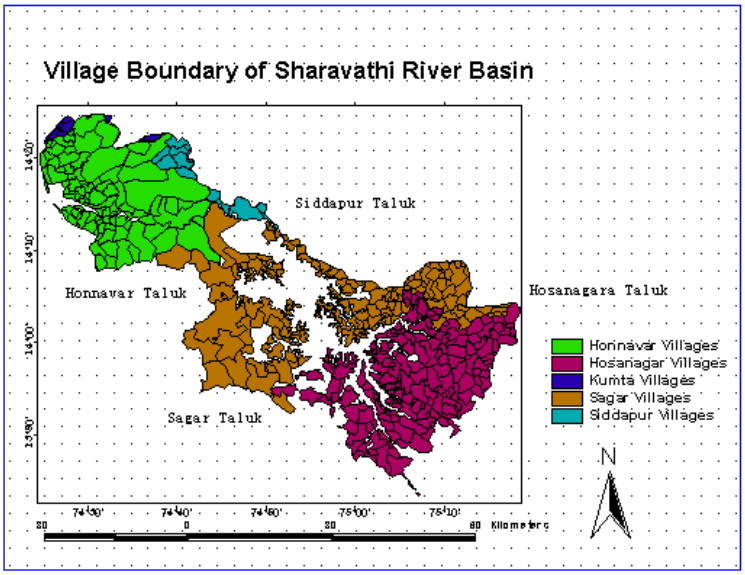

Fig 6.5: Village boundary of Sharavathi river basin

6.4 **Soil Characteristics**

Soil is the product of the weathering of rock and sediments. It is also referred as "relatively loose agglomerate of mineral and organic materials and sediments found above bedrock" (Holtz and Kovacs, 1981). The soils of the district are basically derivatives of Dharwar system - ancient metamorphic rocks in India; rich in iron and Mg. Exposed lateritic rocks along the coastal hills are very infertile and almost barren. During the last 15 years, most of these hills have been brought under forest plantation dominated by *Acacia auriculiformis*. The various types of soil existing in the study area are as shown in the soil characteristic map

in Figure 6.6. Soils are divided on the basis of certain properties as these play a vital role in deciding the susceptibility of a probable landslide. They are classified into three sizes—sand, silt and clay and possess certain specific properties, namely,

a) **Sandy texture soils:** The sandy group includes the sand and loamy sand soil textural classes. The soil is loose when dry and sand particles are plainly visible. It is not at all sticky when wet, but feels very gritty. It cannot be moulded or rolled into sausages. High proportions of fine sand can be identified by comparative lack of grittiness.
b) **Coarse loamy texture soils:** The coarse loamy group includes sandy loam and loam soil textural classes. The sand fraction is plainly visible when dry, but the soil is not so loose. When moist the soil feels very gritty between the fingers. It can just be moulded, but does not retain any impressed shape easily. It does not stick to the fingers very much and cannot be rolled into sausages..
c) **Fine loamy texture soils:** The fine loamy group includes silt, silt loam, sandy clay loam, clay loam, and silty clay loam textural classes. The sand fraction is more difficult to distinguish when dry. The soil is slightly gritty when moist. It moulds readily and retains impressed shapes. It sticks to the fingers slightly. It will roll into sausages with difficulty but the sausages will break up if an attempt is made to roll them to diameters less than 2 mm. Clay loam soil is rather hard when dry. It is distinctly sticky when wet. Only pressing the moist soil hard between the fingers can identify the sand fraction. It will roll into sausages with ease and the sausages will not break up so easily as loam as the diameter falls below 2 mm.
d) **Clayey texture soils:** The clayey group includes sandy clay, silty clay, and clay textural classes and shall be considered provisionally suitable with respect to texture. Clay soil is very hard when dry and very sticky when moist. It is very difficult to detect the sand fraction by pressing the moist soil between the fingers. The soil can be rolled easily into fine sausages of less than 2 mm diameter. The soil particles vary in shape from spherical to angular. They differ in size from gravel and sand to fine clay. Various types of soil and their composition can be seen tabulated in Table 6.2 below.

(http://www.dot.ca.gov/hq/oppd/hdm/pdf/chp0840.pdf).

Soil Class	Percent sand	Percent silt	Percent clay
Clean Sand	80-100	0-20	0-20
Sandy Loam	50-80	0-50	0-20
Loam	30-50	30-50	0-20
Clay Loam	20-50	20-50	20-30
Sandy Clay	50-70	0-20	30-50
Silty Clay	0-20	50-70	30-50
Clay	0-50	0-50	30-100

Table 6.2: Soil composition

Along with these physical compositions, soils also have diverse characteristics in their percentage inorganic composition, which also determines the stability and durability of the soil. The inorganic composition is shown in Table 6.3:

Type	SiO_2	Al_2O_3	Fe_2O_3	MnO	CaO	MgO	K_2O	Na_2O	P_2O_5
Sandy	91.72	2.92	2.36	-	0.35	0.78	0.33	0.08	0.08
Sandy loam	84.84	5.30	4.52-10.89	-	0.06-0.91	0.29-0.52	0.16-0.71	0.03	0.10-0.34
Loam	86.98	4.10	3.52-10.89	-	0.06-0.42	0.29-1.29	0.56-0.71	-	0.06-0.34
Silt loam	86.49	9.16	7.00	0.21	0.14	0.90	1.85	-	0.24
Clay	65.16	13.76	9.27	0.25	1.09-2.18	1.60-2.47	0.14-1.60	0.01	0.23

Table 6.3: Percentage inorganic composition of representative soil

Soil texture is a measure of how much sand, silt, and clay a particular type of soil contains. Soil texture is important because it determines the porosity and permeability *(i.e. how fast water drains through a soil and how much water a soil can hold)*. Slope and aspect affect the moisture and temperature of soil. Steep slopes facing the sun are warmer. Steep soils get eroded and lose their topsoil as they form. Sand is the largest size particle in soil that is 0.05-2 mm in diameter. Clay is less than 0.002 mm in diameter. Clay particles are extremely small, and can be seen only through an electron microscope.

Clay mineralogy along with soil texture is also important as the mineralogy of the clay-sized fraction determines the degree to which some soils swell when wet and thereby affect the size and number of pores available for movement of sewage effluent through the soil. There are two major types of clays, including the 1:1 clays, such as Kaolinite, which do not shrink or swell extensively when dried or made wet; and the 2:1 clays, including mixed mineralogy clays, such as clays containing both Kaolinite and Montmorillonite that shrink and swell when dried and made wet. The type of clay minerals in the clay-sized fraction are determined by a field evaluation of moist soil consistence or of wet soil consistence using Soil Taxonomy. The soils are examined for certain parameters, which are shown in Table 6.4.

Sr. no	Landslide Name	Soil Colour	pH	Bulk density g/cc	WHC %	K_2O kg/ha	Moisture%
1	Kauti	Red	5.3	1.96	35.27	46.4	25.74
2	Yellagadde	Brown sandy	4.8	2.02	14.54	45.1	13.86
3	Athavadi	Brown sandy	5.4	1.89	14.43	199.6	10.50
4	Belmakki	Red	5.5	1.89	29.47	14.2	28.98
5	Kapegi	Red	5.4	2.09	19.64	21.9	16.57
6	Suralli	Brown	5.6	1.99	34.00	12.9	19.36

7	Samse	Brown	6.0	2.12	31.37	15.5	24.61
8	Kalgalli	Red	5.5	1.93	23.86	106.9	22.49
9	Near Nittur	Brown	5.3	1.63	38.97	29.6	26.77
10	Nittur	Red	5.2	1.96	50.50	14.2	21.87
11	Tumri	Red	5.5	2.00	37.90	16.7	14.23
Range @			**4.5-6.0**	**1.63-2.12**	**14.0-50.0**	**12.0-200.0**	**10.0-30.0**

Table 6.4: Parameters of landslide soil analysis

Sandy, loamy and, sandy loam are well drained aerated and workable for most of the year. They are very light and have a very high organic matter content, prone to drying out too quickly, needing additional watering. Clay and clay loamy soils are difficult to work and manage. The main drawbacks are its high water holding capacity and the effort required to work with them i.e. more of porosity and permeability.

Sandy and sandy loamy soils can be identified as prone to landslides because the particle size is large and it contains lot of open spaces between and around the particles. They take up water readily and drain sharply. The slope in the existing area is high and soil is made of larger, gritty particles that do not stick together properly, which creates a probability of hazardous landslides. These two types of soil are imperfectly drained, with loose taxonomy as per its existence near the Arabian Sea. Water drains very slowly through clay soil. Therefore, clay soil remains saturated after a heavy rain. These soils exist in less sloppy area and are deep, well drained but with severe erosion. These clayey skeletal soils are basically gravelly clay; friable, shallow, lateritic layer starting at about 25 cm or lesser depth; being well drained and occurring on undulating to rolling terrain. These soils are moderately and largely stony in places but the study area is hard due to excess of stones, which properly holds the sliding area.

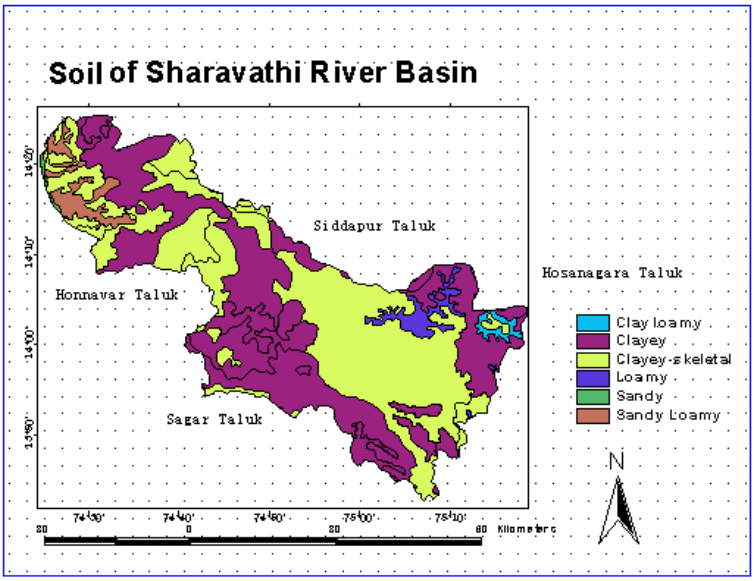

Fig 6.6: Soil of Sharavathi river basin

6.5 **Lithological Distribution:** The Sharavathi river basin belt is made up of various types of Schist, chiefly chloritic and in places micaceous or hornblendic, associated with volcanic rocks of different types. Along with them are found some highly altered sedimentary rocks such as quartzite, conglomerates, limestone, shale and banded ironstones (ferruginous quartzite). The factors of Lithology, which affect the occurrence of landslide, are:

1. Occurrence of fine-grained materials such as shale and unconsolidated alluvium.
2. Distribution of slope angles within a geological unit's outcrop area, affecting the susceptibility ranking of each unit.
3. Rocks rich in clay (montmorillonite, bentonite), mica, calcite, gypsum etc., which are promoters of weathering.
4. Geological structures i.e. occurrence of inclined bedding planes, joints, fault or shear zone are the planes of weakness, which create conditions of instability.

Undercutting along the hill slopes for laying roads or rail tracks can result in instability. Some parts of Uttar Kannada belong to an older group of sediments and intrusives, all very highly metamorphosed with a group of plutonic intrusive, is collectively termed as the *peninsula gneiss*. A capping of laterite, which is locally the source of iron, manganese ores and ocher, frequently overlies both. In detail the main types of rocks, which exist in the Sharavathi river basin area, are

a) **Metamorphic rocks**: These rocks are formed through the operation of various metamorphic processes on the pre-existing rocks involving either textural, structural or change in mineralogical composition. Metamorphic rocks are classified on the basis of texture of structure, degree of metamorphism, mineralogical composition and mode of origin.

   The main rocks of this type are:

   - Migmatites and granodiorite: Characterised as banded rocks consisting of alternating layers of quartz and feldspar of high metamorphic grade. They are banded or striped rocks with alternating layers of dark and light minerals. The dark layers commonly contain biotite, and the light layers commonly contain quartz and feldspar. Shale is the usual parent rock of gneiss. Granite is the parent rock of some gneiss.
   - Greywacke / argillite- is a severely hardened sandstone with mica and feldspar, sometimes containing fossils.
   - Meta grey wake argillite is a mudstone, hardened by pressure.
   - Amphibolitic metapelitic schist/ pelitic schist, calc-silicate rock - are foliated medium-grade metamorphic rocks with parallel layers, vertical to the direction of compaction.

- Quartz chlorite schist with orthoquartzite: metamorphic rock containing abundant obvious micas several millimetres across. Shale is the parent rock of schist.
- Quartzite: represents metamorphosed sandstone with its interlocking grains of quartz. The rock fractures through the grains (rather than between the grains as it does in sandstone). The parent rock is quartz sandstone.

b) **Plutonic rocks:** These are coarse-grained igneous rocks formed at considerable depths, generally between 7-10 km below the surface of earth where there is a very slow rate of cooling.
The main rocks under this are:
- Grey Granite - Granitic rock is much less common on the surfaces of other planets; a fact having to do with the fractionation (where early crystallising minerals separate from the rest of magma), a process that takes place uniquely on earth, due to the prevalence of plate tectonics.

c) **Residual Capping and Unconsolidated sediments:** It is the insoluble products of rock weathering, which have escaped erosion by geological agents and still cover the rock from which they have been derived.
The main rocks under this are: Laterite; Alluvium / beach sand, alluvial soil.

d) **Volcanic / Meta volcanic:** These are igneous rocks formed by the cooling and crystallisation of lava erupted from volcanoes on the surface of the earth.
The main rocks under these are:
- Metabasalt and tuff - (sometimes called greenstone if massive and green, or green schist if foliated and green) - the green colour comes from chlorite (soft and bluish green) and epidotic (pea green). The parent rock is basalt. The grade of metamorphism is very low.
- Metabasalt including thin ironstone.
- Meta basalt thin subardinate metarhyalite and associated metabasic intrusives.
- Amphibolitic metapelitic schist/ pelitic schist, calc-silicate rock: Abundant amphibole is present; may be lineated and subjected to higher temperatures and pressures than Metabasalt, greenstone, or green schist.

Since in the study area the type of rocks are diverse and need to be evaluated precisely, comparative study table for various types of rocks are prepared and the Lithological distribution map was prepared by digitising the geological toposheet, the map is detailed in Table 6.5 and Figure 6.7.

Rock	Compressive strength	Range of toughness	Abrasive hardness	Absorption by wt %	Porosity%	Weight kn/m^3
Igneous	34475 to 413700	7 to 28	37 to 98	0.07 to 0.30	0.4 to 3.84	25.45 to 27.02
Sedimentary	34475 to 137900	2 to 35	2 to 26	3 to 12	1.9 to 27.3	18.70 to 26.39
Metamorphic	110320 to 310275	5 to 30	6 to 42	0.10 to 2.00	1.5 to 2.9	25.92 to 26.71

Table 6.5: Comparative study table for various types of rocks

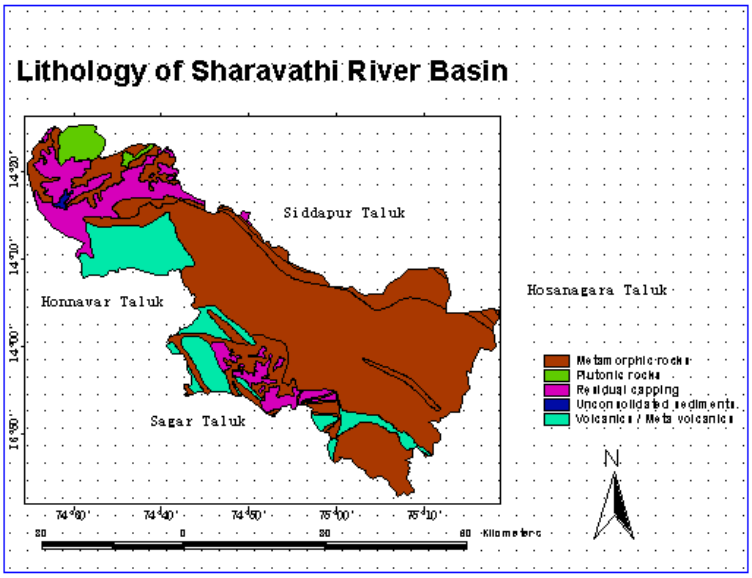

Fig 6.7: Lithology of Sharavathi river basin

6.6 **Structural Geological Analysis – Lineaments:** Where the discontinuity geometry permits sub vertical blocks to be separated from the rock mass through the jointing, movement towards the free face is common. Even where the dip of the base plane (bedding) is less than the natural slope, movement can still occur either by sliding due to the nature of the underlying material or by toppling if the sub vertical joints are opened. A rock plane failure occurs when a set of discontinuities lies parallel to the slope with an angle equal or lower than that of the natural slope. Their influence extends for some 3–5 m on either side of the fracture itself where they appear as a fragmented rock surface in the adjacent area or sheared/ crushed material at the intersection of two such lineaments. This disturbed material assists water infiltration, the lubrication of potential slide planes and the development of pore water pressures. The highest incidence of land sliding can be intercepted in areas where such a linear pattern is interpreted from satellite data in the form of lineaments as shown in Figure 6.8.

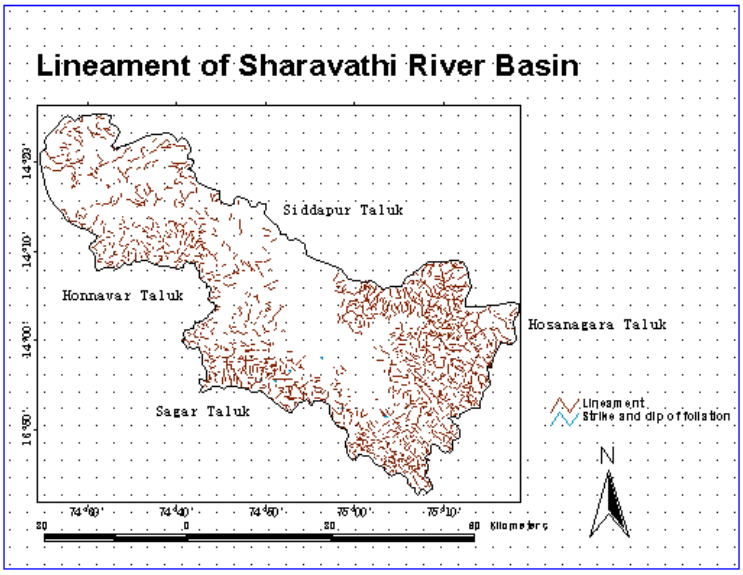

Fig 6.8: Lineament of Sharavathi river basin

Drainage - Sub Basin Analysis: Drainage characterisation is an important factor, which reflects the slope evolution of an area with an indication of the mass wasting and related erosional aspects. Zones with the parallel pattern of drainage associated with strong slope control are the most probable situations for mass movements/ landslides. Drainage is often a crucial measure due to the important role played by pore-water pressure in reducing shear strength. Because of its high stabilisation efficiency in relation to cost, drainage of surface water and groundwater is the most widely used, and generally the most successful stabilisation method. Deep drains that are trenches sunk into the ground to intersect the shear surface, extending below it achieve drainage of the failure surfaces. The drainage in the area is mainly dendritic drainage consisting of a network of channels resembling tree branches. The study area is divided into 16 sub-basins on the basis of major tributaries and existing drainages as shown in Figure 6.10. Areas underlain by nearly horizontal sedimentary rocks and some areas of igneous and metamorphic rocks commonly display dendritic drainage, where tributaries join larger channels at various angles as shown in Figure 6.9, the drainage map of the study area. Table 6.6 shown below gives the details of the sub basins' soil type and lithology.

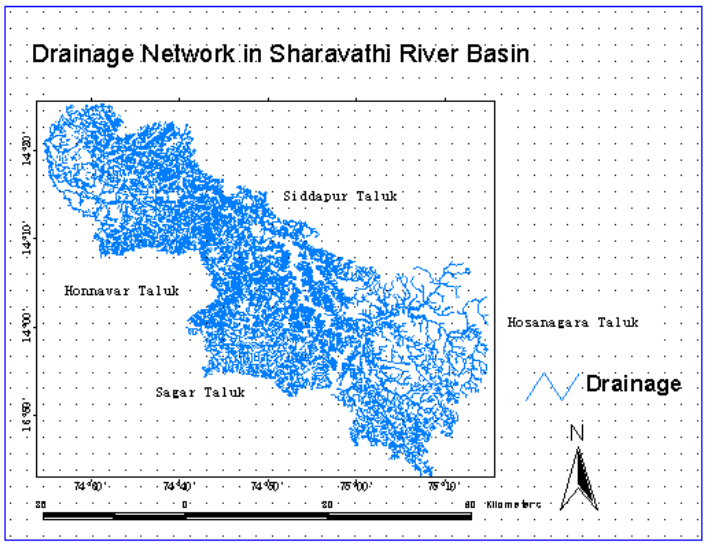

Fig 6.9: Drainage network in Sharavathi river basin

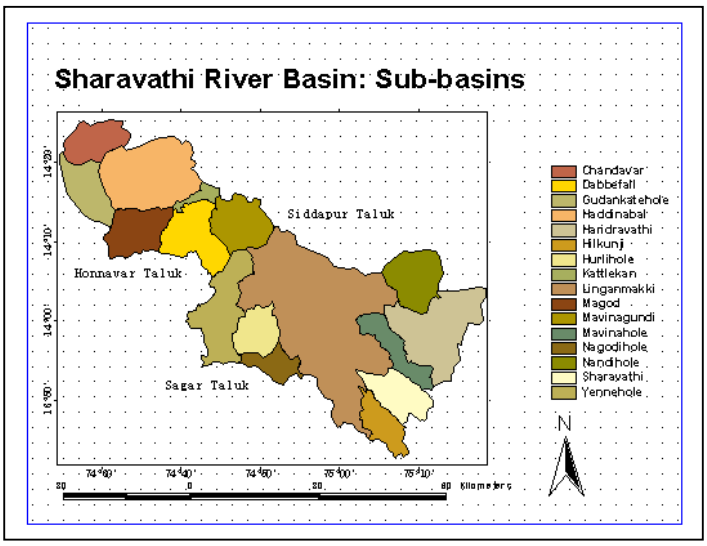

Fig 6.10: Sharavathi river basin: Sub-basins

Table 6.6: Sub-basin details

Sub Basin	Name	Soil Type	Lithology
DS1	Chandavar	Clayey, Clayey skeletal, Sandy loamy	Metamorphic rocks, Plutonic rocks
DS2	Haddinabal	Clayey, Clayey skeletal, Sandy loamy	Volcanic / Meta volcanic, Metamorphic rocks
DS3	Magod	Clayey, Clayey skeletal, Sandy loamy	Volcanic / Meta volcanic, Residual capping
DS4	Dabbefall	Clayey, Clayey skeletal	Metamorphic rocks, Volcanic / Meta volcanic
DS5	Mavinagundi	Clayey, Clayey skeletal	Metamorphic rocks, Residual capping
DS6	Kattlekan	Clayey, Clayey skeletal	Metamorphic rocks, Residual capping
DS7	Gudankateholé	Sandy, Sandy loamy, Clayey skeletal	Metamorphic rocks, Unconsolidated sediments
US1	Nandiholé	Clayey, Clayey skeletal, loamy	Metamorphic rocks
US2	Haridravathi	Clayey, Clayey skeletal, loamy, clay loamy	Metamorphic rocks
US3	Mavinaholé	Clayey skeletal	Metamorphic rocks
US4	Sharavathi	Clayey, Clayey skeletal	Metamorphic rocks, Volcanic / Meta volcanic
US5	Yenneholé	Clayey, Clayey skeletal	Metamorphic rocks, Residual capping
US6	Hurliholé	Clayey	Metamorphic rocks, Residual capping
US7	Nagodiholé	Clayey, Clayey skeletal	Metamorphic rocks, Residual capping
US8	Hilkunji	Clayey, Clayey skeletal	Metamorphic rocks
US9	Linganamakki	Clayey, Clayey skeletal, loamy	Metamorphic rocks, Volcanic / Meta volcanic

6.7 **Rainfall Analysis:** The Sharavathi river basin area receives high rainfall of more than 3000 mm and landslides occur when a high intensity rain follows a prolonged steady rainy season. This normally occurs during the middle phase of southwest monsoon or if the pre-monsoon is high in the initial phase in the month of August or September. A short duration of intense rainfall can be used to predict the likelihood of a landslide. It increases the groundwater level through either short, intense precipitation or prolonged rainfall of lower intensity. The monthly variations of rainfall at all the stations were evaluated to see the intensity of rainfall. For this, the average and standard deviation was calculated as shown in Figures 6.11. Rainfall exceeding 200 mm/day has been found to initiate catastrophic landslides in the Western Ghats area. The data in Table 6.7 of 21 years of 27 locations in the study area is considered as a base layer preparation theme for landslide analysis. The average rainfall data of the locations along with the map generated are shown in Figures 6.12 and 6.13.

Fig 6.11: Monthly variation of rainfall in sub-basins

Monthly variation of rainfall in upstream Sub Basin 1 (Nandiholé)

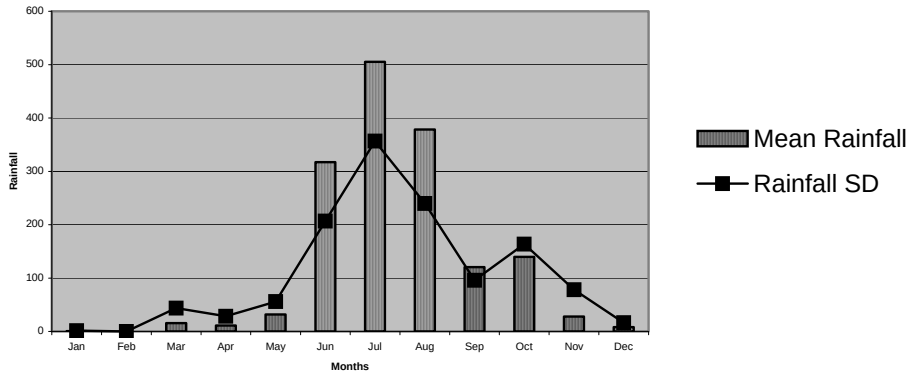

Monthly variation of rainfall in upstream Sub Basin 2 (Haridravathi)

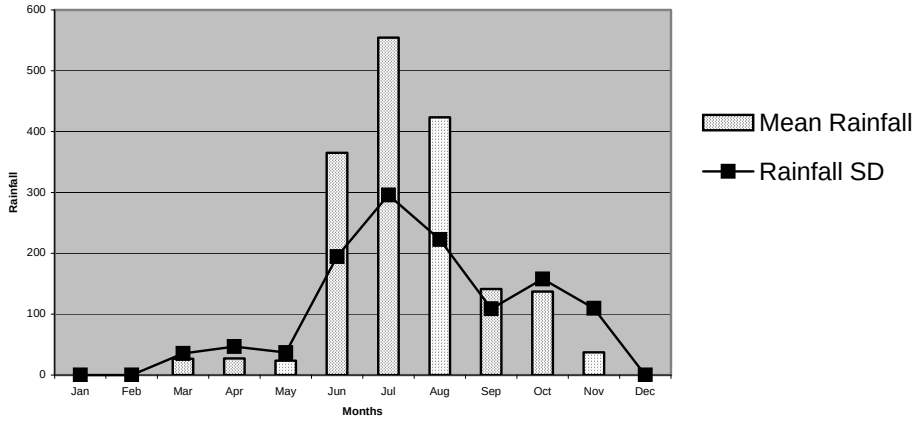

Monthly variation of rainfall in upstream Sub Basin 5 (Yenneholé)

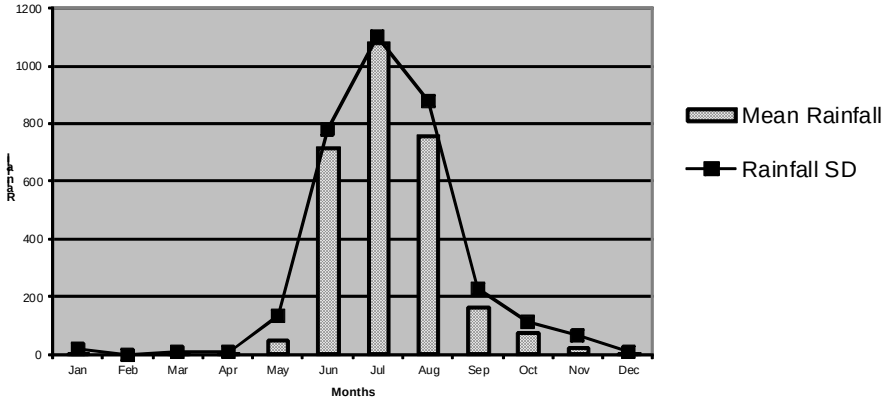

Monthly variation of rainfall in upstream Sub Basin 6 (Hurliholé)

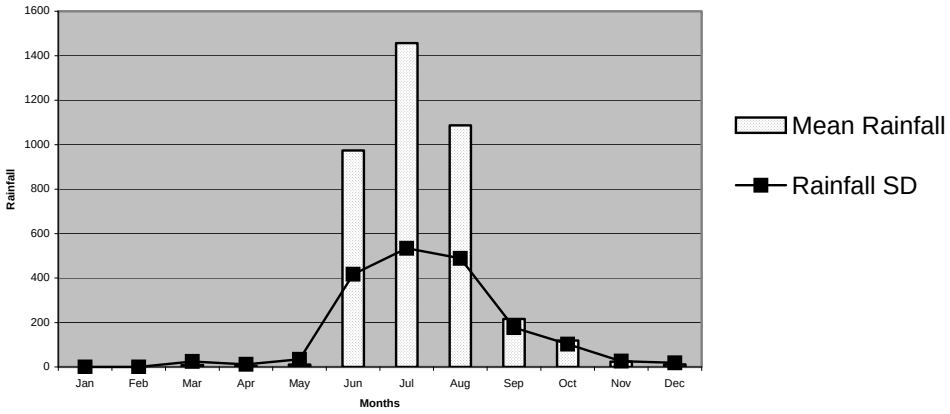

Monthly variation of rainfall in upstream Sub Basin 7 (Nagodiholé)

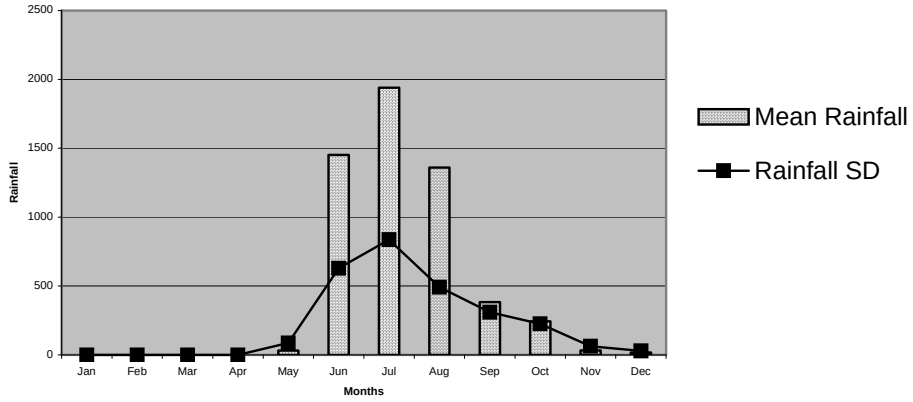

Monthly variation of rainfall in upstream Sub Basin 8 (Hilkunji)

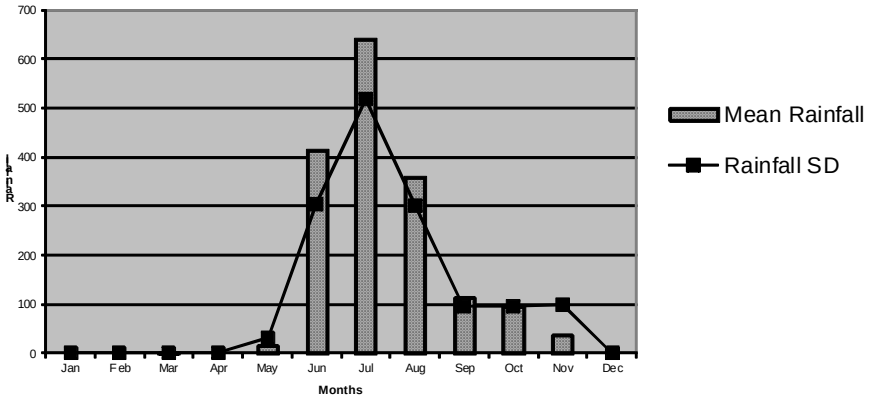

Monthly variation of rainfall in upstream Sub Basin 9 (Linganamakki)

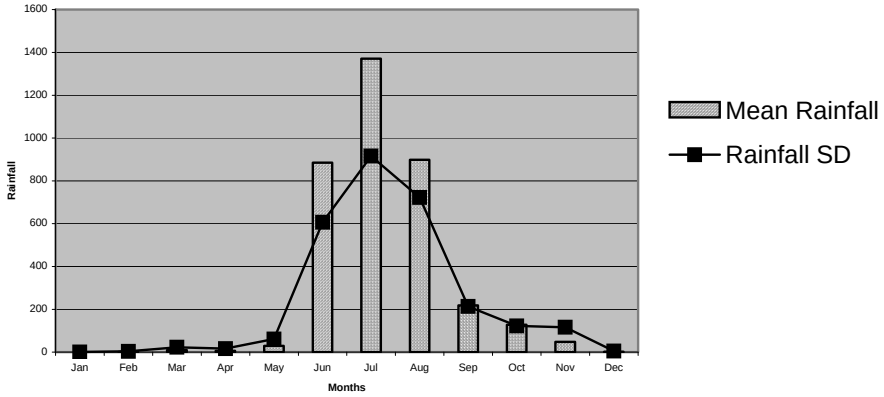

Monthly variation of rainfall in downstream Sub Basin 2 (Haddinabal)

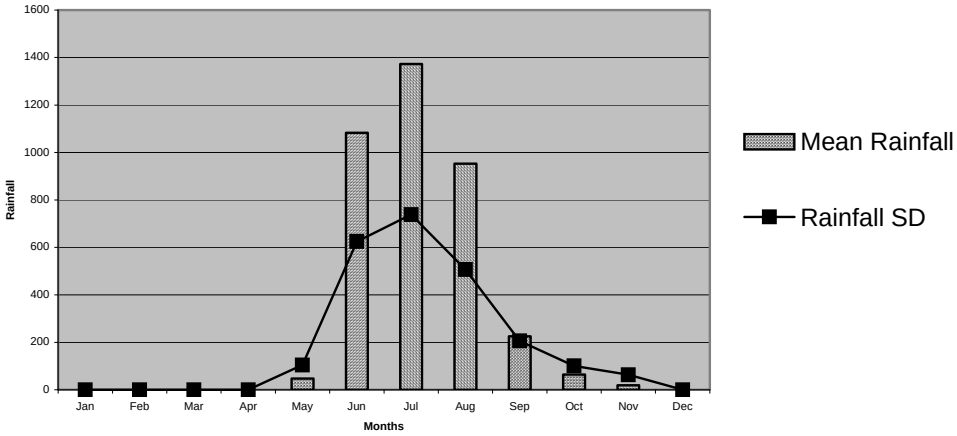

Monthly variation of rainfall in downstream Sub Basin 5 (Mavinagundi)

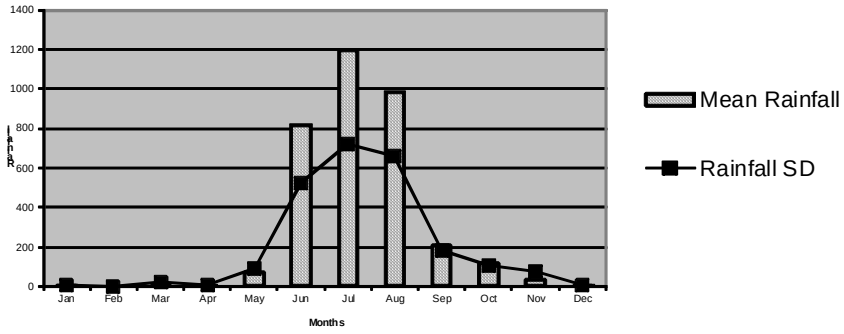

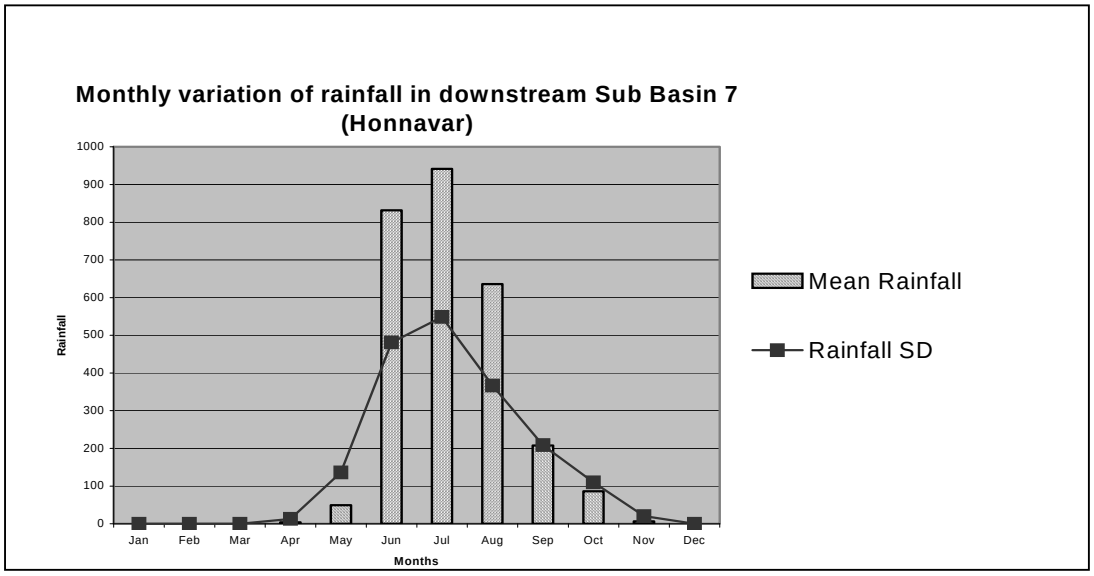

Table 6.7: Rainfall averages of sub-basin stations

Sub Basin	Rainfall Station	Average	Std. Dev	Cumm. Average	Cumm. Std. Dev
US1	Anandapuram	1706.58571	461.5981	**1503.35**	**±798.78**
	Battemallappa	1546.09524	1137.395		
	Ulloru	1257.39524	797.3731		
US2	Rippanapate	1347.44762	482.459	**1675.03**	**±689.81**
	Arasalu	2002.61905	689.8127		
US5	Aralagodu	4682.65714	1070.998	**2830.85**	**±1035.64**
	Kogar	6219.98095	1143.34		
	Kaarani	276.195238	1265.686		
	Biligaaru	144.585714	662.575		
US6	Byakodu	4324.89524	1160.166	**3879.40**	**±937.66**
	Tumari	3433.91429	715.1738		
US7	Nagodi	5693.6	1279.73	**5693.6**	**±1279.73**
US8	Koduru	1638.92857	1115.03	**1638.92**	**±1115.02**
US9	Genasinakuni	1584.7	1014.937	**3546.39**	**±1455.87**
	Sagar	1730.0381	638.4296		
	Nagara	4801.25238	1075.84		
	Chakranagar	5378.65238	1570.547		
	Nilskal	4850.47619	2863.244		
	Mattikai	3669.78095	2097.127		
	Hosanagara	2809.87619	931.0309		
DS2	Gerusoppa	3736.32857	1825.549	**3736.32**	**±1825.54**
DS5	Mavinagundi	263.195238	1206.112	**3374.87**	**±872.26**
	Linganamakki	3436.99048	552.7307		
	Kargal	4144.32381	891.2878		
	Talakalale	4116.33333	598.9735		
	A.B. Site	4913.51429	1112.203		
DS7	Honnavar	2736.60476	1418.18	**2736.60**	**±1418.18**

Fig 6.12: Graphical representation of rainfall averages

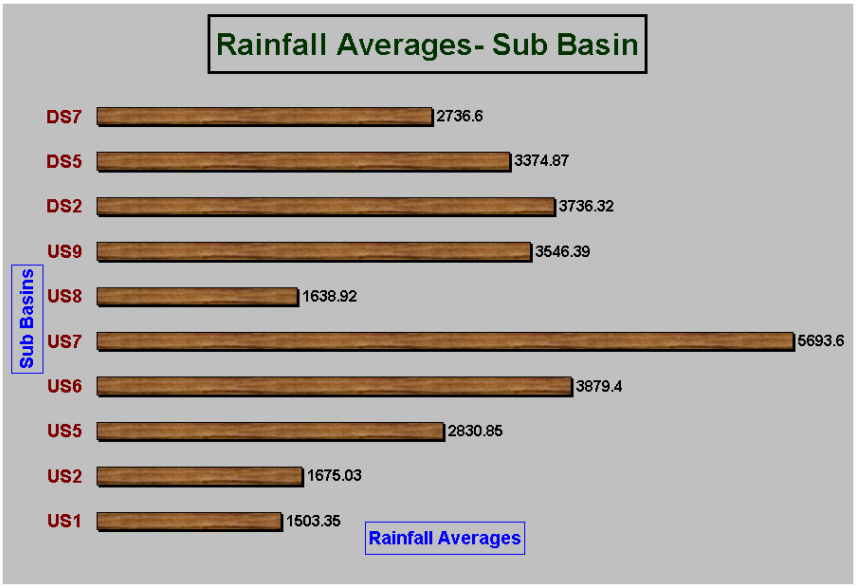

Fig 6.13: Rainfall stations in Sharavathi river basin

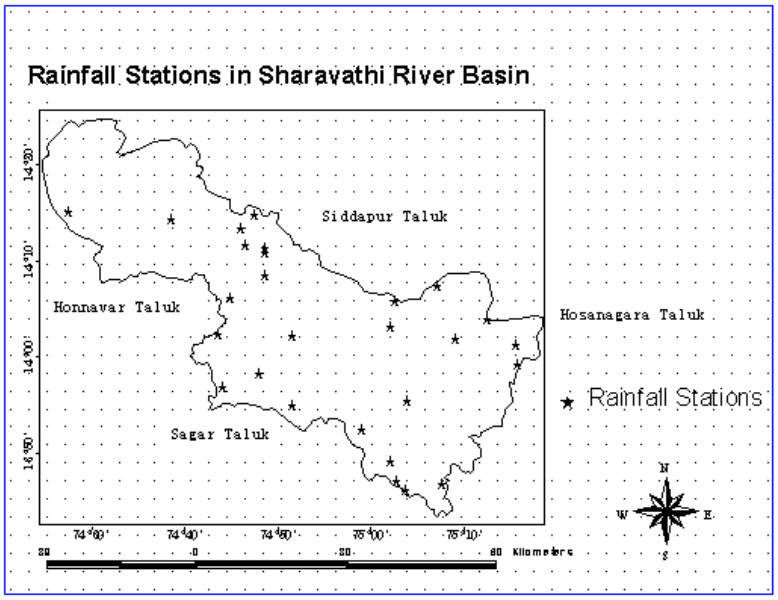

7. REMOTE SENSING DATA ANALYSIS

7.1 Land Cover Analysis - Computation of Normalised Difference Vegetation Indices (NDVI)

Land cover analysis was done using Normalised Difference Vegetation Index (NDVI) that helps in identifying observed physical cover including vegetation (natural or planted) and has an ability to minimise topographic effects while producing a linear measurement scale. NDVI has been computed depending on the extent of the vegetation in a region for the land cover analysis. This is mainly for regions with good vegetation i.e. western and southeast part of the study area where soil reflection is very less because of dense canopy covers.

NDVI is mainly based on the combinations of visible red and near infrared bands and are widely used to generate vegetation Indices. It was computed based on data grabbed by space borne sensors in the range 0.6-0.7 (red band) and 0.7-0.9 (NIR band), which help in delineating vegetation and non-vegetation areas. It is an index derived from reflectance measurements in the red and infrared portions of the electromagnetic spectrum to describe the relative amount of green biomass from one area to the next. The values, which are seen range from –1 to 1, where non-existence is shown at –1 and existence is shown at 1. The values indicate both the status and abundance of green vegetation cover and biomass. This is computed using the algorithm of

$$NDVI = (IR-R) / (IR+R)$$

It is generally seen that:

- High near-infrared reflectance and low visible reflectance yield high values in vegetated areas.
- Features like water and clouds yield negative index values since they have larger visible reflectance than near-infrared reflectance.
- Vegetation indices are seen near zero for rock and bare soil areas since they have similar reflectance in the two bands.

The NDVI image generated for the study area is shown in Figure 7.1 below.

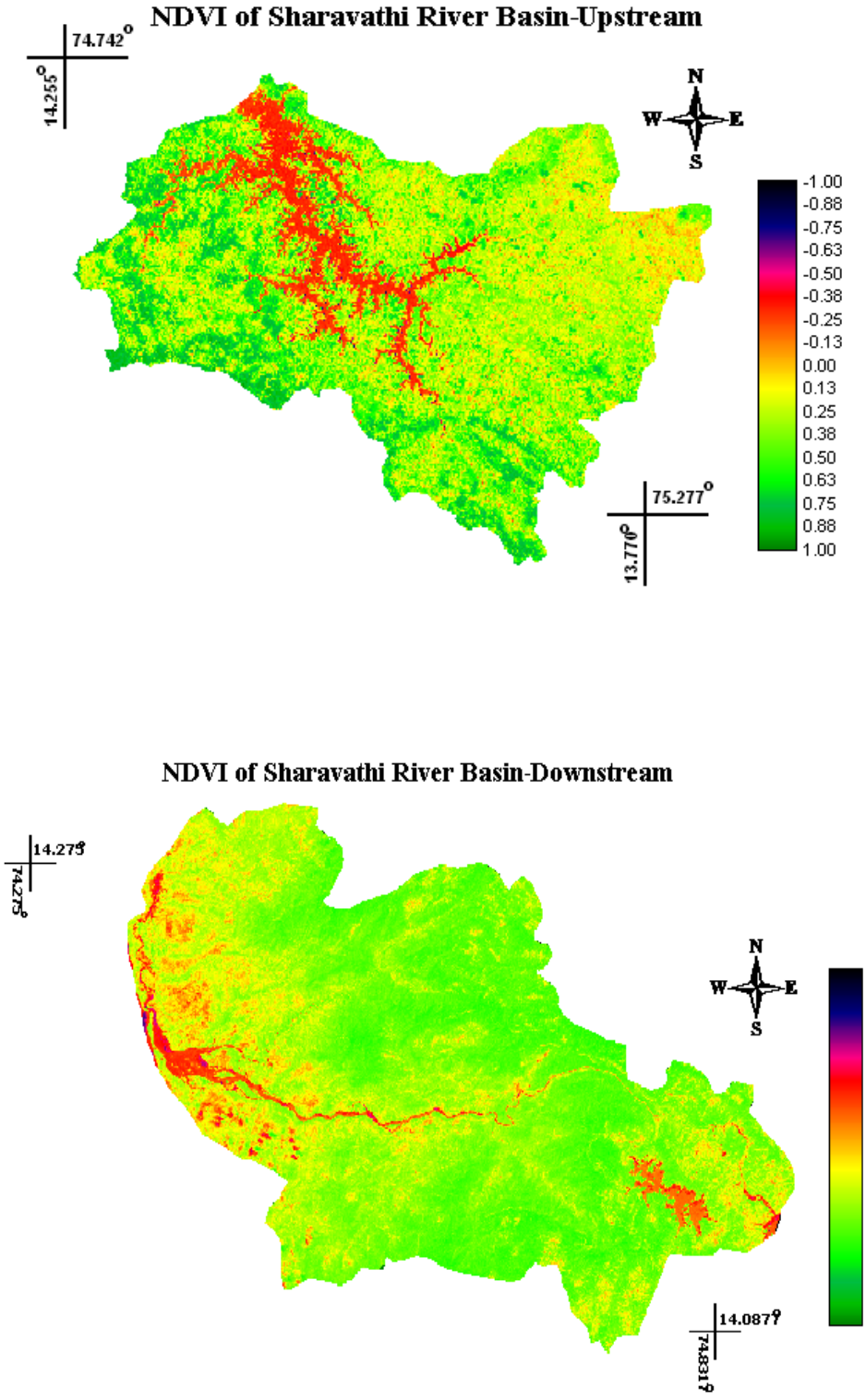

Fig 7.1: NDVI of Sharavathi river basin

7.2 Land Use Analysis - Supervised Classification

- **Data used**: IRS 1D LISS III – MSS Data was used for land cover, land use analyses. Satellite imageries of Path 97 - Row 63, provide the entire image of Sharavathi catchment region. LISS (corresponding to 0.5-0.6, 0.6-0.7, 0.7-0.9 μm of electromagnetic spectrum or Green, Red and NIR bands) sensor data was used for the analysis.
- **Geometric correction**: The existing bands were geometrically corrected taking the known points' latitude and longitude values from the image and the existing accurate corresponding ground values existing in Survey of India toposheets and Ground Control Points taken from field using GPS. Resampling of the images was done considering the polynomial model because it uses polynomial coefficients to map between image spaces. The projection for raw satellite imagery used was UTM and to do that, first order polynomial is normally good and was taken. The GCP tool references for images were taken from toposheets. The image obtained after this was re-sampled with these points to get the correct image.
- **Field data**: Field data, which was uniformly distributed all over the basin, was collected using GPS over the entire basin so as to represent all land use categories . This helped in considering all spectral classes constituting each information class for adequate representation in the training set statistics used to classify an image. The test areas are taken as prototype of representative areas and they are located during the training stage of supervised classification by intentionally designating more training areas than that which was actually needed to develop the classification statistics.
- **Vegetation classification**: Data regarding trees were noted down in quadrants of 20 x 20 m^2, which mainly contain trees species; density and canopy cover along with the GPS value.

Supervised classification requires more input and experience by the analyst but it can produce more accurate and useful results than unsupervised classification. The strategy is to identify homogenous, representative samples of the different land cover types of interest. These samples are called *training areas.* The selection of appropriate training areas is based on the analyst's familiarity with the area and it is ideally supported by reliable ancillary sources, such as aerial photos, maps, or other *ground truth* data. The spectral information in all spectral bands for the pixels comprising these training areas is used to recognise spectrally similar areas for each class. The computer uses a special algorithm (of which there are several variations) to determine "the *spectral signatures"* for each training class, although there are a number of different algorithms available for performing supervised classification. If the classification is accurate, the resulting classes represent the categories within the data that the user originally identified. Thus, in a supervised classification we are first

identifying the information classes, which are then used to determine the spectral classes, which represent them. In supervised training, it is important to have a set of desired classes in mind, and then create the appropriate signatures from the data. The various types of algorithms, which are used in supervised classification, include: Maximum likelihood, Mahalanobis distance and minimum distance. *Maximum likelihood decision rule is based on the probability that a pixel belongs to a particular class. The basic equation assumes that these probabilities are equal for all classes, and that the input bands have normal distributions.*

- **Maximum likelihood supervised classifier**: In comparison with various classification algorithms, maximum likelihood classification approach has higher accuracy. Maximum likelihood classification is a supervised classification for which training sites were selected and sufficient training data and Ground Control Points (GCP) were used. Accurate mapping or inventory of natural resources requires ground control points (GCP), which are necessary to fit details extracted from satellite images. Based on the training data collected in the field, remote sensing data was classified in the land use pattern of built up areas (open rocky area, buildings, etc.), evergreen to semi evergreen forest, moist deciduous forest, plantation (acacia + areca), agricultural areas, open area (barren area, open uncultivated agriculture land, dry grasslands, dry river bed, etc.) and waterbodies.
- **Accuracy assessment**: The overall objective of the training process is to assemble a set of statistics that describe the spectral response pattern for each land cover type to be classified in an image. Two of the most commonly employed approaches are as follows.
    - Homogeneous test areas selected by the analyst.
    - Test pixels or areas selected randomly.

This requires substantial reference data and a thorough knowledge of the geographic area. Most importantly, the quality of the training process determines the success of the classification stage and, therefore, the value of the information generated from the classification. The recognising pixel that represents the classes that has been extracted is shown in Figure 7.2 below.

Fig 7.2: Landuse of Sharavathi River Basin

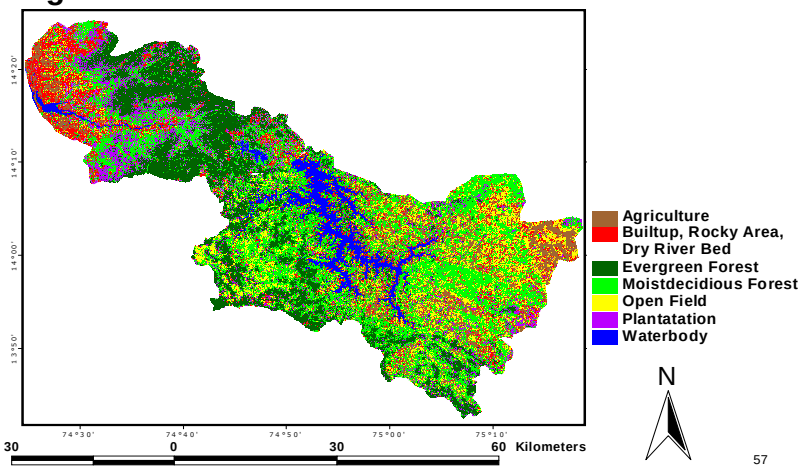

57

8. LANDSLIDE PRONE ZONE MAPPING

In order to do landslide prone zone mapping, suitable map layers along with attribute tables were considered necessary for inclusion in the GIS. Giving relative weightages of susceptibility to the classified objects of these maps, weights' map is prepared that also incorporated image processing techniques. Weight value for landslide susceptibility is calculated from the landslide density of each class of each control factor category. This helped in the division of the entire study area in various zones of hazard classes as per the weight assigned for various classes. The various layers, which were finally used for assigning weights for ranking, are as follows.

1. Slope
2. Aspect
3. Landuse/ Landcover
4. N.D.V.I image i.e. vegetation
5. Geology i.e. Lithological distribution
6. Soil characteristics
7. Drainage density
8. Lineament density
9. Road density
10. Rainfall intensity

The parameters are prioritised based on the hazard potential i.e. higher the ranking higher is the area prone to landslide. The study area is divided into zones of landslide vulnerability viz., very high, high, very moderate, moderate, poor and very poor. The landslide magnitude definition says that the rankings, which are given to various factors, are.

- Rank 1 (Very Poor): No damage to infrastructure because of low-lying areas.
- Rank 2 (Poor): Injury, burial or death of people is likely.
- Rank 3 (Very Moderate): Destruction of smaller trees, powerlines, damage to houses possible, and removal of roadways are likely.
- Rank 4 (Moderate): Destruction of large trees, and burial of small houses possible.
- Rank 5(High): Destruction of large infrastructure, and derailment of trains likely.
- Rank 6(Very High): Destruction and burial to multiple infrastructures, parts of towns and villages.

8.1 Ranking of Study Area based on Slope, Land Use, and other GIS Database

The study area is ranked on various parameters discussed earlier considering the sub basin clusters as a base and weights are calculated on the ranking basis, which is as follows:

a) Slope: The slope map of the study area was derived from the contours and Digital elevation model, as explained in the methodology. The slopes of the study area are defined at an interval of 10 degrees as shown in Figure 8.1 below.

Fig 8.1: Slope -Sharavathi river basin

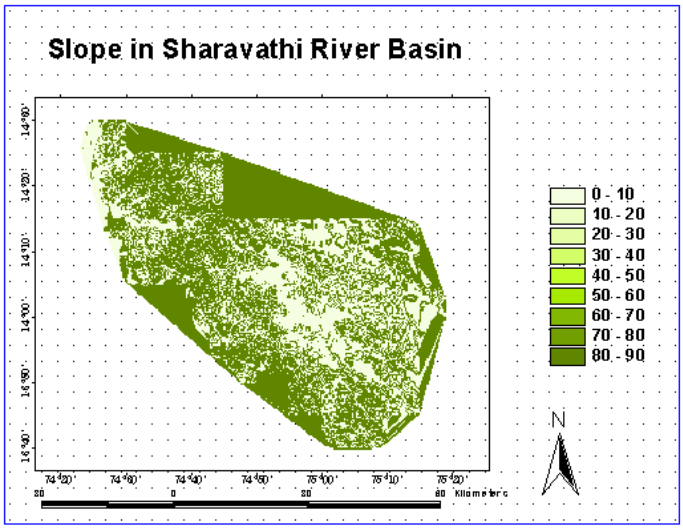

Slope is a very important parameter in any landslide hazard zonation mapping. In the study area slope varies from 0 to 60 degrees. If the slope is higher, then there is a chance of occurrence of landslide. The final ranking is done on the basis of the amount of existence of high sloping in a cluster and weight values are given to slope parameters using Table 8.1 and map was prepared.

Table 8.1: Criteria for ranking terrain based on Slope

Sr. No	Slope value	Rank
1	0-10°	1
2	10-20°	2
3	20-30°	3
4	30-40°	4
5	40-50°	5
6	>50°	6

As the terrain is undulating, each sub basin has heterogeneous slopes. Hence, the cumulative weights were calculated based on the share of each slope range in a cluster for each sub basin. The final ranking was computed based on cumulative weights as

listed in Table 8.2. Based on this, the slope-ranking map for the river basin was generated and is given in Figure 8.2.

Cumulative Values	Weights
1-1.2	1
1.2-1.4	2
1.4-1.6	3
1.6-1.8	4
1.8-2.5	5

Table 8.2: Cumulative weights of Slope

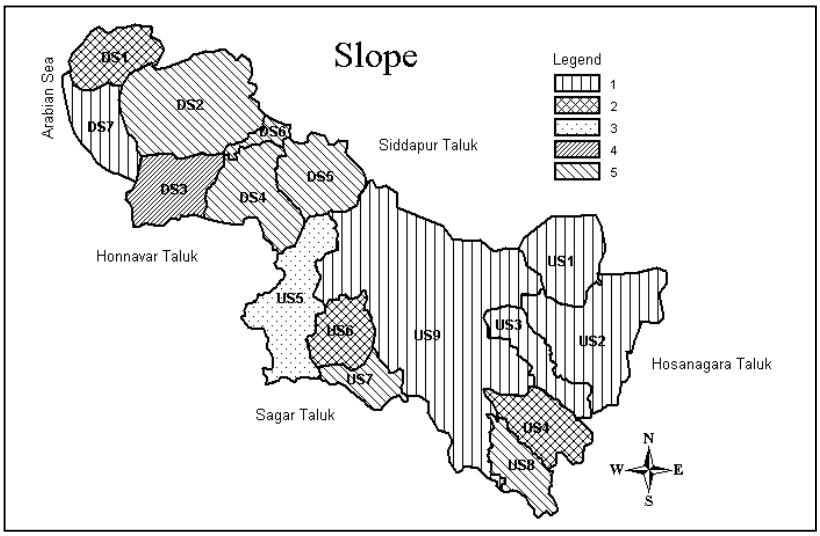

Fig 8.2: Ranking based on Slope

b) Aspect: The aspect is the direction in which the maximum slope exists. This is used to determine the direction of downhill faces in the line of steepest descent. Aspects are output in decimal degrees and use standard azimuth designations from north. In regions where the surface is perfectly flat with slope = 0, aspect is assigned a value of flat terrain. All the sides of the slope were assigned the value of its present existence, which is shown in Figure 8.3 below.

Fig 8.3: Aspect of Sharavathi river basin

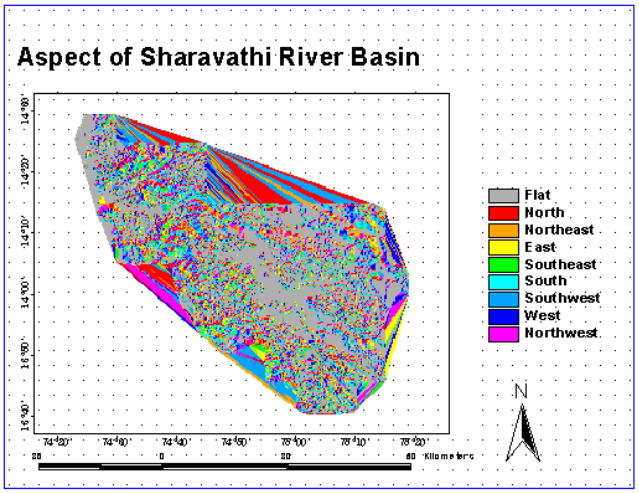

Aspect is also one of the important phenomena, which alters the existence of landslide. To monitor this, as the southwest area is having sea and wind blowing from that side, which could affect landslide generation, aspect map was prepared as shown in Figure 8.4 and map was created taking the ranking values shown in Table 8.3.

Table 8.3: Criteria for ranking terrain based on Aspect

Sr. No	Aspect	Rank
1	North or East	1
2	North West	2
3	West	3
4	South East	4
5	South	5
6	South west	6

Fig 8.4: Ranking based on Aspect

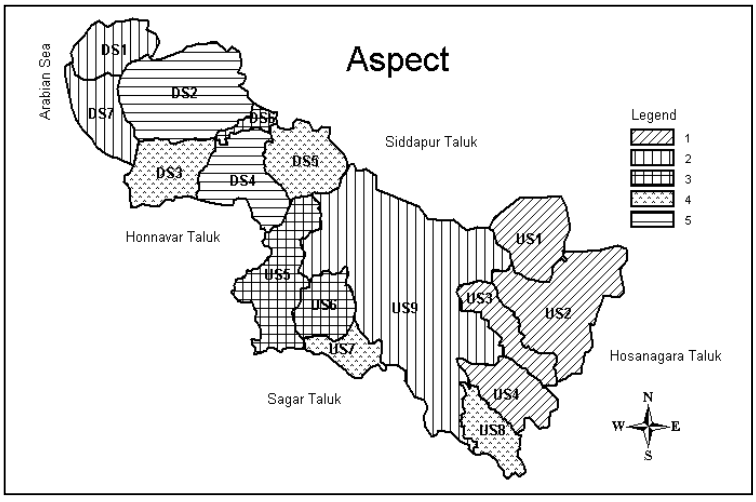

c) Landuse/ Landcover: The remote sensing data (MSS data) of the study area was classified by supervised classification approach using maximum likelihood classifier. The types of classification falling in various sub basins on the basis of their area existing in that was used to calculate the susceptibility for landslide. The ranks given in Table 8.4 were used and maps generated for the same is shown in Figure 8.5.

Sr. No	Landuse type	Rank
1	Built up	1
2	Water	2
3	Evergreen forest	3
4	Moist deciduous forest	4
5	Plantation	5
6	Agriculture	6
7	Open area	7

Table 8.4: Criteria for ranking based on Land use

Classified image indicate that each sub-basin has different level / extent of land use. Hence, based on the extent of each type and on ranking for each category, a composite ranking is derived for each sub-basin as given in the Table 8.5 below. This takes into account susceptibility for landslide by each category and its spread in each sub-basin.

Table 8.5: Cumulative weights of Land use

Cumulative Values	Weights
3.25-3.5	1
3.5-3.75	2
3.75-4.0	3
4.0-4.25	4
4.25-4.5	5
4.5-5.0	6

Fig 8.5: Ranking based on Land use

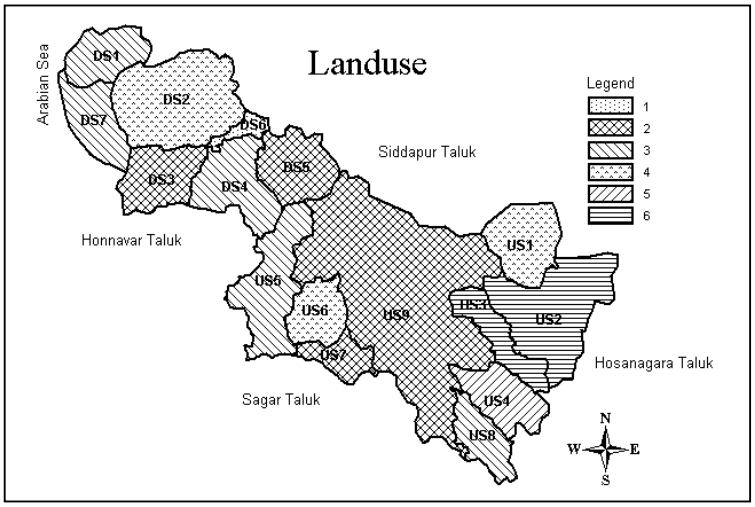

d) N.D.V.I image: N.D.V.I was computed for the study area reflecting the amount of vegetation lying in a particular sub basin. NDVI values normally range from –1 to +1. Values greater than 0 show vegetation and the range indicate extent of canopy cover / vegetation in the region. Higher values reflect good canopy cover or good vegetation. The amount and extent of each range of NDVI for each sub basin was evaluated using their value given in Table 8.6 and depicted pictorially in Figure 8.6.

Table 8.6: Criteria for ranking terrain based on NDVI ranges

Sr. No	Vegetation range	Rank
1	> -0.4	5
2	-0.4 to 0	4
3	0 to 0.2	3
4	0.2 to 0.4	2
5	> 0.4	1

Fig 8.6: Ranking based on NDVI

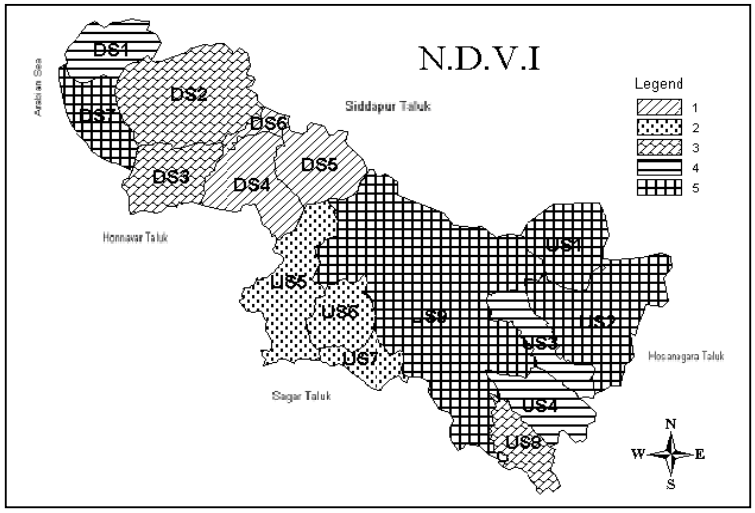

e) Lithological distribution: An important aspect is the existence of rocks, for instance, when the underlying bedrock is porous due to the presence of sandstone or some volcanic-formed rock, it drains faster. Impermeable bedrock, such as granite, keeps water in the soil. Over the time, excess water is transferred down to the water table or to stream channels, and some is stored for future use by plants. Bedrock type can also determine slide potential. Some rocks, such as shale and volcanic-formed rocks weather to form sticky clay soils. Sandstones, granites, and micas wear down into coarse porous soils that are easily moved. In the study area, the existing rock types are classified on

their various properties with the rank ranging 4-5 due to lot of lineaments crack, water content, thin soft week beds. The existing landslide is also taken into consideration to decide the stability of the existing rocks. For the hardened rocks, which rank lowly, i.e. 3, it is mainly due to existing of major river and dam areas with lots of water percolation and seepage. The area with laterite also faces mining and excavation, which loosens that rock type. And lastly for high ranking i.e. 2 and 1, the factors considered are high weathering, high permeability, and presence of unconsolidated and weak material in lesser quantity. Existence of Metabasalt or basalt is mainly due to its hardness with less weathering and no seepage of water due to absence of layering. The rankings are shown in Table 8.7.

Table 8.7: Criteria for ranking based on Lithology

Sr. No	Lithology	Rank
1	Amphibolitic metapelitic schist/ pelitic schist, calc-silicate rock	4
2	Greywacke / argillite	4
3	Meta grey wake argillite	4
4	Quartz chlorite schist with orthoquartzite	4
5	Laterite	3
6	Migmatites and granodiorite - tonalitic gneiss	3
7	Grey granite	2
8	Meta basalt thin subardinate metarhyalite & assosiated metabasic intrusives	2
9	Metabasalt & tuff	2
10	Metabasalt including thin iron stone	2
11	Quartzite	2
12	Alluvium / beach sand, alluvial soil	1

Investigation of lithology of the Sharavathi river basin shows that each sub basin has heterogeneous lithological features. In view of this, depending on share of lithological features in each sub basin, a composite ranking is derived based on weighted averages as shown in Table 8.8 and the map is given in Figure 8.7.

Table 8.8: Cumulative weights of Lithology

Cumulative Values	Weights
2.0-2.50	1
2.50-3.0	2
3.0-3.5	3
3.5-4.0	4

Fig 8.7: Ranking based on Lithology

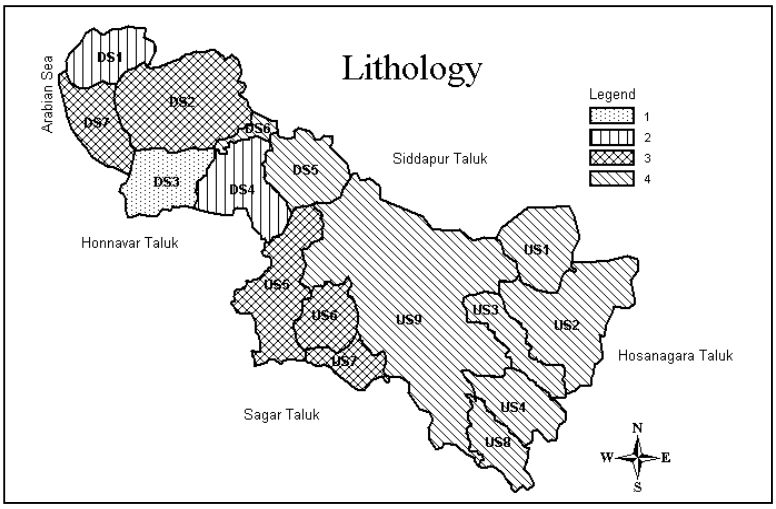

f) Soil types: In the study area, occurrence of landslide is mainly found due to the presence of huge thickness of loose soils when mixed with water near the Sharavathi river area. As discussed earlier, the ranking is mainly done keeping the water holding capacity, bulk density, porosity and permeability of the soil in concern. The area of a certain soil falling in a sub basin with other soils helps in determining the prone area of the sub basin for landslide. The ranking Table 8.9 and map generated for the same in Figure 8.8 are as follows.

Table 8.9: Criteria for ranking terrain based on Soil

Sr.	Soil	Rank
1	Clayey	6
2	Clay loamy	5
3	Clayey-skeletal	4
4	Loamy	3
5	Sandy loamy	2
6	Sandy	1

Cumulative values were evaluated through the relevance of the lithological map as soil types vary with the type in cluster so the percentage area was calculated for various types to calculate the weights for the map as is shown in Table 8.10.

Table 8.10: Cumulative weights of Soil

Cumulative Values	Weights
2.5-3.0	1
3.0-3.5	2
3.5-4.0	3
4.0-4.5	4
4.5-5.0	5
5.0-6.0	6

Fig 8.8: Ranking based on Soil

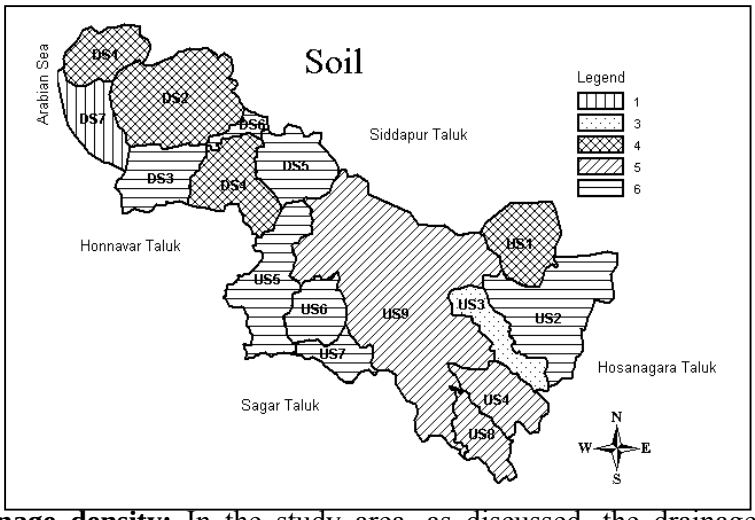

g) Drainage density: In the study area, as discussed, the drainage is mainly dendritic, where the density was computed by using the area in square kilometre of individual sub basins and number of drains falling in that area. This is mainly done to see the dependence of the type of drain on the involvement of water in percolation. The first order drains have various aspects in their drainage with respect to the third order due to lesser water flow and percolation. The drainage density also decides the susceptibility for landslides. The ranking shown in Table 8.11, which was considered in making the map for drainage density as shown in Figure 8.9, is as follows.

Table 8.11: Criteria for ranking based on Drainage density

Sr. No	Drainage density	Rank
1	0-1.0	1
2	1.0-2.0	2
3	2.0-3.0	3
4	3.0-4.0	4
5	4.0-5.0	5
6	>5.0	6

Fig 8.9: Ranking based on Drainage density

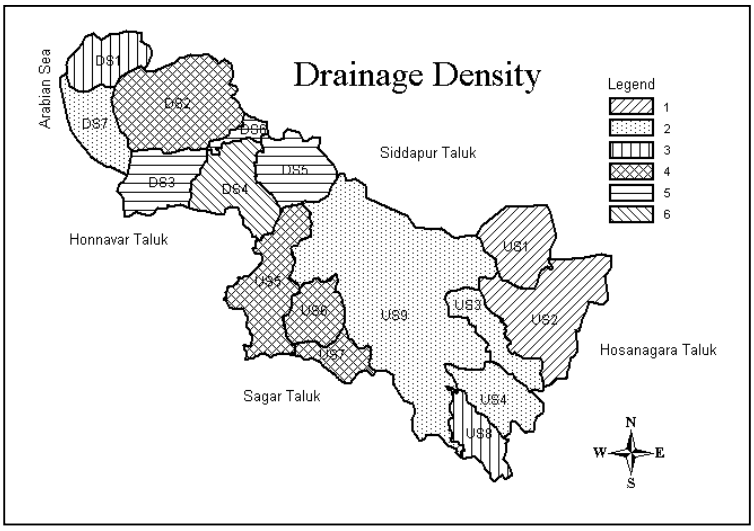

h) Lineament density: As discussed earlier, the influence of landslide lies on 3–5 m on either side of the fracture itself where they appear as a fragmented rock surface in the adjacent area or sheared/crushed material at the intersection of two such lineaments. To evaluate the amount of effects the lineaments impart on landslide, the density was calculated similar to the calculation of drainage density. The ranking criteria based on the density are given in Table 8.12 and the same for each sub basin is shown pictorially in Figure 8.10.

Table 8.12: Criteria for ranking based on Lineament density

Sr. No	Lineament density	Rank
1	0-0.25	1
2	0.25-0.5	2
3	0.5-0.75	3
4	0.75-1.0	4
5	1.0-1.25	5
6	1.25-1.50	6

Fig 8.10: Ranking based on Lineament density

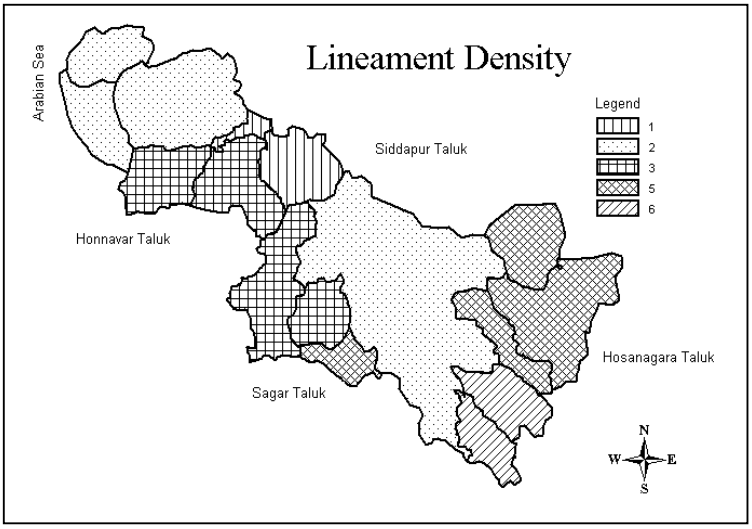

i) Road density: The areas close to the existing roads in an undulating terrain are more prone for landslide as they are built across the toe of hills and have removed the support. The criteria tables for ranking, which was used, and map generated are shown in Table 8.13 and Figure 8.11 respectively.

Table 8.13: Criteria for ranking terrain based on Road density

Sr. No	Road density	Rank
1	0-0.25	1
2	0.25-0.5	2
3	0.5-0.75	3
4	0.75-1.0	4
5	1.0-1.25	5
6	1.25-1.50	6

Fig 8.11: Ranking based on Road density

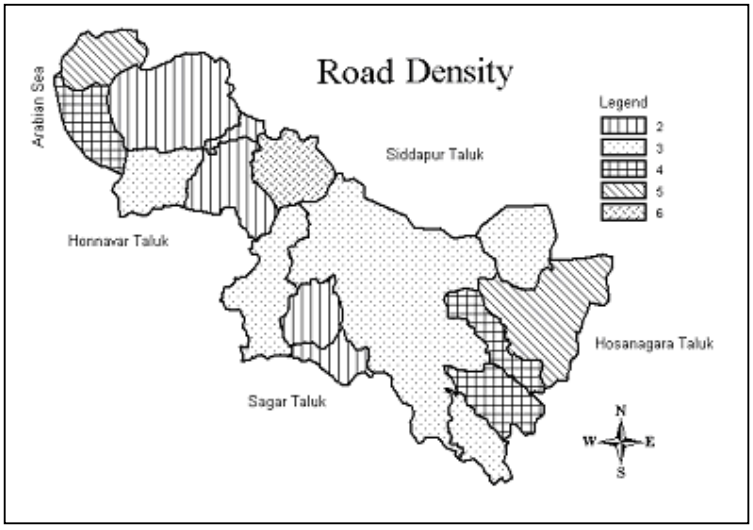

j) Rainfall: The relationship between rainfall and landslides aids in the understanding of the landslide processes and also provides a basis for predicting widespread slope failures. Heavy antecedent rainfall or a short duration of intense rainfall triggers most of the landslides. The ranking as shown in Table 8.14 and the map 8.12 created on the basis of amount of rainfall occurred at 27 locations in various sub basins is as follows.

Table 8.14: Criteria for ranking terrain based on Rainfall

Sr. No	Rainfall	Rank
1	0-2000 mm	1
2	2000-3000 mm	2
3	3000-3500 mm	3
4	3500-3750 mm	4
5	>3750 mm	5

Fig 8.12: Ranking based on rainfall

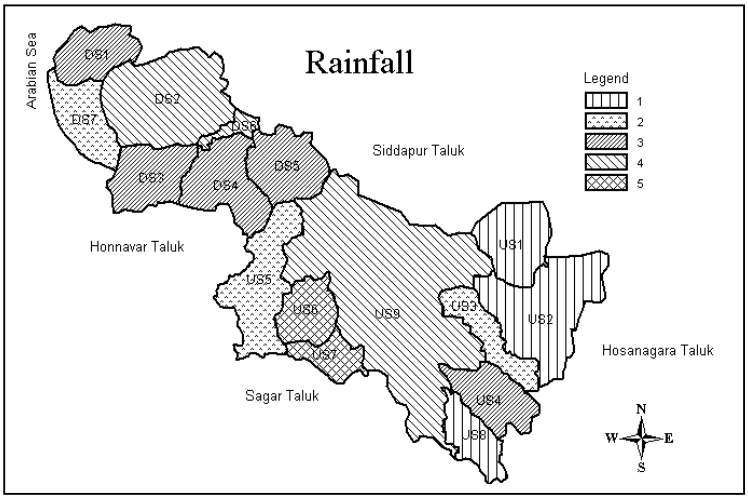

8.2 Resultant Layers Creation- Overlaying

In order to map landslide susceptibility zones in the river basin, considering various causal factors discussed so far, a composite map is generated in GIS by overlaying all causal factor-ranking layers. Higher weights indicate the sub-basin's susceptibility for landslides. Percentage share of each sub basin's weights is computed and are given in the Table 8.15. Values greater than 65.353 % or cumulative weights of 32.6765 were considered to confer the sub-basins' susceptibility to landslides.

Table 8.15: Final ranking values of factors in all Sub-basins

Sub-basin	Aspect	NDVI	Drainage	Landuse	Lineament	Road	Lithology	Slope	Soil	Rain	Sum	% Share
DS7	2	5	2	3.76	2	4	3.12	1.12	2.95	2	**27.95**	55.9
US1	1	5	1	4.15	5	3	4	1.05	4.5	1	**29.70**	59.4
US9	2	5	2	3.7	2	3	3.75	1.15	4.7	4	**31.30**	62.6
US3	1	4	2	4.62	5	4	4	1.1	4	2	**31.72**	63.44
US5	3	2	4	3.94	3	3	3.25	1.47	5.6	2	**31.26**	63.44
DS1	2	4	3	3.79	2	5	2.69	1.32	4.5	3	**31.30**	62.6
DS6	3	1	5	3.44	1	2	3.52	1.99	5.4	4	**30.35**	60.7
US2	1	5	1	4.93	5	5	4	1.05	5.3	1	**33.28**	66.56
US4	1	4	2	4.39	6	4	3.66	1.2	5	3	**34.25**	68.5
DS3	4	3	5	3.57	3	3	2.05	1.77	5.1	3	**33.49**	66.98
US6	3	2	4	4.12	3	2	3.32	1.37	6	5	**33.81**	67.62
DS2	5	3	5	4.15	2	2	3.16	1.97	4.2	4	**34.48**	68.96
US7	4	2	4	3.68	5	2	3.18	1.9	5.8	5	**36.56**	73.12
US8	4	3	3	3.98	6	3	4	2	5	1	**34.98**	69.96
DS4	5	1	6	3.97	3	2	2.94	1.97	4.2	3	**33.08**	66.16
DS5	4	1	5	3.57	1	6	3.98	2.1	5.2	3	**34.85**	69.7
Ranks	**5**	**5**	**6**	**5**	**6**	**6**	**4**	**2**	**6**	**5**	**50.00**	
										Maximum		**73.12**
										Minimum		**55.9**
										Average		**65.353**

The sub basins were grouped into landslide susceptibility zones on the basis of their weights of all causal factors. The zones prone for landslide are classified into 6 zones from very high to very poor based on the relative share of causal factors. Within susceptible sub-basins, considering slope and aspect, data regions were identified that are prone to landslides. This was also compared with the field data of existing landslides. The landslide prone zones with regions of higher susceptibility are depicted in Figure 8.13.

Fig 8.13: Landslide Prone Zones in Sharavathi River Basin

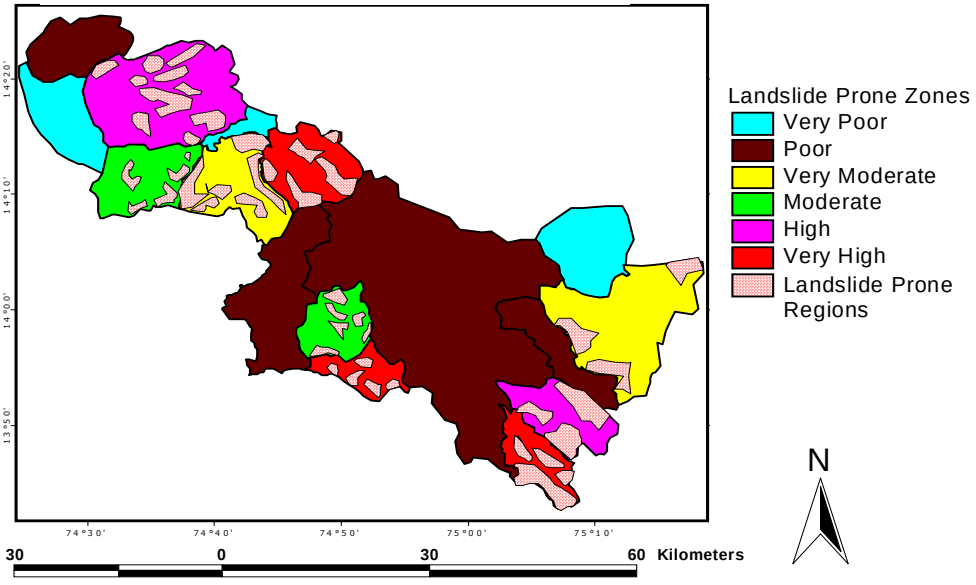

8.3 Data Analysis

In order to understand the role of various causal factors on landslide in a region, parametric analysis was carried out. Field data of landslides is overlaid on the landslide zonation map as shown in Figure 8.14, and corresponding attribute values for the respective field points were derived from the map and listed in Table 8.16.

Regression analysis of each causal factors (as independent variable) and landslide proneness as dependent variable did not reveal any significant relationship (at $p < 0.05$). In order to understand cumulative effects, stepwise regression was carried out and the probable relationship is given by:

LS= -1.05801- (0.345238797) S + (0.204210801) L + (0.646266454) RD + (0.615561311) L D – (0.089156743) DD + (0.07793196) R +(1.888490458) A - (1.49700461) Sl – (0.00015434) Lu – (0.296976094) N

R = correlation coefficient = 0.5948, standard error of y estimate= 1.008

Where dependent causal factors are: LS= Landslide Susceptibility, S= Soil, L=Lithology, RD= Road Density, LD= Lineament Density, DD= Drainage Density, R= Rainfall, A= Aspect, Sl= Slope, Lu= Landuse and N= NDVI.

Table 8.16: Ranking of landslide variables for analysis

Landslide	Landslide Group	Soil	Lithology	Road density	Lineament density	Drainage density	Rainfall	Aspect	Slope	Landuse	NDVI
1	4	2	3	5	2	3	3	2	2	7	3
2	3	2	3	5	2	3	3	2	2	1	3
3	4	4	3	5	2	3	3	2	2	6	3
4	3	4	3	5	2	3	3	2	2	5	2
5	3	4	4	4	2	2	2	2	1	6	3
6	5	4	4	4	2	2	2	2	1	1	3
7	5	4	4	4	2	2	2	2	1	7	3
8	3	4	1	4	2	2	2	2	1	1	3
9	3	4	1	4	2	2	2	2	1	1	3
10	3	4	1	4	2	2	2	2	1	5	3
11	3	2	3	4	2	2	2	2	1	6	3
12	3	2	3	4	2	2	2	2	1	6	4
13	4	2	3	4	2	2	2	2	1	7	2
14	2	2	2	3	3	5	3	4	4	7	2
15	1	4	2	3	3	5	3	4	4	1	3
16	3	4	4	2	2	5	4	5	5	1	2
17	2	4	4	2	2	5	4	5	5	5	1
18	2	4	4	2	2	5	4	5	5	5	1
19	1	6	4	6	1	5	3	4	5	3	1
20	5	4	2	2	3	6	3	5	5	3	1
21	3	4	4	2	3	6	3	5	5	3	1
22	1	6	4	6	1	5	3	4	5	4	2
23	2	6	4	6	1	5	3	4	5	5	1
24	3	4	4	3	3	4	2	3	3	4	2
25	2	6	4	2	3	4	4	3	2	4	3
26	3	6	4	2	3	4	4	3	2	4	3
27	2	6	2	2	3	4	4	3	2	3	2
28	2	6	4	3	2	2	4	2	1	1	2
29	3	6	4	3	2	2	4	2	1	1	2
30	3	6	4	3	2	2	4	2	1	3	2
31	2	6	4	3	2	2	4	2	1	5	2
32	5	4	4	3	2	2	4	2	1	5	3
33	2	4	4	3	2	2	4	2	1	1	3
34	2	6	4	2	5	4	5	4	5	4	2
35	1	6	4	2	5	4	5	4	5	7	3
36	2	6	4	3	2	2	4	2	1	4	2
37	1	4	4	3	3	4	2	3	3	4	2

Fig 8.14: Landslide Prone Zones with Existing Landslides in Sharavathi River Basin

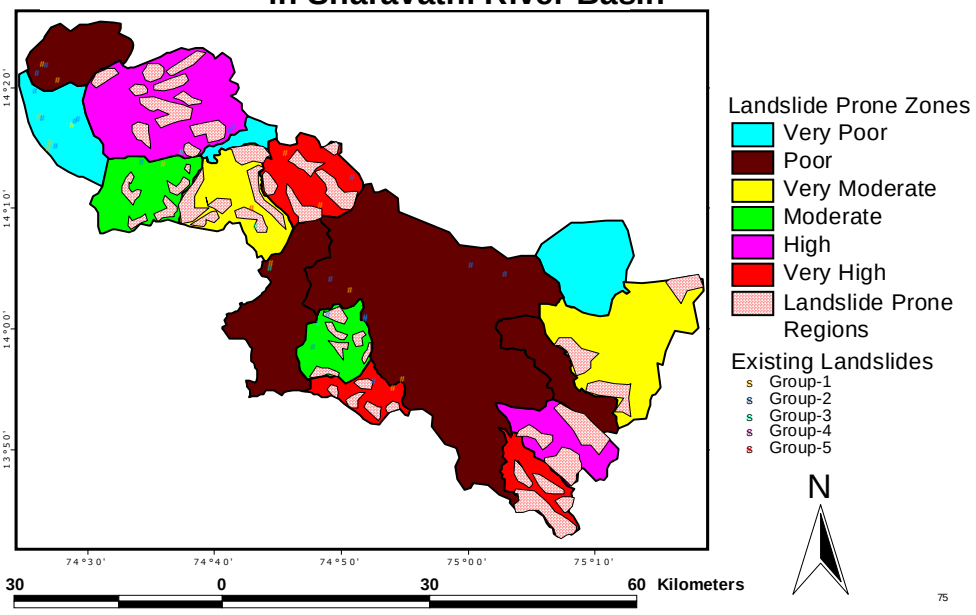

8.4 Socio-Economic Analysis of Highly Sensitive Landslide Areas

Landslide tampers the landscape and disturbs the habitats of flora and fauna. It severely degrades the environment and declines the quality of life for many people. Landslides have incapacitating effect on the economy and generally the people in the lower economic strata are affected the most, as they are economically ill and cannot cope with the disruption of life due to this natural hazard. Socio-economic survey was carried out while doing the field survey for existing landslide areas and the problems people face due to landslides were enumerated after evaluating the landslide prone areas as per the village boundary and population of 1991 census. The villages with the population that would be affected due to landslide are shown in Table 8.17. Proper remedial/corrective measures and preventive actions can be implemented at this stage so that impact can be minimised and distortions due to this are less and controllable.

Table 8.17: Village and population affected due to landslides

SR. NO	VILLAGE NAME	AREA IN HECTARE	TOTAL POPULATION	POPULATION DENSITY NO /HECTARE	PER CAPITA AGRICULTURE LAND IN HECTARE
1	PAVINKURVE	183.32	1031	5.62	0.06
2	KARKI	1149.18	5429	4.72	0.05
3	MALLAPUR	56.75	261	4.60	0.60
4	CHANDAVAR	2134.16	2881	1.35	0.02
5	HOSAKULI	574.19	2767	4.82	0.01
6	DUGGUR	142.67	297	2.08	0.21
7	KADLE	822.11	1605	1.95	0.04
8	NILKOD	688.04	806	1.17	0.28
9	VANDOOR	375.23	925	2.47	0.41
10	MAVINKURVE	657.54	3335	5.07	0.00
11	HADINBAL	383.57	2156	5.62	0.06
12	MUTTA	244.12	1065	4.36	0.07
13	GUNDABALA	937.86	1112	1.19	0.03
14	JANKADKAL	3374.11	731	0.22	0.18
15	SARALGI	685.29	1285	1.88	0.26
16	HULEGAR	565.39	362	0.64	0.01
17	KASARKOD	391.23	6719	17.17	0.00
18	NAGODI	2566.83	1963	0.76	0.10
19	VARAMBALLI	422.48	456	1.08	0.27
20	DEVARASALIKE	68.58	45	0.66	0.26
21	KALLUVIDIABBIGALLA	1252.34	447	0.36	0.18
22	BILLODI	352.01	320	0.91	0.34
23	TOGARE	1199.65	623	0.52	0.21
24	HONNEBYLU	1106.56	934	0.84	0.22
25	ANEGADDE	359.46	235	0.65	0.25
26	SONALE	931.19	1064	1.14	0.24
27	ADAVALLI	115.77	90	0.78	0.32
28	KOLAGI	628.16	459	0.73	0.27
29	KODASE	865.90	248	0.29	0.27
30	SAVANTHUR	671.66	569	0.85	0.24
31	RYAVE	1572.41	702	0.45	0.22
32	HILUKUNGI	930.98	323	0.35	0.14
33	HIRIYOGI	181.66	245	1.35	0.19
34	THNNIVE	842.77	893	1.06	0.15
35	RAMACHANDRAPURA	489.93	606	1.24	0.13
36	NELLUNDE	210.38	159	0.76	0.09
37	BELUR	1716.26	662	0.39	0.22
38	MUMBARU	1054.58	1122	1.06	0.21
39	URALAGALLU	3194.56	118	0.04	0.82
40	KANURU	1702.84	275	0.16	0.24
41	KANAPAGARU	3056.32	659	0.22	0.24
42	MARATI	2100.86	784	0.37	0.19
43	VALUR	1035.03	165	0.16	1.25
44	ADAGALALE	960.35	424	0.44	0.32
45	KODANAVALLI	2448.55	782	0.32	0.17
46	MARUTHIPURA	787.68	765	0.97	0.12
47	KODUR	844.5	1296	1.50	0.01
48	HIREMAITHE	802.99	635	0.79	0.02
49	ALAVALI	1211.99	683	0.563	0.06

After evaluating the socio economic aspects, the following points were evaluated for the study area:

- 51518 persons reside in the areas/villages, which are prone to landslides.
- The 12 villages having higher average density of population can be affected more due to this natural hazard, and the average population density is 1.841.
- Total area of villages falling under landslide prone zone is 490 square kilometres.
- Among all the villages, 64 % of area falls in forest and the remaining 36% is the area where the people reside in and use for their needs.
- In the villages, per capita agriculture land on an average is 0.22, which reflects the vital role played by agriculture in their lives.
- Some existing landslide occurrences is due to anthropogenic activities i.e. diversion of streams for increase of agriculture area or for better irrigation.
- Total literacy in the area is roughly around 55%.
- Since the literacy rate is high, it is important to tell them about the hazardous impacts and how they can be avoided.

9. RESULTS AND DISCUSSION

The landslide prone zone mapping of Sharavathi river basin reveals that sub basins, namely, Haddinabal (DS2), Magod (DS3), Dabbefall (DS4), Mavinagundi (DS5), Haridravathi (US2), Sharavathi (US4), Hurliholé (US6), Nagodiholé (US7) and Hilkunji (US8) show higher probability of landslide occurrence, mainly due to the following aspects:

- Heavy rain in particular months would cause enough erosive force to erode significant bank areas along meanders (which have relatively poor vegetation cover) and trigger highly prone slope failures.
- The establishment of reservoirs has ushered a change in the flow regime of the streams, leading to higher susceptibility for slope failures and consequent damages in the downstream of the Sharavathi river basin.
- With the inherent fragility of the terrain, the slides may occur due to high precipitation and the existence of reservoirs, which enhance the pore-water pressure beyond the threshold limits.
- Sub basins, which are found prone to landslide, are in undulating terrains.
- Laterite, which is locally the source of iron and manganese ores and ocher, lie in all the downstream and coastal areas and is generally extracted for mining and construction use. These disturbed laterite slopes may slide as the prone areas have abundance of this Lithological unit.

- The sub basins in the study area, which are identified as prone are having close proximity of lineaments that render some areas more vulnerable to hazards.
- Slopes are high in the identified sub basins and may fail if disturbed, i.e. highly prone for landslides due to any human disturbance that is likely to affect the equilibrium.
- It is seen clearly that the study area is having an abundance of road network and due to it's the presence of hilly terrain, new tracks are being laid to reduce the discomfort of circuitous routes. These creations of new tracks in hilly area or through mountains have led to imbalances in the terrain.
- In addition to these, anthropogenic activities like diversion of streams, encroachment of valley for areca plantations and agriculture are aggravating landslide proneness.

Remedial Measures

This hazard can be avoided through implementing protective measures considering delicately positioned properties of the study area as follows:

- To minimise any future slope failure the construction of the road should be at a properly planned position and haphazard road constructions must be avoided.
- Planting vegetation or maintaining slope terraces can also reduce slope-runoff so regulating the amount of vegetation clearing reduces the risk of increasing the number of landslide-prone areas.
- In view of recurring danger to life and property, an appropriate management strategy should be adopted to prevent diversion of streams, deforestation, conversion of hilly areas for plantation and agricultural activities. This would minimise landslides and mass failures.
- Construction of establishments without considering past or estimated peak flow stages may cause extensive damage to property that can be avoided by proper planning.
- Any disturbance that would contribute to deforestation must be avoided. This may fail slope in an above normal monsoon year.
- Socio economic survey reveals that the literacy rate is high in the area and the local residents must be made aware of the consequences of landslide hazards and the causal factors that aggravate the situation due to unplanned anthropogenic activities.

10. CONCLUSION

As per the landslide prone zone mapping, slides may occur due to infiltration of water in the unconsolidated material due to reservoirs and toe cutting of the hilly area for developmental activities.

The study area with heavy rainfall of more than 4500 mm and instances of high intensity rainfall, which not only increases the surface flow in river basin but also induces a high piezometric head in the unsorted colluvium of clayey soil and metamorphic rocks. The area of study is having an abundance of wet surface due to heavy rainfall and surface water. The stability of the wet surface further reduces because of the existence of clayey soil due to its low porosity and permeability. Geological existence of metamorphic rocks along the lineament features increases hydrostatic pressures on the existing unconsolidated material, which trigger down slope movement.

In the study area it is found that the slope excavation is mainly done in order to develop residential sites or build roads on sloping terrain as the area is having completely forested hilly terrain full and as a result now some slopes are much steeper than the pre-existing natural slopes. The added weight of fill placed on slopes can also result in an area prone for landslide hazards. Small landslides are common along roads, in either the road cut or the road fill. During the field visit it was found that most of the existing landslides are near the roads. Road associated landslides are good indicators of the potential impacts of excavation on new construction.

12. REFERENCES

- Abhishankar, K (1975) Gazetteer of India, Karnataka state gazetteer, Shimoga district, Government of Karnataka Publication, Bangalore
- Akgun A, Serhat Dag S, and Bulut F (2007) Landslide susceptibility mapping for a landslide-prone area (Findikli, NE of Turkey) by likelihood-frequency ratio and weighted linear combination models. Environ Geol. doi:10.1007/s00254-007-0882-8
- Alca´ntara-Ayala, I., 2002. Geomorphology, natural hazards, vulnerability and prevention of natural disasters in developing countries. Geomorphology 47 (2–4), 107– 124.
- Anbalagan R, 1992. Landslide hazard evaluation and zonation mapping in mountainous terrain. Eng Geol 32, pp. 269–277.
- Atkinson, P.M., Massari, R., 1998. Generalized linear modelling of landslide susceptibility in the central Apennines, Italy. Computers & Geosciences 24, 373–385.

- Bernard W.P and Trent D.D, 2001. Geology and the Environment, Brooks/Cole, Pacific Grove, USA. pp.269
- Cannon, S.H., 2000. Debris flow response of southern California watersheds burned by wildfire. In: Wieczorec, G.F., Naeser, N.D. (Eds.), Debris Flow Hazards Mitigation: Mechanics, Prediction and Assessment. Balkema, Rotterdam, pp. 45– 52.
- Clerici A, Perego S, Tellini C, Vescovi P (2002) A procedure for landslide susceptibility zonation by the conditional analysis method. Geomorphology 48:349–364.
- Cooke R., Doornkamp,J., 1990.Geomorphology in Environmental Management: A New Introduction, Oxford Univ. Press, Oxford.
- *D. O'Leary, J. Friedman and H. Pohn, 1976. Lineament, linear, lineation: some proposed new standards for old terms, Geological Society of America Bulletin 87, pp. 1463–1469*
- Dai, F.C., Lee, C.F., 2001. Terrain-based mapping of landslide susceptibility using a geographical information system: a case study. Canadian Geotechnical Journal 38, 911 – 923.
- Das, B.K. (1981) District census handbook: Shimoga district, Census of India 1981 series 9: Karnataka Government Press, Bangalore.
- Das, B.K. (1981) District census handbook: Uttara Kannada district, Census of India 1981 series 9: Karnataka Government Press, Bangalore.
- David F. Maune (2001) Digital elevation model technologies and applications: the DTM users manual, ASPRS, Maryland
- Derruau M., 1983. Geomorfologia, Ariel Geografia, Barcelona.
- Donati L, Turrini MC (2002) An objective method to rank the importance of the factors predisposing to landslides with the GIS methodology: application to an area of the Apennines (Valnerina; Perugia, Italy). Eng Geol 63:277–289.
- Fausto Guzzetti (2005), Probabilistic landslide hazard assessment at the basin, doi:10.1016/j.geomorph.2005.06.002
- Garcı´a-Ruiz, J.M., Arna´ez, J., Ortigosa, L., Go´mez Villar, A., 1988.Debris flows subsequent to a forest fire in the Najerilla River Valley (Iberian System, Spain). Pirineos 131, pp.3– 24.
- Giacomo D'Amato Avanzi, Roberto Giannecchini, Alberto Puccinelli., 2004. The influence of the geological and geomorphological settings on shallow landslides. An example in a temperate climate environment: the June 19, 1996 event in northwestern
- Gómez H., Kavzoglu T., 2005. Assessment of shallow landslide susceptibility using artificial neural networks in Jabonosa River Basin, Venezuela, Eng Geol 78, pp-11-27.
- Greenbaum, D., Tutton, M., Bowker, M., Browne, T., Buleka, J., Greally, K., Kuna, G., McDonald, A., Marsh, S., O'Connor, E., Tragheim, D., 1995. Rapid Methods of Landslide Hazard Mapping: Papua New Guinea Case Study. British Geological Survey. Technical Report WC/95/27.
- Greenway, D.R., 1987. "Vegetation and Slope Stability." Slope Stability, John Wiley & Sons Ltd., pp.187 - 230.
- Gupta, R.P, 2002 Remote Sensing Geology, 2nd edition, Springer-Verlag, Heidelberg. pp. 445.

- Guzzetti F., Reichenbach P., Cardinali M., Galli M., Ardizzone F., (2005), Probabilistic landslide hazard assessment at the basin scale, doi:10.1016/ j.geomorph.2005.06.002
- H. Chen and C. F. Lee, A dynamic model for rainfall-induced landslides on natural slopes, Geomorphology, Volume 51, Issue 4, 25 April 2003, Pages 269-288
- Hutchinson JN (1995) Landslide hazard assessment. In: Proc VI Int Symp on Landslides, Christchurch, 1 : 1805–1842
- Jibson WR, Edwin LH, John AM (2000) A method for producing digital frequency seismic landslide hazard maps. Eng Geol 58:271–289.
- Jiu J.J., Xu-Sheng, W., Subhas N., 2005, Confined groundwater zone and slope instability in weathered igneous rocks in Hong Kong, Engineering Geology 80 pp.71-92
- Kamat, S.U. (1985) Gazetteer of India, Karnataka state gazetteer, Uttara Kannada district, Government of Karnataka Publication, Bangalore
- Kesavulu C.N, 1997. Textbook of Engineering geology, Macmillan India Limited, New Delhi.
- Lee S, Choi J, Min K (2004a) Frequency landslide hazard mapping using GIS and remote sensing data at Boun, Korea. Inter J Remote Sens 25(11):2037–2052.
- Lee S, Choi U (2003) Development of GIS based geological hazard information system and its application for landslide analysis in Korea. Geosci J 7:243–252.
- Lee S, Chwae U, Min K (2002) Landslide susceptibility mapping by correlation between topography and geological structure: the Janghung area, Korea. Geomorphology 46:49–162.
- Lee S, Min K (2001) Statistical analysis of landslide susceptibility at Yongin, Korea. Environ Geol 40:1095–1113
- Lee S, Pradhan B (2006) Landslide hazard assessment at Cameron Highland Malaysia using frequency ratio and logistic regression models. Geophy Res Abstracts, 8:SRef-ID:1607–7962/gra/ EGU06-A-03241.
- Lee S, Pradhan B (2007) Landslide hazard mapping at Selangor, Malaysia using frequency ratio and logistic regression models. Landslides 4(1):33–41
- Luzi L, Pergalani F, Terlien MTJ (2000) Slope vulnerability to earthquakes at sub-regional scale, using frequency techniques and geographic information systems. Eng Geol 58:313–336.
- McDermid G. and Franklin S., 1995.Remote sensing and geomorphometric discrimination of slope processes, Zeitschrift für Geomorphologie 101, pp.165–185.
- Mohammad Israil and A. K. Pachauri (2003) Geophysical characterization of a landslide site in the Himalayan foothill region, Journal of Asian Earth Sciences
- Nagarajan R, Khire MV (1998) Debris slides of Varandh ghat, west coast of India. Bull Eng Geol Environ 57: 59–63
- Nagarajan, R., A. Roy, R. Vinodkumar, A. Mukherjee, & M.V. Khire (2000), Landslide hazard susceptibility mapping based on terrain and climatic factors for tropical monsoon regions. Bull Eng. Geol. Env. (2000) 58
- Pachauri AK, Pant M (1992) Landslide hazard mapping based on geological attributes. Eng Geol 32: 81–100

- Piyoosh Rautela and Ramesh Chandra Lakhera (2000) Landslide risk analysis between Giri and Tons Rivers in Himachal Himalaya (India), JAG l Volume 2 – Issue 3/4
- R. Anbalagan, (1992), Landslide hazard evaluation and zonation mapping in mountainous terrain. Engineering Geology, 32 (1992) 269-277
- Radhakrishna B.P., Vidyanadhan R. (1994) Geology of Karnataka, Geological Society of India, Bangalore.
- Reed W, James S.M, 2002.Essentials of Geology, 3rd edition, Brooks/Cole, Pacific Grove, USA. pp.269.
- S.K. Paul, S.K. Bartarya, Piyoosh Rautela, A.K. Mahajan (2000) Catastrophic mass movement of 1998 monsoons at Malpa in Kali Valley, Kumaun Himalaya India, Geomorphology 35 2000: 169–180
- Selby M., 1993. Hillslope Materials and Processes, Oxford Univ. Press, Oxford.
- Shiva Prasad, et al. Soils of Karnataka for optimizing landuse, National Bureau of Soil survey and Landuse Planning, Nagpur
- Squier, L.R., Harvey, A.F., 2000. Two debris flows in Coast Range, Oregon, USA: logging and public policy impacts. In: Wieczorec, G.F., Naeser, N.D. (Eds.), Debris Flow Hazards Mitigation: Mechanics, Prediction and Assessment. Balkema, Rotterdam, pp- 127– 138.
- Terzaghi, K., Peck, R.B., 1967. Soil Mechanics in Engineering Practice. John Wiley and Sons, New York. p. 432
- Tuscany (Italy), Eng Geol 73, pp. 215–228
- Varnes, 1984; landslide hazard zonation: a review of principles and practices. UNESCO, Paris, pp.1-63.
- Vijith H., Madhu G., 2007,Estimating potential landslide sites of an upland sub-watershed in Western Ghat's of Kerala (India) through frequency ratio and GIS, Environ Geol.doi:10.1007/s00254-007-1090-2.
- Wu, W., Sidle, R.C., 1995. A distributed slope stability model for steep forested basins. Water Resources Research 31, 2097– 2110.
- Zezere JL, Reis E, Garcia R, Oliveira S, Rodrigues ML, Vieira G, Ferreira AB (2004) Integration of spatial and temporal data for the definition of different landslide hazard scenarios in the area north of Lisbon (Portugal). Natural Haz Earth Sys Sciences 4:133–146.
- http://www.gisdevelopment.net/application/natural_hazards/landslides/nhls0013pf.htm
- http://www.gisdevelopment.net/application/natural_hazards/landslides/nhls0010pf.htm
- http://www.gisdevelopment.net/application/natural_hazards/landslides/nhls0011pf.htm
- http://www.cnr.colostate.edu/~denis/pubs_online/Litschert_and_Dean_2000.PDF
- http://www.gisdevelopment.net/application/natural_hazards/landslides/mi03128.htm
- http://www.gisdevelopment.net/application/natural_hazards/landslides/mi03040.htm
- http://www.gisdevelopment.net/application/natural_hazards/landslides/nhls0012.htm
- http://www.geospatialtoday.com/articles/article_4.asp

- http://www.gisdevelopment.net/application/natural_hazards/landslides/nhls0005.htm
- http://www.gisdevelopment.net/application/natural_hazards/landslides/nhls0006.htm
- http://www.gisdevelopment.net/aars/acrs/1994/ts3/ts3004.shtml
- http://www.gisdevelopment.net/aars/acrs/1997/ps3/ps3006.shtml
- http://www.gisdevelopment.net/aars/acrs/1996/ts3/ts3003.shtml
- http://www.gisdevelopment.net/aars/acrs/2000/ts12/laus0010.shtml
- http://www.gisdevelopment.net/application/natural_hazards/landslides/mi03098abs.htm
- http://dionysos.gssr.sk/ig_home/exchange/ppaudits/p2002_Praha(Handlova,Paudits-Bednarik).pdf

13. BIBLIOGRAPHY

- Drury, S.A. (1987) Image interpretation in geology, Allen and Unwin, London
- Prost, Gary L. (2001) Remote sensing for geologists: a guide to image interpretation, 2nd Gordon and Breach Science Publishers, Australia
- Lillesand, Thomas M.; Kiefer, Ralph W. (2002) Remote sensing and image interpretation, 4th John Wiley & Sons, Inc., New York
- Majumdar, S.P., Singh, R.A. (2000) Analysis of soil physical properties, Agro bios, Jodhpur
- Verbyla, David L. (2002) Practical GIS analysis, Taylor & Francis, London
- Prabin Singh (1996) A textbook of engineering and general geology, S.K.Kataria and sons, Delhi.
- Kessavulu channa N. (1997) Textbook of engineering geology, Macmillan India Limited, Delhi.
- Radhakrishna B.P. (1996) Mineral resources of Karnataka, Geological society of India, Bangalore
- http://www.gisdevelopment.net/application/natural_hazards/landslides/nhls0007pf.htm
- http://convention.allacademic.com/aag2003/sessions.html?letter=R
- http://www.gisdevelopment.net/application/natural_hazards/landslides/index.htm
- http://www.onid.orst.edu/~chevallj/GIS.landslides.htm
- http://convention.allacademic.com/aag2003/sessions.html?letter=R
- http://www.gisdevelopment.net/application/natural_hazards/landslides/index.htm
- http://www.onid.orst.edu/~chevallj/GIS.landslides.htm
- http://www.geologyuk.co.uk/downloads/kathmandu_seminar.doc
- http://www.gisdevelopment.net/aars/acrs/1997/ps3/ps3006pf.htm
- http://gisweb.athena.bcit.ca/students/class02-03/gisb009/litreview.htm
- http://www.gisdevelopment.net/aars/acrs/2000/ps1/ps102pf.htm
- http://geosun.sjsu.edu/paula/285/285/eb_sem.htm
- http://rst.gsfc.nasa.gov/Front/tofc.html
- http://www.gisdevelopment.net/aars/acrs/1997/ts3/ts3001pf.htm
- http://www.geogr.muni.cz/lgc/gis98/proceed/PAVELKA.html
- http://www.mysteries-megasite.com/main/bigsearch/landslides.html
- http://staff.aist.go.jp/s.tsuchida/itit/f_report/3odaji.pdf
- http://www.mysteries-megasite.com/main/bigsearch/landslides.html
- http://www.onid.orst.edu/~chevallj/GIS.landslides.htm
- http://moose.cee.usu.edu/sinmap/sinmap_poster.ppt
- http://www.fes.uwaterloo.ca/crs/gp555/gisp.pdf
- http://www.onid.orst.edu/~chevallj/GIS.landslides.htm
- http://staff.aist.go.jp/s.tsuchida/itit/f_report/3odaji.pdf

- http://www.cnr.uidaho.edu/remotesensing/Projects/Landslide_hazard.html
- http://www.mountaingis.org/
- http://www.cnr.uidaho.edu/remotesensing/Projects/Strategic_Research2002/Landslide%20Hazard.htm
- http://www.ceworld.org/ceworld/Presentations/Computing/Rose1.cfm
- http://moose.cee.usu.edu/sinmap/sinmap_poster.ppt
- http://www.ceeraindia.org/cgi-bin/ceera_indown.pl?filename=about.pl
- http://deis158.deis.unibo.it/gis/chapt0.htm
- http://www.geoplace.com/asiapac/2000/0700/0700lnd.asp
- http://www.gisdevelopment.net/proceedings/mapindia/2000/poster/pos001.htm
- http://ag.arizona.edu/classes/rnr271/articles/logic/logic.html
- http://www.gisdevelopment.net/application/natural_hazards/landslides/mi03128pf.htm
- http://www.geovista.psu.edu/sites/geocomp99/Gc99/054/gc_054.htm
- http://www-public.tu-bs.de:8080/~aguenthe/bmbf/bmbf01_eng.html
- http://www.itc.nl/ilwis/applications/application07.asp
- http://www.oas.org/en/cdmp/document/kma/udspub5.htm
- http://www.geohaz.com/kingston.htm
- http://geopubs.wr.usgs.gov/map-mf/mf2378/berkpamph.pdf
- http://csd.unl.edu/csd/illustrations/landslides/landslide.html#1.0
- http://landslides.usgs.gov/html_files/nlic/nlicpub.html
- http://www.cityofseattle.net/projectimpact/pioverview/hazardmapping/landslide.htm
- http://www.adpc.ait.ac.th/audmp/rllw/themes/th1-bandara.pdf
- http://www.oregonshowcase.org/projects/state/downloads/hazard_trg_6_2000/08_landslide.pdf
- http://3d.wr.usgs.gov/docs/wgmt/3d/pp02.html#task5
- http://www.geol.pdx.edu/People/DCP/G424-GIS/metrosld.doc
- http://www.yapirehberi.net/Heyelan.htm
- http://www.saguenay.ggl.ulaval.ca/saguenay/publi/urgeles2.pdf
- http://anaheim-landslide.com/features.htm
- http://pubs.usgs.gov/of/1995/ofr-95-0213/TABLE.HTML#TABLE
- http://www.ce.berkeley.edu/~khazai/Research/Report/index2.html
- http://www.geospatialtoday.com/articles/article_4.asp
- http://ceos.cnes.fr:8100/cdrom-00b2/ceos1/science/gdta/ang/a2an/78.htm
- http://www.toprak.org.tr/isd/can_41.htm#
- http://www.toprak.org.tr/bildiri_can.htm

Landslide susceptibility mapping in the downstream region of Sharavathi river basin, Central Western Ghats

Abstract—**Landslides are hazards encountered during monsoon in undulating terrains of Western Ghats causing geomorphic make over of earth surface resulting in significant damages to life and property. An attempt is made in this paper to identify landslides susceptibility regions in the Sharavathi river basin downstream using frequency ratio method based on the field investigations during July- November 2007. In this regard, base layers of spatial data such as topography, land cover, geology and soil were considered. This is supplemented with the field investigations of landslides. Factors that influence landslide were extracted from the spatial database. The probabilistic model -frequency ratio is computed based on these factors. Landslide susceptibility indices were computed and grouped into five classes. Validation of LHS, showed an accuracy of 89% as 25 of the 28 regions tallied with the field condition of highly vulnerable landslide regions. The landslide susceptible map generated for the downstream would be useful for the district officials to implement appropriate mitigation measures to reduce hazards.**

INTRODUCTION

Movement of a mass of rock, debris, or earth down a slope resulting geomorphic make over of earth surface and this active process contributes to erosion and landscape evolution is often referred as landslide [1,2]. This could be due to the temporal conjunction of several factors [3-5], such as: (i) the quasi-static variables, which contribute to landslide susceptibility, such as geology, slope characteristics (gradient, slope aspect, elevation, etc.), geotechnical properties, and long-term drainage patterns, etc.; and (ii) the dynamic variables, which tend to trigger landslides in an area of a given landslide susceptibility, such as rainfall and earthquakes.

Depending on quasi static and triggering factors, landslides vary in composition as well as in the rate of movement ($0.5x10^{-6}$ to $5x10^{3}$ mm/sec). Landslides in vulnerable zones in India have lead to large scale loss of life and property [6]. In this context, identification, mapping and monitoring of landslide susceptible pockets would help in the mitigation as well as in the rehabilitation. These vulnerable pockets can be identified by by both direct and indirect techniques based on significance of causative factors in inducing instability. The assumptions that are generally made in identifying landslide hazard susceptibility (LHS) regions [7, 8] are: Occurrence of landslides follows past history in the region depending on geological, geomorphological, hydrogeological and climatic conditions. Identification of LHS involves dividing the region into zones depending on degrees of stability, significance of causative factors inducing instability, etc.

Identification and mapping of LHS zones aid in delineating unstable hazard-prone areas, so that environmental mitigation measures can be initiated. This also helps planners to choose favourable locations for site development projects. Even if the hazardous areas can not be avoided altogether, their recognition in the initial stages of planning will help to adopt suitable precautionary remedial measures.

Identification of LHS and mapping: Quasi static variables and dynamic variables are considered for likelihood frequency ratio (LRM) model and weighted linear combination (WLC) model. In this regard, slope angle, slope aspect, lithology, distance from drainage lines, distance from roads and the land-cover of the study area are considered as the landslide-conditioning parameters. [9] Other attempts considering lithology, slope angle, bedding attitude along with dynamic variable like rainfall [10]; distance from faults, parallelism between the fractures and the landslide scarps, land use, lithology, distance from the streams, orientation and steepness of slopes, orientation of layers compared to the slope [11]; slope, aspect, and curvature of topography, texture, material, drainage, and effective soil thickness and type, age, diameter, and density of timber, lithology, land use in probability and logistic regression methods [12]; geological structure of foliation, slope aspect and slope of the topography for frequency ratio analysis [13]; slope, curvature, soil texture, soil drainage, soil effective thickness, timber age, and timber diameter in ANN and frequency ratio methods [12-16]; rainfall, slope angle, aspect, curvature, lithology, superficial deposits, geomorphology, and land use in the probabilistic evaluation of landslide hazard [17]; slope angle, slope aspect, slope curvature, slope length, distance from drainage, distance from lineaments, lithology, and land use and geomorphology in frequency ratio method [18].
The objective of the study is identification and mapping landslide prone zones of Sharavathi downstream using frequency ratio analysis. The Sharavathi river basin is situated in Central Western Ghats. Due to undulating terrain coupled with high

intensity rainfall, ghats are prone to landslides causing significant damage to property and agriculture. Most of the episodes are triggered by rainfall with the changes in land cover. Effort is made to identifify landslide susceptible regions.

STUDY AREA

The Sharavathi River (74.408°-75.32° E and 13.717°-14.432° N) is one of the important west flowing rivers of central Western Ghats, India (Fig 1). A hydro-electric dam was commissioned in 1964 at Linganamakki, which has waterspread area of 357 sq.km.). Subsequent to the dam, Sharavathi river loses height of 253m as series of rapids. The catchment area is about 2985km², with up-stream being 1988 km² and the downstream being 997km².

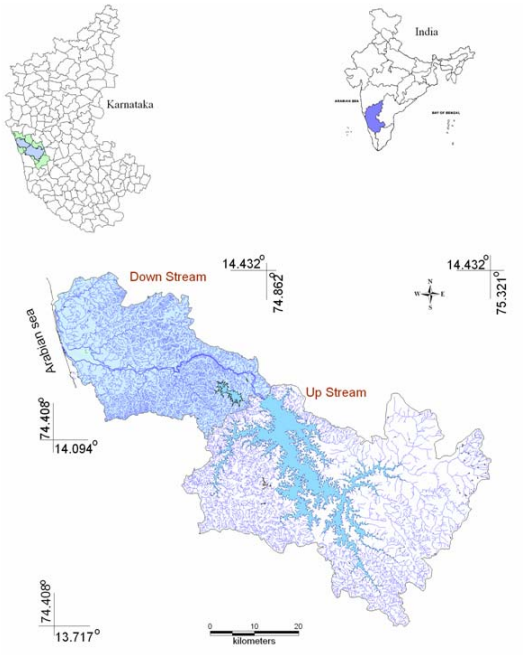

Fig 1: Sharavathi river basin, Central Western Ghats

Down stream of Sharavathi situated at 74.408° – 74.862° E and 14.094°–14.431° N, with elevation varies from zero eters at sea level to 760 m at the ghats and having an average altitude of 237 m. The soil texture is mainly clayey, clayey-skeletal, sandy loam and sand distributed only along the mouth of the catchment. The region is made up laterite, migmatites and granodiorite. grey granite, metabasalt, greywacke, alluvium, and quartz chlorite schist with orthoquartzite are spread across the study area. Annual rainfall in the region ranges from …3521±619 mm (Honavar) 4339±1249 mm (Gerusoppa). Field investigations were carried out in the downstream region during August, September, and October months and 120 landslide locations were located.

METHOD

Method adopted for landslide susceptibility analysis is given in Fig 2. Field investigations were carried out in the Sharavathi river basin located in central Western Ghats. Major components of the study are:

i.) Identification of causal variables: Review of literature indicates the major causal variables are: topographical (aspect, slope, curvature, drainage network), geo-morphological (lineament, genesis), lithological (lithology, soil texture, soil permeability and soil depth), infrastructure (road network, location of buildings), land cover (NDVI), land-use (agriculture, waterbodies, forests, built-up, barren land). Field surveys were carried out of landslide spots (temporal as well as latest ones), attribute data of training polygons of land use analysis using pre-calibrated GPS.

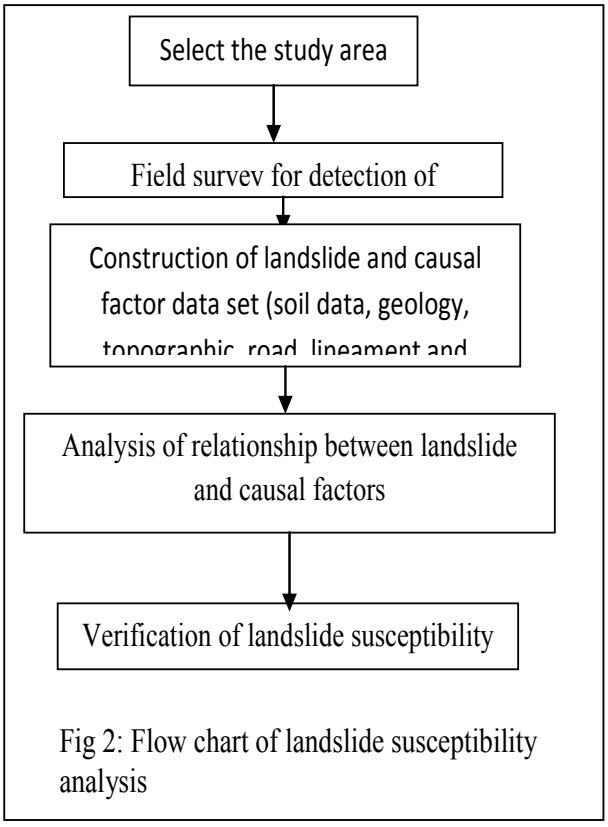

Fig 2: Flow chart of landslide susceptibility analysis

Table 1: Spatial data

Classification	Sub-classification	Data Type	Scale
Base layers	Topographic	Lines and points	1:50000
	Geological	Lines and polygons	1:250,000
	Soil	Polygon	1:250,000
	Elevation	GRID (SRTM)	90m x 90m
Remote sensing data	Land cover	GRID (IRS-1D)	23.5m x 23.5m
	Rainfall	Points	Taluk level
Geological Hazard	Landslide	Points	

ii.) Creation of base layers of spatial data – soil, geology, topography, geo-morphology, land use, etc. These information were collected from the respective government agencies and supplemented with the remote sensing data and other spatial layers. Indian Remote Sensing (IRS) 1C/1D satellite, LISS III (linear imaging self scanner) data of spatial resolution 23.5 m (acquired during Nov 2004), of bands 2, 3 and 4 (corresponding to G, R and IR bands of electro magnetic spectrum) were used for land use and land cover (NDVI) analysis. Supervised classification using Gaussian maximum likelihood classifier was carried out for deriving seven land use categories- agricultural, barren land, built up, moist deciduous forest, plantation, semi-evergreen forest and water body. Road and drainage networks with administrative boundaries were digitised from Survey of India (SOI) topographic maps (1:50,000 scale). Soil types and spatial extent were digitised from the soil map of National Bureau of Soil Sampling and land use planning (NBSS& LUP) of 1:250,000 scale. From this, texture, depth and permeability were derived. Spatial data with type are listed in Table 1.

Geomorphological variables such as lithology, lineament, rock type were extracted from geological and structural maps of Geological Survey of India (1:250,000 scale). Shuttle radar topographic mapping (SRTM 3 arc-sec) of 90 m resolution was used to derive layers of slope, aspect and curvature. This constitutes predisposing factors for the landslide activity.

Slope was classified into 10 classes. Aspect represents the angle between the geographic north and a horizontal plain for a certain point. This was classified in eight major orientations (N, NE, E, SE, S, SW, W, NW). The curvature controls the superficial and subsurface hydrological regime of the slope and the classes considered are concave, flat and convex slope areas, which were directly derived from the DEM.

The distance from drainage and road was calculated using the vectorised drainage and road from the topographical sheets of scale 1:50,000. The drainage and road buffer was calculated at 90 m intervals. The lithology and genesis was extracted from the available geology map prepared by the Geological Survey of India (GSI). In addition the lineament database from GSI, was used to create distance from lineaments map. The lineament buffer was calculated at 90 m intervals.

iii.) Development of spatial database: Considering the spatial resolution of the data available, all data layers were resampled to 90 m. Landslides (both latest and earlier ones) corresponding to 120 occurrences were used for computing LSI as well as for sensitivity analysis.

iv.) Frequency ratio: Frequency ratio is the ratio of occurrence of probability to non-occurrence probability, for specific attributes. In the case of landslides; if landslide occurrence event is set to B and the specific factor's attribute to D, the frequency ratio for D is a ratio of conditional probability. If the ratio is greater than 1, greater is the relationship between a landslide and the specific factor's attribute; and if the ratio is less than 1, the lower the relationship between a landslide and the specific factor's attribute.

v.) Computation of Landslide Susceptibility Index (LSI): Landslide Susceptibility Index (LSI) is the summation of each factor's frequency ratio values as in Eq. 1. Landslide susceptibility value represents the relative hazard to landslide occurrence, as higher values are associated with landslide hazards.

$$LSI = \sum_{i=1}^{n} Fr_i \qquad \text{---------- (1)}$$

(where, LSI: Landslide Susceptibility Index; Fr: rating of each factor's type or range). The landslide hazard map was made using the LSI values.

Table 2: Frequency ratio – Spatial relationship between landslides and related factors

Factors with domain	No of pixels in domain	No of landslide	% of domain	% of landslide	Frequency ratio
Aspect					
South	15924	24	0.135	0.261	1.939
South-West	16018	13	0.135	0.141	1.044
North-West	16308	13	0.138	0.141	1.026
North-East	13337	11	0.113	0.120	1.061
South-East	12758	12	0.108	0.130	1.210
West	16085	5	0.136	0.054	0.400
East	11159	6	0.094	0.065	0.692
North	16795	8	0.142	0.087	0.613
Land use					
Agriculture land	25933	40	0.219	0.435	1.985
Barren Land	4536	6	0.038	0.065	1.702
Builtup	1145	2	0.010	0.022	2.248
Moist Deciduous Forest	32271	9	0.273	0.098	0.359
Plantation	3877	0	0.033	0.000	0.000
Semi-Evergreen Forest	45460	35	0.384	0.380	0.991
Water body	5162	0	0.044	0.000	0.000
Topographic curvature					
Convex	95956	77	0.811	0.837	1.033
Concave	22428	15	0.189	0.163	0.861
Distance from Drainage (m)					
Buffer 90	65833	30	0.5561	0.3261	0.5864
Buffer 180	32190	34	0.2719	0.3696	1.3591
Buffer -270	11125	22	0.0940	0.2391	2.5446
Buffer 360	4513	5	0.0381	0.0543	1.4256
Buffer 450	2074	0	0.0175	0.0000	0.0000
Buffer 540	1073	0	0.0091	0.0000	0.0000
Buffer 630	583	1	0.0049	0.0109	2.2072
Buffer 630<	993	0	0.0084	0.0000	0.0000
Rock type					
Plutonic rocks	8674	0	0.073	0.000	0.000
Metamorphic rocks	51253	55	0.433	0.598	1.381
Residual capping	32837	33	0.277	0.359	1.293
Unconsolidated sediments.	735	1	0.006	0.011	1.751
Volcanics / Meta volcanics	24885	3	0.210	0.033	0.155
Lithologic unit					
Grey granite	8675	0	0.073	0.000	0.000
Migmatites and granodiorite - tonalitic gneiss	31698	38	0.268	0.413	1.543
Laterite	32836	33	0.277	0.359	1.293
Alluvium / beach sand, alluvial soil	735	1	0.006	0.011	1.751
Greywacke / argillite	16343	11	0.138	0.120	0.866
Metabasalt & tuff	24885	3	0.210	0.033	0.155
Quartz chlorite schist with orthoquartzite	3212	6	0.027	0.065	2.404
Limeament (m)					

Buffer 90	9028	5	0.076	0.054	0.713
Buffer 180	10145	7	0.086	0.076	0.888
Buffer 270	10509	14	0.089	0.152	1.714
Buffer 360	10387	4	0.088	0.043	0.496
Buffer 450	9720	4	0.082	0.043	0.530
Buffer 540	8911	2	0.075	0.022	0.289
Buffer 630	8038	4	0.068	0.043	0.640
Buffer 720	7001	3	0.059	0.033	0.551
Buffer 810	6184	5	0.052	0.054	1.040
Buffer 900	5345	5	0.045	0.054	1.204
Buffer 900<	33116	39	0.280	0.424	1.515
NDVI					
<=-0.5	192	0	0.002	0.000	0.000
>0.5	47954	57	0.405	0.620	1.530
>10^-7 and <=0.5	62070	33	0.524	0.359	0.684
>-0.5 and <=-10^-7	8168	2	0.069	0.022	0.315
Slope (degree)					
0-5	534	0	0.005	0.000	0.000
5-10	1369	0	0.012	0.000	0.000
10-15	1647	4	0.014	0.043	3.125
15-20	1798	0	0.015	0.000	0.000
20-25	2162	3	0.018	0.033	1.786
25-30	2647	10	0.022	0.109	4.861
30-35	2476	1	0.021	0.011	0.520
35-40	2837	10	0.024	0.109	4.536
40-45	3782	14	0.032	0.152	4.763
45-90	99226	50	0.838	0.543	0.648
Soil depth					
Moderately shallow	21094	40	0.178	0.435	2.440
Deep	71508	49	0.604	0.533	0.882
Very deep	22732	2	0.192	0.022	0.113
Moderately deep	3050	1	0.026	0.011	0.422
Soil permability					
Somewhat excessively drained	11104	17	0.094	0.185	1.970
Imperfectely drained	12740	15	0.108	0.163	1.515
Well drained	94540	60	0.799	0.652	0.817
Soil texture					
Sandy	895	0	0.008	0.000	0.000
Clayey	45088	15	0.381	0.163	0.428
Clayey-skeletal	60556	57	0.512	0.620	1.211
Sandy loamy	11845	20	0.100	0.217	2.173
Distance form road(m)					
Buffer 90	16992	74	0.131	0.804	6.144
Buffer 180	14707	9	0.113	0.098	0.863
Buffer 270	12278	3	0.095	0.033	0.345
Buffer 360	10279	1	0.079	0.011	0.137
Buffer 450	8606	2	0.066	0.022	0.328
Buffer 540	7256	1	0.056	0.011	0.194
Buffer 630	5108	0	0.043	0.000	0.000
Buffer 720	6295	0	0.053	0.000	0.000
Buffer 810	4348	1	0.034	0.011	0.324
Buffer 810<	32515	1	0.251	0.011	0.043

IV. RESULTS AND DISCUSSION

Frequency ratio computed for related factors are listed in Table 2. With high intensity rainfall, slope in the range of 35º to 45º with convex curvature, south and south–west aspect, land uses like barren or agricultural or built up and geological aspects such as metamorphic rocks (migmatites and granodiorite - tonalitic gneiss, laterite, and quartz chlorite schist with orthoquartzite) or residual capping or unconsolidated sediments are highly susceptible to landslides. LSI values computed were classified into five classes (Very high, High, Moderate, Low and Least) based the degree of vulnerability are listed in Table 3 and LHS map is given in Fig. 3. Higher values (14.39 % of study area) of LSI indicate higher probability of landslide occurrences (which coincides with the field data of latest occurrences). Validation of LHS map, showed an accuracy of 89% as 25 of the 28 regions tallied with the field data of highly vulnerable landslides.

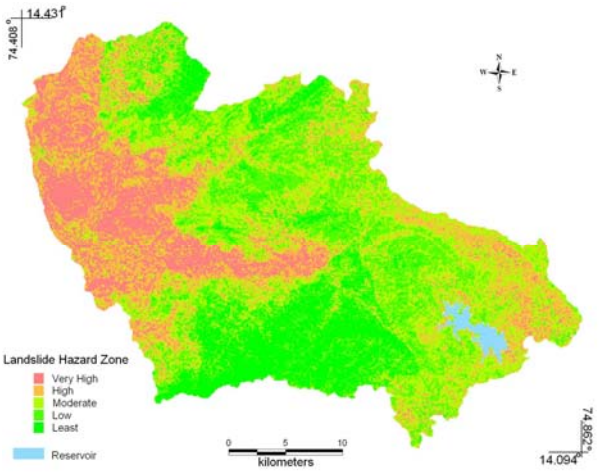

Fig 3: LHS map for Sharavathi Down stream using Frequency ratio

Table 3: LHS for the downstream of Sharavathi river basin

Category	LSI	Spatial Coverage	Validation Accuracy
Very high	18.3-27.8	14.39%	89%
High	14.9-18.3	21%,	
Moderate	12.3-14.9	27.98%	
Low	10.1-12.3	22.54%	
least	5.3-10.1	14.09	

V. CONCLUSION

Frequency ratio method based mapping of landslide for Sharavathi river downstream show that 14.39% of the study area is very highly susceptible to landslide and 14.09% of the area being very safe or least prone to landslide. The validation of the LHS map generated had an agreement of 89% between the susceptibility map and the field data.

VI. REFERENCE

[1] Cruden, D.M., 1991. A Simple Definition of a Landslide. Bulletin of the International Association of Engineering Geology, No. 43, pp. 27-29

[2] Guzzetti F (2005), Probabilistic landslide hazard assessment at the basin, doi:10.1016/j.geomorph.2005.06.002

[3] Atkinson, P.M., Massari, R., 1998. Generalized linear modelling of landslide susceptibility in the central Apennines, Italy. Computers & Geosciences 24, 373– 385.

[4] Dai, F.C., Lee, C.F., 2001. Terrain-based mapping of landslide susceptibility using a geographical information system: a case study. Canadian Geotechnical Journal 38, 911 – 923

[5] Wu, W., Sidle, R.C., 1995. A distributed slope stability model for steep forested basins. Water Resources Research 31, 2097– 2110.

[6] International Federation of the Red Cross and Red Crescent Societies, I. (2001). World disasters report 2001.

[7] Hutchinson JN (1995) Landslide hazard assessment. In: Proc VI Int Symp on Landslides, Christchurch, 1: 1805–1842

[8] Varnes DJ, IAEG Commission on Landslides (1984) Landslide hazard zonation – a review of principles and practice. UNESCO, Paris, 63.

[9] Akgun A, Serhat Dag S, and Bulut F (2007) Landslide susceptibility mapping for a landslide-prone area (Findikli, NE of Turkey) by likelihood-frequency ratio and weighted linear combination models. Environ Geol. doi:10.1007/s00254-007-0882-8

[10] Clerici A, Perego S, Tellini C, Vescovi P (2002) A procedure for landslide susceptibility zonation by the conditional analysis method. Geomorphology 48:349–364.

[11] Donati L, Turrini MC (2002) An objective method to rank the importance of the factors predisposing to landslides with the GIS methodology: application to an area of the Apennines (Valnerina; Perugia, Italy). Eng Geol 63:277–289.

[12] Lee S, Min K (2001) Statistical analysis of landslide susceptibility at Yongin, Korea. Environ Geol 40:1095–1113

[13] Lee S, Chwae U, Min K (2002) Landslide susceptibility mapping by correlation between topography and geological structure: the Janghung area, Korea. Geomorphology 46:49–162

[14] Lee S, Choi U (2003) Development of GIS based geological hazard information system and its application for landslide analysis in Korea. Geosci J 7:243–252.

[15] Lee S, Pradhan B (2007) Landslide hazard mapping at Selangor, Malaysia using frequency ratio and logistic regression models. Landslides 4(1):33–41

[16] Lee S, Talib JA. 2005. Probabilistic landslide susceptibility and factor effect analysis. Environmental Geology 47: 982–990.

[17] Zezere JL, Reis E, Garcia R, Oliveira S, Rodrigues ML, Vieira G, Ferreira AB (2004) Integration of spatial and temporal data for the definition of different landslide hazard scenarios in the area north of Lisbon (Portugal). Natural Haz Earth Sys Sciences 4:133–146

[18] Vijith H., Madhu G., 2007,Estimating potential landslide sites of an upland sub-watershed in Western Ghat's of Kerala (India) through frequency ratio and GIS, Environ Geol.doi:10.1007/s00254-007-1090-2.

Landslide Hazard Mapping of Aghnashini River Catchment, Central Western Ghats, India

Abstract

Landslides are encountered during the monsoon season in the undulating terrains of the Western Ghats. These cause geomorphic makeovers of the earth's surface resulting in significant damage to life and property. An attempt is made in this paper to identify landslide susceptibility regions in the Aghnashini river catchment of Uttara Kannada district of Karnataka, India using the frequency ratio method based on field investigations during 2007-2008. In this regard, base layers of spatial data such as topography, land cover, geology and soil were considered. Factors that influence landslides were extracted from the spatial database. This was supplemented by the field investigations of landslides. The frequency ratio which is the ratio of probability of occurrence to probability of non-occurrence, for specific attributes. Landslide susceptibility indices were computed and grouped into five classes. A landslide susceptibility map generated for the Aghnashini river catchment would be useful for the Government and other development agencies to implement appropriate mitigation measures to reduce hazards.

Introduction

The movement of a mass of rocks, debris, or earth down a slope resulting in geomorphic makeover of earth's surface which contributes to erosion and landscape evolution is often referred as a landslide [1, 2]. Landslides could be due to the temporal conjunction of several factors [3-5], like:

1. Quasi-static variables, which contribute to landslide susceptibility, such as geology, slope characteristics (gradient, slope aspect, elevation, etc.), geotechnical properties, long-term drainage patterns, etc.
2. Dynamic variables, which tend to trigger landslides, such as rainfall and earthquakes. Depending on quasi static and triggering factors, landslides vary in composition as well as in the rate of movement (0.5x10-6 to 5x103 mm/sec) [6]. Landslides in vulnerable zones in India have lead to large scale loss of life and property [7].

In this context, identification, mapping and monitoring of landslide susceptible pockets would help in the mitigation of landslides as well as in rehabilitation of victims. These vulnerable pockets can be identified by both direct and indirect techniques based on the significance of causative factors in inducing instability. The assumption that is generally made in identifying landslide hazard susceptibility (LHS) regions [8, 9] is that occurrence of landslides follows past history in the region depending on geological, geomorphological, hydrogeological and climatic conditions. Identification of LHS involves dividing the region into zones depending on degrees of stability, significance of causative factors inducing instability, etc. Identification and mapping of LHS zones aids in delineating unstable hazard-prone areas which help planners choose favourable locations for siting development projects. It also assists in putting into place environmental mitigation measures. Even if the hazardous areas cannot be avoided altogether, their recognition in the initial stages of planning will help to adopt suitable precautionary remedial measures.

Identification of LHS and Mapping: Quasistatic variables and dynamic variables are considered for the likelihood frequency ratio (LRM) model in modelling landslides by various authors. In this regard slope, aspect, curvature, soil texture, soil drainage, soil effective thickness, timber age, timber diameter, distance from drainage, distance from roads, distance from faults, distance from lineaments, parallelism between the fractures, landslide scarps, lithology, geological structure of foliation, geomorphology, normalized difference vegetation index (NDVI) and land use are some of the parameters used by several authors[10-19]. Even a dynamic variable like rainfall is considered in the analysis. The objective of the study is identification and mapping of landslide prone zones of Aghnashini River catchment using frequency ratio analysis. The Aghnashini River is situated in the

Central Western Ghats. Due to undulating terrain coupled with high intensity rainfall, the ghats are prone to landslides causing significant damage to property and agriculture. Most of the episodes are triggered by rainfall with the changes in land cover. Effort is made in this paper to identify landslide susceptible regions of Aghnashini river catchment

Study Area

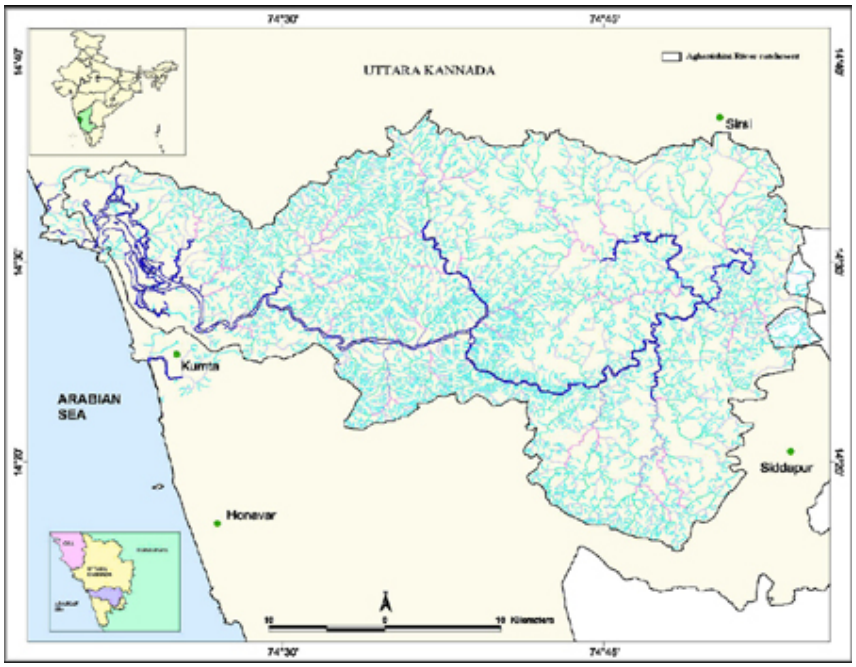

Figure1: Aghnashini River catchment, Central Western Ghats

The Aghnashini River catchment (74.32°-74.92° E and 14.26°-14.62° N) is one of the important west flowing rivers of central Western Ghats, India (Fig 1). This river catchment is of the Uttara Kannada District is neither disturbed by major projects or industries nor does it have a major town in the catchment. The catchment area is about 2985km² (due to lack of data 18.25 km² of catchment which\ falls in Havery district has been excluded). The Aghnashini river catchment with elevation varying from zero meters at sea level to 784 m at the Ghats has an average altitude of 396 m. The soil texture is mainly clayey, gravelly clayey which comprises of 85% of the catchment. The region is made up of laterite, migmatites and granodiorite, pink granite, metabasalt, greywacke, alluvium, and quartz chlorite schist with orthoquartzite spread across the study area. Annual rainfall in the region varies from 3581±687 mm (Kumta), 2450±485 mm (Sirsi) and 2969±704 mm (Siddapur) (all the three rain gauge stations are just outside the catchment). Field investigations were carried out in the region during post monsoon months of 2007 and 2008 with 237 and 53 landslide locations being located respectively of the total number of landslides 83% were due to road cutting.

Classification	Sub-classification	Data Type	Scale
Base layers	Topographic	Lines and points	1:50000
	Geological	Lines and polygons	1:250,000
	Soil	Polygon	1:250,000
	Elevation	GRID (SRTM)	90m x 90m
Remote sensing data	Land cover	GRID (LANDSAT ETM)	30m x 30m
Geological Hazard	Landslide	Points	

Table 1:Spatial data Work Flow/ Methodology

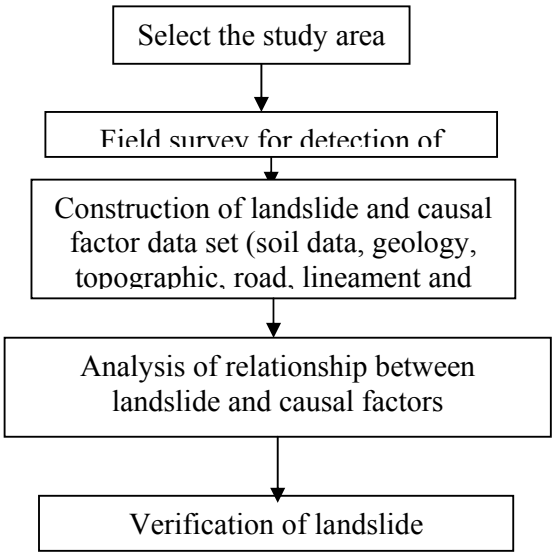

Fig 2: Flow chart of landslide susceptibility analysis

Creation of base layers of spatial data – soil, geology, topography, geo-morphology, land use, etc. This information was collected from the respective government agencies and supplemented with the remote sensing data. Landsat, ETM (Enhanced Thematic Mapper) data of spatial resolution 30 m of bands 2, 3, 4 and 5 (corresponding to Green, Red, Infra Red and Near Infra Red bands of the electromagnetic spectrum) were used for land use and land cover (NDVI) analysis. Road networks with administrative boundaries were digitised from Survey of India (SOI) topographic maps (1:50,000 scale). Soil types and spatial extents were digitised from the soil map of the National Bureau of Soil Sampling and land use planning (NBSS& LUP) of 1:250,000 scale. From this, texture, depth and permeability were derived. Spatial data with type are listed in Table 1.Geomorphological variables such as lithology, lineament, and rock type were extracted from geological and structural maps of the Geological Survey of India (1:250,000 scale). Shuttle radar topographic mapping (SRTM 3 arc-sec) of 90 m resolution was used to derive layers of analysis slope, aspect and toposhapes. This constitutes predisposing factors for the landslide activity. Slope was classified into 10 classes. Aspect represents the angle between the geographic north and a horizontal plain for a certain point. This was classified in nine orientations (flat, N, NE, E, SE, S, SW, W and NW). The topographic features control the superficial and subsurface hydrological regime of the slope and the classes considered are peak, ridge, saddle, ravine, pit, convex hillside, saddle hillside, slope hillside, inflection hillside, concave hillside and unknown hillside which were directly derived from the digital elevation model (DEM). The distance from lineaments and road was calculated by buffering at 90 m intervals.

Development of Spatial Database: Considering the spatial resolution of the data available, all data layers were resampled to 90 m and total number of cells was 165042. Landslides corresponding to 237 and 53 occurrences in 2007 and 2008 respectively were used for computing LSI as well as for sensitivity analysis. Frequency ratio: Frequency ratio is the ratio of occurrence probability to non-occurrence probability for specific attributes. In the case of landslides; if landslide occurrence event is set to B and the specific factor's attribute to D, the frequency ratio for D is a ratio of conditional probability. If the ratio is greater than 1, greater is the relationship between a landslide and the specific factor's attribute; and if the ratio is less than 1, the lesser will be the relationship between a landslide and the specific factor's attribute. Computation of Landslide Susceptibility Index (LSI): Landslide Susceptibility Index (LSI) is the summation of each factor's frequency ratio values as in

equation 1. Landslide susceptibility value represents the relative hazard to landslide occurrence, as higher values are associated with landslide hazards.

$$LSI = \sum_{i=1}^{n} Fr_i \qquad \text{---------} (1)$$

(where, LSI: Landslide Susceptibility Index; Fr: rating of each factor's type or range). The landslide hazard map was made using the LSI values.

Results and Discussion

Frequency ratios computed for related factors are listed in equation 1. With high intensity rainfall, slope in the range above 45º with concave and ridge hillside, south–west, north-west, and south-east aspect, and geological aspects such as metamorphic rocks (greywacke / argillite and metabasalt) or Volcanic / Meta volcanic are highly susceptible to landslides. Gravely clay soil with moderate erosion, moderately deep, and well drained has high susceptibility. LSI values computed were classified into five classes (Very high, High, Moderate, Low and Least) based on the degree of vulnerability. These are listed in Table 2 and LHS map is given in Figure 3. Higher values (16.95 % of study area) of LSI indicate higher probability of landslide occurrences (which coincide with the field data of latest occurrences). Validation of LHS map showed an accuracy of 11% and 47% of the 53 regions tallied with the field data of highly vulnerable landslides.

Table 2: LHS for the downstream of Aghnashini River catchment

Category	LHS	Spatial Coverage (%)	Validation Accuracy (%)
Very high	16.4-21.8	16.95	11
High	14.5-16.4	25.43	47
Moderate	14.5-13.1	27	
Low	13.1-11.1	21.3	
Least	11.1-4.2	9.3	

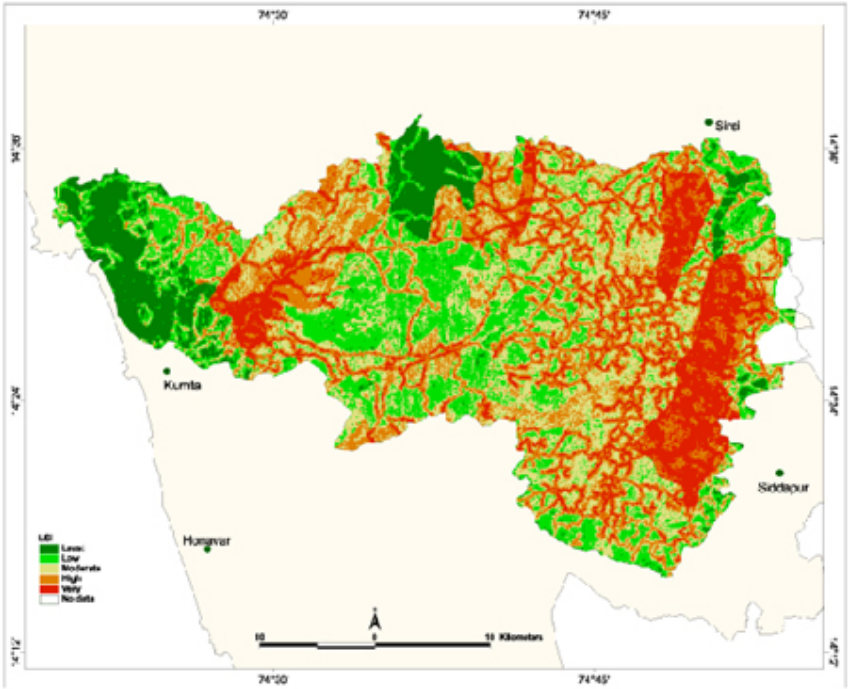

Figure 3: LHS Map of Aghnashini River catchment

References

1. Cruden, D.M., 1991. A Simple Definition of a Landslide. Bulletin of the International Association of Engineering Geology, No. 43, pp. 27-29
2. Guzzetti F (2005), Probabilistic landslide hazard assessment at the basin, doi:10.1016/j.geomorph.2005.06.002
3. Atkinson, P.M., Massari, R., 1998. Generalized linear modelling of landslide susceptibility in the central Apennines, Italy. Computers & Geosciences 24, 373– 385.
4. Dai, F.C., Lee, C.F., 2001. Terrain-based mapping of landslide susceptibility using a geographical information system: a case study. Canadian Geotechnical Journal 38, 911 – 923
5. Wu, W., Sidle, R.C., 1995. A distributed slope stability model for steep forested basins. Water Resources Research 31, 2097– 2110.
6. International Union of Geological Sciences Working Group on Landslides, 1995, A suggested method for describing the rate of movement of a landslide, Bulletin of the International Association of Engineering Geology, 52, 75-78.
7. International Federation of the Red Cross and Red Crescent Societies, I. (2001). World disasters report 2001.
8. Hutchinson JN (1995) Landslide hazard assessment. In: Proc VI Int Symp on Landslides, Christchurch, 1: 1805–1842
9. Varnes DJ, IAEG Commission on Landslides (1984) Landslide hazard zonation – a review of principles and practice. UNESCO, Paris, 63.
10. Akgun A, Serhat Dag S, and Bulut F (2007) Landslide susceptibility mapping for a landslide prone area (Findikli, NE of Turkey) by likelihood-frequency ratio and weighted linear combination models. Environ Geol. doi:10.1007/s00254-007-0882-8
11. Clerici A, Perego S, Tellini C, Vescovi P (2002) A procedure for landslide susceptibility zonation by the conditional analysis method. Geomorphology 48:349–364.
12. Donati L, Turrini MC (2002) An objective method to rank the importance of the factors predisposing to landslides with the GIS methodology: application to an area of the Apennines (Valnerina; Perugia, Italy). Eng Geol 63:277–289.
13. Lee S, Min K (2001) Statistical analysis of landslide susceptibility at Yongin, Korea. Environ Geol 40:1095–1113
14. Lee S, Chwae U, Min K (2002) Landslide susceptibility mapping by correlation between topography and geological structure: the Janghung area, Korea. Geomorphology 46:49– 162
15. Lee S, Choi U (2003) Development of GIS based geological hazard information system and its application for landslide analysis in Korea. Geosci J 7:243–252.
16. Lee S, Pradhan B (2007) Landslide hazard mapping at Selangor, Malaysias using frequency ratio and logistic regression models. Landslides 4(1):33–41
17. Lee S, Talib JA. 2005. Probabilistic landslide susceptibility and factor effect analysis. Environmental Geology 47: 982–990.
18. Zezere JL, Reis E, Garcia R, Oliveira S, Rodrigues ML, Vieira G, Ferreira AB (2004) Integration of spatial and temporal data for the definition of different landslide hazard scenarios in the area north of Lisbon (Portugal). Natural Haz Earth Sys Sciences 4:133– 146
19. Vijith H., Madhu G., (2007), Estimating potential landslide sites of an upland subwatershed in Western Ghat's of Kerala (India) through frequency ratio and GIS, Environ Geol.doi:10.1007/s00254-007-1090-2.

Land cover Assessment using À Trous Wavelet fusion and K-Nearest Neighbour classification

***Abstract*—Landslide is induced by a wide range of ground movements, such as rock falls, deep failure of slopes, shallow debris flows, etc. These ground movements are caused when the stability of a slope changes from a stable to an unstable condition. A change in the stability of a slope can be caused by a number of factors acting together such as loss or absence of vegetation (changes in land cover), soil structure, etc. Loss of vegetation happens when the forest patch is fragmented that can be either anthropogenic or natural. Hence land cover mapping with forest fragmentation can provide an opportunity for visualising the areas that require immediate attention from slope stability aspects. In this paper, À Trous algorithm based wavelet transform is used to merge IRS 1D LISS-III MSS (23.5 m) and PAN (5.8 m) images. The fused images are classified using K-nearest neighbour for land cover categories . A fragmentation model is developed to analyse the extent of forest fragmentation in Uttara Kannada district, Karnataka, India. This helped in visualising the effect of land use changes in five west flowing river basins in the district. Field investigation of land slide region confirm that land cover plays a very vital role in landslides. Change in land cover in the catchment area of these rivers has triggered landslide.**

***Index Terms*—Landslide, à trous, multiresolution**

INTRODUCTION

A LANDSLIDE is a geological phenomenon involving small to medium to large ground movements caused due to change in stability of a slope to an unstable condition. Change in the stability of a slope can be induced by a number of factors, acting together or alone such as rock falls, deep failure of slopes, shallow debris flows, ground water pressure, loss or absence of vegetative cover, erosion, soil nutrients, soil structure, etc. Although the action of gravity is the primary driving force for a landslide to occur, there are other contributing factors affecting the original slope stability. The pre-conditional factors build up specific sub-surface conditions that make the area/slope prone to failure, whereas the actual landslide often requires a trigger before being released. A change in land cover due to the loss of vegetation is a primary factor that builds up specific sub-surface conditions for landslide to occur. The losses in vegetation cover results in fragmenting large, continuous area of forest into two or more fragments. Forest fragmentation apart from affecting the biodiversity and ecology of the region has a significant influence in the movement of soil (silt) and debris in an undulating terrains with high intensity rainfall. Forest fragmentation analysis spatially aids in visualizing the regions that require immediate attention to minimize landslides. Spatial fragmentation map depicts the type and extent of fragmentation. These are derived from land use (LU) data which are obtained from multi-source, multi-sensor, multi-temporal, multi-frequency or multi-polarization remote sensing (RS) data. The objectives of this paper are

i.) Pixel based image fusion of LISS (Linear Imaging Self Scanner)-III MSS (Multispectral) images of 23.5 m spatial resolution with PAN (Panchromatic) image of 5.8 m spatial resolution using À Trous algorithm based wavelet transform (ATW).
ii.) Classification of fused image using K-nearest neighbour to obtain LU map.
iii.) Forest fragmentation analysis to characterise the type and extent of fragmentation or loss of vegetation cover.

METHODS

Pixel based image fusion: Earth observation satellites provide data at different spatial, spectral and temporal resolutions. Satellites, such as IRS bundle a 4:1 ratio of a high resolution PAN band and low resolution MSS bands in order to support both colour and best spatial resolution while minimizing on-board data handling needs [1]. For many applications, the fusion of spatial and spectral data from multiple sensors aids in delineating objects with comprehensive information due to the integration of spatial information present in the PAN image and spectral information present in the low resolution MSS data. Pixel based image fusion refers to the merging of measured physical parameters or fusion at the lowest processing level of co-registered or geocoded data. Many fusion techniques are developed to integrate both PAN and MSS data considering, application of the user. In this communication we use the À Trous algorithm based wavelet transform (ATW).

Multiresolution analysis based on the wavelet theory (WT) is based on the decomposition of the image into multiple channels depending on their local frequency content. While the Fourier transform gives an idea of the frequency content in image, the wavelet representation is an intermediate representation and provides a good localisation in both frequency and space domain [2]. The WT of a distribution f(t) is expressed as

$$W(\mathrm{f})\,(a,b) = |a|^{-\frac{1}{2}} \int_{-\infty}^{+\infty} f(t)\psi\left(\frac{t-b}{a}\right)dt \qquad (1)$$

where a and b are scaling and transitional parameters, respectively. Each base function $\psi\left(\frac{t-b}{a}\right)dt$ is a scaled and translated version of a function ψ called *Mother Wavelet*. These base functions are $\int\psi\left(\frac{t-b}{a}\right)=0$. Most of the WT algorithms produce results that are not shift invariant. An algorithm proposed by Starck and Murtagh [3] uses a WT known as à trous to decompose the image into wavelet planes that overcomes this problem. Given an image $\mathbf{p}$ we construct the sequence of approximations: $F_1(\mathbf{p})=\mathbf{p}_1$, $F_2(\mathbf{p}_1)=\mathbf{p}_2$, $F_3(\mathbf{p}_2)=\mathbf{p}_3$, …. by performing successive convolutions with a filter obtained from an auxiliary function named scaling function which has a $\mathbf{B_3}$

cubic spline profile. The use of a $\mathbf{B_3}$ cubic spline leads to a convolution with a mask of 5 x 5:

$$\frac{1}{256}\begin{pmatrix} 1 & 4 & 6 & 4 & 1 \\ 4 & 16 & 24 & 16 & 4 \\ 6 & 24 & 36 & 24 & 6 \\ 4 & 16 & 24 & 16 & 4 \\ 1 & 4 & 6 & 4 & 1 \end{pmatrix}. \quad (2)$$

The wavelet planes are computed as the differences between two consecutive approximations $\mathbf{p}_{l-1}$ and $\mathbf{p}_l$. Letting $w_l = \mathbf{p}_{l-1} - \mathbf{p}_l$ ($l = 1, \ldots, n$), in which $\mathbf{p}_0 = \mathbf{p}$, the reconstruction formula can be written as

$$\mathrm{p} = \sum_{l=1}^{n} w_l + \mathrm{p_r}. \quad (3)$$

The image $\mathbf{p}_l$ (l = 0, …, n) are versions of original image $\mathbf{p}$, $\mathbf{w}_l$ (l = 1, …, n) are the multiresolution wavelet planes, and $\mathbf{p}_r$ is a residual image. The wavelet merger method is based on the fact that, in the wavelet decomposition, the images $\mathbf{p}_l$ (l = 0, …, n) are the successive versions of the original image. Thus the first wavelet planes of the high resolution PAN image have spatial information that is not present in the MSS image. In this paper, we follow the Additive method [2] where the high resolution PAN image is decomposed to n wavelet planes. For 1:4 fusion (as in IRS 1D) n is set to 2.

$$\mathbf{PAN} = \sum_{l=1}^{n} w_{\mathrm{P}l} + \mathbf{PAN}_r \quad (4)$$

The wavelet planes of the PAN decomposition are added to the low resolution MSS images individually to get high resolution MSS images.

K-nearest neighbour classification: Two of the main challenges in RS data interpretation with using parametric techniques are high dimensional class data modeling and the associated parameter estimates. While the Gaussian normal distribution model has been adopted widely, the need to estimate a large number of covariance terms leads to a high demand on the number of training samples required for each class of interest. In addition, multimode class data cannot be handled properly with a unimodal Gaussian description. Nonparametric methods, such as K-nearest neighbour (KNN) have the advantage of not needing class density function estimation thereby obviating the training set size problem and the need to resolve multimodality [4]. The KNN algorithm [5] assumes that pixels close to each other in feature space are likely to belong to the same class. It bypasses density function estimation and goes directly to a decision rule. Several decision rules have been developed, including a direct majority vote from the nearest k neighbours in the feature space among the training samples, a distance-weighted result and a Bayesian version [6].

Let $\mathbf{x}$ be an unknown pixel vector and suppose there are k_i neighbours labelled as class ω_i out of k nearest neighbours.

$\sum_{i=1}^{M} k_i = k$ (M is the number of class defined).

The basic KNN rule is

$x \in \omega_i, \ if \ m_i(x) > m_j(x)$ for all $\mathrm{j} \neq \mathrm{i}$, where

$$m_i(x) = k_i \quad (5)$$

If the training data of each class is not in proportion to its respective population, $p(\omega_i)$, in the image, a Bayesian Nearest-Neighbour rule is suggested based on Bayes' theorem

$$m_i(x) = \frac{p(x \mid \omega_i)p(\omega_i)}{\sum_{j=1}^{M} p(x \mid \omega_i)p(\omega_j)} = \frac{k_j p(\omega_i)}{\sum_{j=1}^{M} k_j p(\omega_j)} \quad (6)$$

The basic rule does not take the distance of each neighbour to the current pixel vector into account and may lead to tied results every now and then. Weighted-distance rule is used to improve upon this as

$$m_i(x) = \frac{\sum_{j=1}^{k_i} 1/d_{ij}}{\sum_{i=1}^{M}\sum_{j=1}^{k_i} 1/d_{ij}} \quad (7)$$

where d_{ij} is Euclidean distance. Assuming there are S training samples, one needs to find the k nearest neighbours from S training samples for every pixel in a large image. This means S spectral distances must be evaluated for each pixel. The above algorithm is summarised as follows:

The variable unknown denotes the number of pixels whose class is unknown and the variable wrong denotes the number of pixels which have been wrongly classified.
set No: of pixels = 0.
set unknown = 0.
set wrong = 0.
For all the pixels in the test image
do
{
1. Get the feature vector of the pixel and increment no. of pixels by 1.

2. Among all the feature vectors in the training set, find the sample feature vector which is nearest (nearest neighbor) to the feature vector of the pixel.

3. If the no. of nearest neighbors is more than 1, then

Check whether the corresponding class labels of all the nearest sample feature vectors are the same.

If the corresponding class labels are not the same, then increment unknown by 1 and go to Step 1 to process the next pixel else go to Step 4.

4. Class label of the image pixel=class label of the nearest sample vector. Go to Step 1 to process the next pixel.
}

Forest fragmentation: Forest fragmentation is the process whereby a large, continuous area of forest is both reduced in area and divided into two or more fragments. The decline in the size of the forest and the increasing isolation between the two remnant patches of the forest has been the major cause of declining biodiversity [7, 8, 9, 10 and 11]. The primary concern is direct loss of forest area, and all disturbed forests are subject to "edge effects" of one kind or another. Forest fragmentation is of additional concern, insofar as the edge effect is mitigated by the residual spatial pattern [12, 13 and 14].

LU map indicate only the location and type of forest, and further analysis is needed to quantify the forest fragmentation. Total extent of forest and its occurrence as adjacent pixels, fixed-area windows surrounding each forest pixel is used for calculating type of fragmentation. The result is stored at the location of the centre pixel. Thus, a pixel value in the derived map refers to between-pixel fragmentation around the corresponding forest location. As an example [15] if *Pf* is the proportion of pixels in the window that are forested and *Pff* is the proportion of all adjacent (cardinal directions only) pixel pairs that include at least one forest pixel, for which both pixels are forested. Pff estimates the conditional probability that, given a pixel of forest, its neighbour is also forest. The six fragmentation model that identifies six fragmentation categories are: (1) interior, for which Pf = 1.0; (2), patch, Pf < 0.4; (3) transtitional, 0.4 < Pf < 0.6; (4) edge, Pf > 0.6 and Pf-Pff > 0; (5) perforated, Pf > 0.6 and Pf-Pff < 0, and (6) undetermined, Pf > 0.6 and Pf = Pff. When Pff is larger than Pf, the implication is that forest is clumped; the probability that an immediate neighbour is also forest is greater than the average probability of forest within the window. Conversely, when Pff is smaller than Pf, the implication is that whatever is nonforest is clumped. The difference (Pf-Pff) characterises a gradient from forest clumping (edge) to nonforest clumping (perforated). When Pff = Pf, the model cannot distinguish forest or nonforest clumping. The case of Pf = 1 (interior) represents a completely forested window for which Pff must be 1.

STUDY AREA AND DATA

The Uttara Kannada district lies 74°9' to 75°10' east longitude and 13°55' to 15°31' north latitude, extending over an area of 10,291 km^2 in the mid-western part of Karnataka state (Fig. 1). It accounts for 5.37 % of the total area of the state with a population above 1.2 million [16]. This region has gentle undulating hills, rising steeply from a narrow coastal strip bordering the Arabian sea to a plateau at an altitude of 500 m with occasional hills rising above 600–860 m. This district, with 11 taluks, can be broadly categorised into three distinct regions — coastal lands (Karwar, Ankola, Kumta, Honnavar and Bhatkal taluks), mostly forested Sahyadrian interior (Supa, Yellapur, Sirsi and Siddapur taluks) and the eastern margin where the table land begins (Haliyal, Yellapur and Mundgod taluks). Climatic conditions range from arid to humid due to physiographic conditions ranging from plains, mountains to coast.

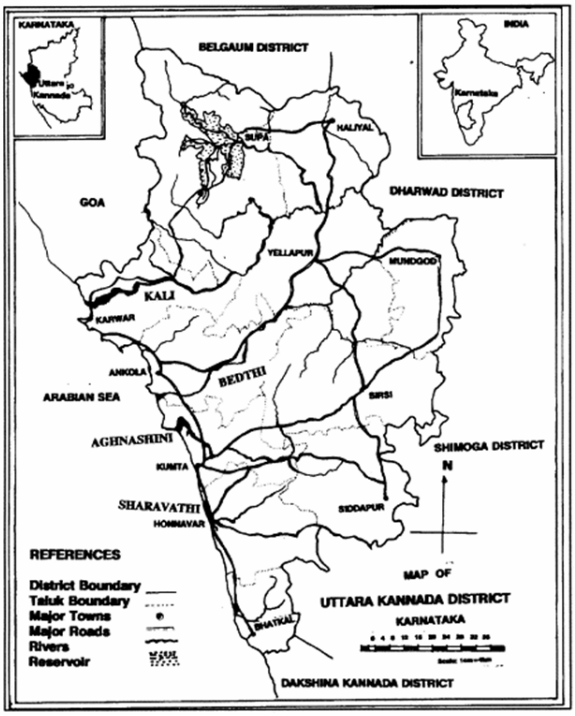

Fig. 1. Uttara Kannada district, Karnataka, India

Survey of India (SOI) toposheets of 1:50000 and 1:250000 scales were used to generate base layers – district and taluk boundaries, water bodies, drainage network, etc. Field data were collected with a handheld GPS. RS data used in the study were LISS-III MSS (in Blue, Green and Red bands) and PAN band, procured from NRSA, Hyderabad, India. Google Earth data (http://earth.google.com) served in pre and post classification process and validation of the results.

Results and Discussion

RS data were geometrically corrected on a pixel by pixel basis. The low resolution MSS images (7562 x 4790) were upsampled to the size of high resolution PAN image (30284 x 19160). MSS and PAN data were fused using ATW method and the decomposition level (n) was set to 2. Land cover (LC) mapping (Fig. 2) was done using normalised difference vegetation index (NDVI) given as

$$\frac{\text{NIR-Red}}{\text{NIR+Red}} \qquad (8)$$

NDVI values range from -1 to +1; increasing values from 0 indicate presence of vegetation and negative values indicate absence of greenery. LC analysis showed 94 % green (agriculture, forest and plantation) and remaining 6 % other categories (builtup, sand, fallow, water).

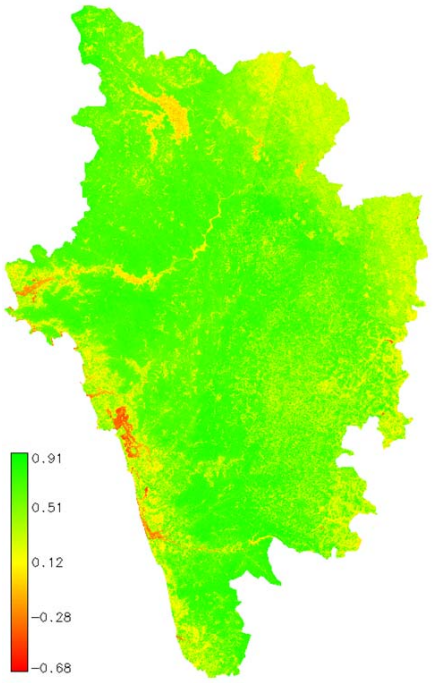

Fig. 2. LC of Uttara Kannada district.

Mapping of water bodies (Fig. 3) was done using normalised difference water index (NDWI) [17] given as

$$\frac{\text{Green-NIR}}{\text{Green+NIR}} \quad (9)$$

NDWI values above 0 indicate presence of water bodies and values below 0 indicate other classes. The major rivers in Uttara Kannada are showed in blue in Fig. 3 that constitute approximately 2.5 % (25000 ha) of the entire district. The class spectral characteristics for six LU categories (agriculture, builtup, forest, plantation, waste land / fallow / sand, and water bodies) using LISS-III MSS bands 2, 3 and 4 were obtained from the training pixels spectra to assess their inter-class separability and the images were classified using KNN with training data uniformly distributed over the study area collected with pre calibrated GPS (Fig. 4). This was validated with the representative field data (training sets collected covering the entire city and validation covering ~ 10% of the study area) and also using Google Earth image. LU statistics, producer's accuracy, user's accuracy and overall accuracy computed are listed in table 1. Using the results from classification, forest fragmentation model was used to obtain fragmentation indices as shown in Fig. 5 and the statistics are presented in table 2.

TABLE I: LU DETAILS OF UTTARA KANNADA DISTRICT

CLASS	AREA (HA)	AREA (%)	P* (%)	U* (%)	O* (%)
AGRICULTURE	38023	3.71	85.21	84.54	89.63
BUILTUP	6638	0.65	86.47	83.11	
FOREST	448815	43.79	94.73	96.20	
PLANTATION	484389	47.26	92.27	91.73	
WASTE LAND / FALLOW / SAND	22311	2.18	88.49	87.88	
WATER BODIES	24663	2.41	93.13	94.33	
TOTAL	1024839	100	-	-	-

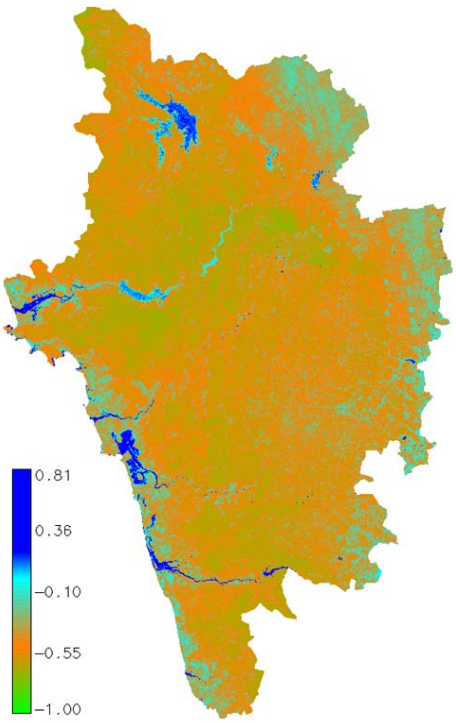

Fig. 3. Water Index of Uttara Kannada district.

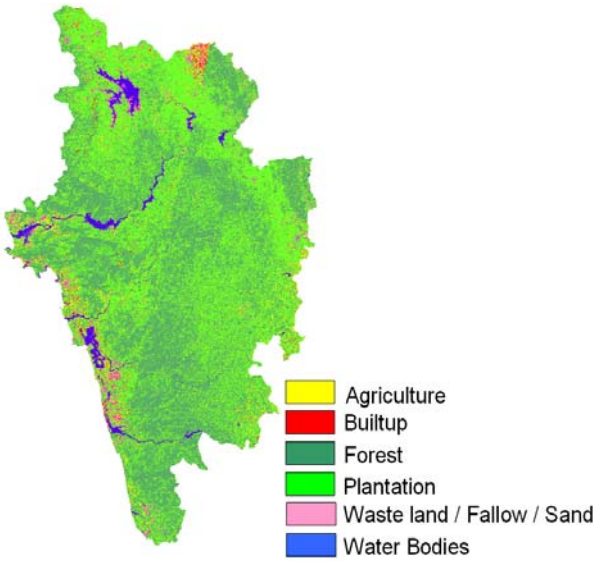

Fig. 4. LU in Uttara Kannada district.

Forest and plantation were considered as a single class - forest and all other classes were considered as non-forest as the extent of land cover is a decisive factor in landslides. It is seen that majority of the area (97 %) is interior forest.

TABLE II: FOREST FRAGMENTAION DETAILS

CLASS	AREA (HA)	AREA (%)
PATCH	917	0.10
TRANSITIONAL	2838	0.33
EDGE	11529	1.24
PERFORATED	9115	0.98
INTERIOR	906946	97.38
TOTAL	931345	100.00

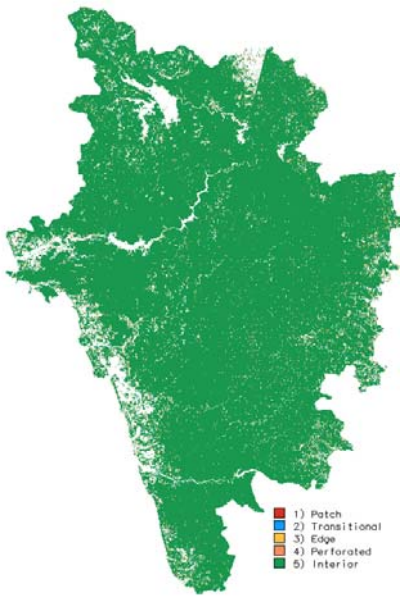

Fig. 5. Fragmentation of forests in Uttara Kannada district.

While the forest fragmentation map produced valuable information, it also helped to visualise the state of forest for tracking the trends and to identify the areas where forest restoration might prove appropriate to reduce the impact of forest fragmentation. Forest fragmentation also depends on the scale of analysis (window size) and various consequences of increasing the window size are reported in [15]. The measurements are also sensitive to pixel size. Nepstad et al., (1999a, 1999b) [18, 19] reported higher fragmentation when using finer grain maps over a fixed extent (window size) of tropical rain forest. Finer grain maps identify more nonforest area where forest cover is dominant but not exclusive. The strict criterion for interior forest is more difficult to satisfy over larger areas. Although knowledge of the feasible parameter space is not critical, there are geometric constraints [20]. For example, it is not possible to obtain a low value of Pff when Pf is large. Percolation theory applies strictly to maps resulting from random processes; hence, the critical values of Pf (0.4 and 0.6) are only approximate and may vary with actual pattern. As a practical matter, when Pf > 0.6, nonforest types generally appeared as "islands" on a forest background, and when Pf < 0.4, forests appeared as "islands" on a nonforest background. There are five major west flowing rivers – Kali, Bedthi, Aginashini, Sharavathi and Venkatpura. Since LU in the catchment area of a river plays an important role in defining the course of the river, water quality and water retaining properties of the soil grains due to the presence of vegetation, the analysis was done for each watershed separately. LU map and forest fragmentation map of the five river basins are shown in Fig. 6 and statistics are given in table III. All the rivers are perennial since the catchment areas are mainly composed of interior forest. However, people have started converting forest patches for agricultural purposes. In addition, the dams present in the major rivers of the district have inundated large vegetation areas. These areas have silt deposit at the river beds and have been classified as sand / waste land. If the vegetative areas have been cleared, the water retaining capacity of the soil has decreased, triggering landslides in those areas. There is a immediate need to restore those vegetative by forestation to ensure that the soil is retained on the hill slopes and do not activate any downward movement of the hill tops.

CONCLUSION

The analysis showed that although the proportion of vegetation (natural forest and plantation which include – Acacea, Araca, Euclyptus, etc.) constitute major part of the LU in the district, recent field survey indicate many forest patches being used for agricultural activities. Conversions of land from forests to agriculture in undulating terrains have contributed to land slides, evident from the field data of landslides in the region. Hence, forest restoration is required to avoid erosion and prevent landslides.

REFERENCES

[1] H. I. Cakir, and S. Khorram, "Pixel Level Fusion of Panchromatic and Multispectral Images Based on Correspondence Analysis," *Photogrammetric Engineering & Remote Sensing,*vol. 74(2), pp. 183-192, 2008.

[2] J. Nunez, X. Otazu, O. Fors, A. Prades, V. Pala, and R. Arbiol, "Multiresolution-Based Image Fusion with Additive Wavelet Decomposition," *IEEE Transactions of Geoscience and Remote Sensing*, vol. 37(3), pp. 1204-1221, 1999.

[3] J. L. Starck and F. Murtagh, "Image restoration with noise suppression using the wavelet transform," *Astron. Astrophys*, vol. 228, pp. 342-350, 1994.

[4] Venkatesh, Y.V., KumarRaja, S., 2003. On the classification of multispectral satellite images using the multilayer perceptron. Pattern Recognition, vol. 36, pp. 2161 – 2175.

[5] B. V. Dasarathy (Editor), Nearest neighbor (NN) norms: NN pattern classification techniques, IEEE Computer Society Press, Los Alamitos, California, 1990.

[6] P. J. Hardin, "Parametric and Nearest-neighbor methods for hybrid classification: A comparison of pixel assignment accuracy," Photogrammetric Engineering & Remote Sensing, vol. 60, pp. 1439-1448, Dec, 1994.

[7] R. P. Tucker, and J. F. Richards, "*Global deforestation and the nineteenth century world economy*," Duke University Press, Durham, North Carolina, USA, 1983.

[8] B. L. Turner, W. C. Clark, R. W. Kates, J. F. Richards, J. T. Mathews, and W. B. Meyer, "*The Earth as transformed by human action*," Cambridge University Press, Cambridge, UK, 1990.

[9] W. B. Meyer, and B. L. Turner, "*Changes in land use and land cover: a global perspective*," Cambridge University Press, Cambridge, UK, 1994.

[10] R. A. Houghton, "The worldwide extent of land-use change," BioScience, vol. 44, pp. 305-313, 1994.

[11] J. D. Hurd, E. H. Wilson, S. G. Lammey, and D. L. Civco, "Characterization of Forest Fragmentation and Urban Sprawl using time sequential Landsat Imagery," In ASPRS 2001 Annual Convention, St. Louis, MO, 2001.

[12] R. T. T. Forman, and M. Godron, "*Landscape Ecology*," John Wiley, New York, 1986.

[13] M. G. Turner, "*Landscape ecology: the effect of pattern on process*," Annual Review of Ecology and Systematics, vol. 20, pp. 171-197, 1989.

[14] S. A. Levin, "*The problem of pattern and scale in ecology*," Ecology, vol. 73, pp. 1943-1967, 1992.

[15] K., J. Riitters, R. O' Neill. Wickham, B. Jones, and E. Smith, "*Global-scale patterns of forest fragmentation*," Conservation Ecology, vol. 4(2-3), 2000.

[16] T. V. Ramachandra and A. V. Nagarathna, "Energetics in paddy cultivation in Uttara Kannada district," Energy Conservation and Management, vol. 42(2), pp. 131-155, 2001.

[17] McFeeters, S. K., 1996. The use of normalized difference water index (NDWI) in the delineation of open water features, *International Journal of Remote Sensing*, 17(7): 1425–1432.

[18] D. C. Nepstad, P. Lefebvre, and E. A. Davidson, "*Positive feedbacks in the fire dynamic of closed canopy tropical forests,"* Science, vol. 284, pp. 1832-1835, 1999a.

[19] D. C. Nepstad, A. Verissimo, A. Alencar, C. Nobre, E. Lima, P. Lefebvre, P. Schlesinger, C. Potter, P. Moutinho, E. Mendoza, M. Cochrane, and V. Brooks, "*Large-scale impoverishment of Amazonian forests by logging and fire*," Nature, vol. 98, pp. 505-508, 1999b.

[20] R. V. O'Neill, C. T. Hunsaker, S. P. Timmins, B. L. Jackson, K. B. Jones, K. H. Ritters, and J. D. Wickham, "*Scale problems in reporting landscape pattern at the regional scale*," Landscape Ecology, vol. 11, pp. 169-180, 1996.

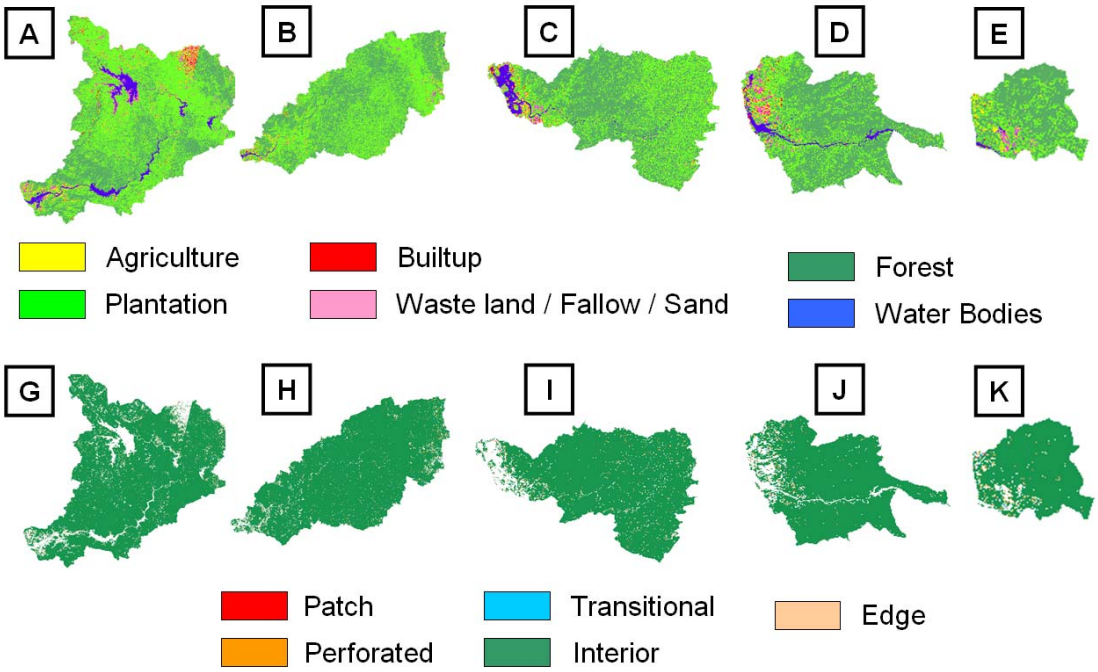

Fig. 6. LU in the catchments of five major river basins in Uttara Kannada district – (A) Kali, (B) Bedthi, (C) Aginashini, (D) Sharavathi, (E) Venkatpura. Forest fragmentation in five river basins in Uttara Kannada district – (G) Kali, (H) Bedthi, (I) Aginashini, (J) Sharavathi, (K) Venkatpura.

TABLE III: LU DETAILS OF THE FIVE RIVER BASINS

CLASSES →	AGRICULTURE		BUILTUP		FOREST		PLANTATION		WASTE LAND / FALLOW / SAND		WATER BODIES	
AREA →	Ha	%	Ha	%	Ha	%	Ha	%	Ha	%	Ha	%
KALI	13305	3.56	3176	0.85	127311	34	203491	54.4	11240	3	15023	4
BEDTHI	5671	2	652.4	0.24	126532	46.3	136746	50	2616	0.96	1242	0.45
AGINASHINI	3654	2.68	673	0.49	72356	53	53604	39.3	1929	1.41	4323	3.17
SHARAVATHI	2537	3.13	607.7	0.75	49367	61	23794	29.4	2093	2.58	2627	3.24
VENKATPURA	778	3.45	73	0.32	14491	64.3	6507	28.8	509	2.26	197.8	0.88

TABLE IV: FOREST FRAGMENTATION DETAILS OF THE FIVE RIVER BASINS

CLASSES →	PATCH		TRANSITIONAL		EDGE		PERFORATED		INTERIOR	
AREA →	Ha	%	Ha	%	Ha	%	Ha	%	Ha	%
KALI	359	0.11	1085	0.33	4119	1.25	3027	0.92	321589	97.4
BEDTHI	159	0.06	501	0.19	2462	0.94	1655	0.63	258209	98.18
AGINASHINI	70.8	0.06	234.6	0.19	1191	0.95	961	0.76	123265	98.05
SHARAVATHI	53	0.07	163.3	0.22	632.2	0.87	571.1	0.78	71465.8	98.05
VENKATPURA	23.49	0.11	67.08	0.32	246.3	1.18	225	1.07	20379	97.32

Landslide Susceptible Locations in Western Ghats: Prediction through openModeller

***Abstract*— Many shallow landslides are triggered by heavy rainfall on hill slopes resulting in enormous casualties and huge economic losses in mountainous regions. Hill slope failure usually occurs as soil resistance deteriorates in the presence of the acting stress developed due to a number of reasons such as increased soil moisture content, change in land use causing slope instability, etc. Landslides triggered by rainfall can possibly be foreseen in real time by jointly using rainfall intensity-duration and information related to land surface susceptibility. Terrain analysis applications using spatial data such as aspect, slope, flow direction, compound topographic index, etc. along with information derived from remotely sensed data such as land cover / land use maps permit us to quantify and characterise the physical processes governing the landslide occurrence phenomenon. In this work, the probable landslide prone areas are predicted using two different algorithms – GARP (Genetic Algorithm for Rule-set Prediction) and Support Vector Machine (SVM) in a free and open source software package - openModeller. Several environmental layers such as aspect, digital elevation data, flow accumulation, flow direction, slope, land cover, compound topographic index, and precipitation data were used in modelling. A comparison of the simulated outputs, validated by overlaying the actual landslide occurrence points showed 92% accuracy with GARP and 96% accuracy with SVM in predicting landslide prone areas considering precipitation in the wettest month whereas 91% and 94% accuracy were obtained from GARP and SVM considering precipitation in the wettest quarter of the year.**

***Index Terms*—Landslide, GARP, SVM, openModeller**

INTRODUCTION

Landslides are one of the most widespread natural hazards on Earth causing casualties and property loses. They are sudden hydrogeomorphic events due to the combination of i) predisposing factors (e.g. lithology and morphology), ii) triggering factors (e.g. excessive and intense precipitations) and iii) accelerating factors (e.g. human activities altering natural slope stability) [1]. Among landslide typologies, shallow landsliding is common on steep topographies covered by colluvial or residual soils whose texture can vary from sand to clayey silt [2], playing a significant role in hill slope denudation and catchment sediment dynamics. The possible time and locations where landslides are likely to occur should thus be identified in advance in order to avoid or reduce the harm. In this regard, establishing a landslide warning system which provides information for evacuation and hazard mitigating is a top priority.

Prediction of rainfall-triggered hill slope disasters has relied mostly on the valley slope [3 and 4], rainfall intensity and duration that can cause hill slope failure [5, 6, 7 and 8]. Recently, theoretical models have been developed to predict landslide susceptibility based on watershed topographic, geologic and hydrological variables as well as changes in landuse [9, 10, 11, 12, 13 and 14]. The rapidly growing availability of relatively detailed digital elevation data, coupled with simple slope-instability mechanism and hill slope hydrological models, has led to advances in physically-based modeling of shallow landslide hazard [9, 15]. Casadei et al., [16] proposed a landslide warming system using a slope-instability analysis and a hydrological model to predict the time and location of landslides that were verified using historical data of landslide events for Montara Mountains of California from 1953–1998 [17].

Given the complex spatial dynamics of the process, most of the hazard evaluation tools make use of Geographical Information Systems (GIS), capable of geospatial and multitemporal data integration. The availability of digital elevation models (DEMs) and precipitation data at higher spatial and temporal resolution [1] encourage the development of more sophisticated techniques for shallow landslide hazard modelling [9, 15, 18, 19, 20, 21 and 13]. Several of these methods are based on the infinite slope stability equation [22] coupled with hydrological models (e.g. [9, 15 and 13]), extensively applied for the estimation of spatially variable soil wetness (e.g. [23, 24 and 25]). SHALSTAB [9 and 26] is one of these models. Various models have been developed in order to assess landslide incidence potential [27, 28, 29 and 30]. Among these techniques, deterministic, heuristic and statistical methods are the most common ones. Deterministic methods deal with the estimation of quantitative values of stability variables, over a defined area where the landslide types are simple with homogeneous intrinsic properties [31]. The required data include soil strength, depth below the terrain surface, soil layer thickness, slope angle and water pressure. These methods have been employed in translational landslides studies [32] and are applicable at large scale over small areas. One of the main drawbacks of these methods is their high degree of oversimplification when the data are incomplete. Another problem is that the data requirements for deterministic models can be prohibitive, and frequently it is impossible to acquire the input data necessary to use the model effectively.

In this context, the present study explores the suitability of pattern recognition techniques to predict the probable distribution of landslide occurrence

points based on several environmental layers along with the known points of occurrence of landslides. The aims of the study are:

i.) to apply and evaluate Genetic Algorithm for Rule-set Prediction and Support Vector Machine based models for predicting landslides;
ii.) to compare and assess the results of these analyses;
iii.) to suggest management strategies for preventing potential losses.

The model utilises precipitation and six site factors including aspect, DEM, flow accumulation, flow direction, slope, land cover, compound topographic index and historical landslide occurrence points. Both precipitation in the wettest month and precipitation in the wettest quarter of the year were considered separately to analyse the effect of rainfall on hill slope failure for generating scenarios to predict landslides.

Methods

Genetic Algorithm for Rule-set Prediction (GARP): GARP is based on genetic algorithms originally meant to generate niche models for biological species. In this case, the models describe environmental conditions under which the species should be able to maintain populations. GARP is used in the current work here to predict the locations susceptible for landslides with the known landslide occurrence points.

For input, GARP uses a set of point localities where the landslide is known to occur and a set of geographic layers representing the environmental parameters that might limit the landslide existence. Genetic Algorithms (GAs) are a class of computational models that mimic the natural evolution to solve problems in a wide variety of domains. GAs are suitable for solving complex optimisation problems and for applications that require adaptive problem-solving strategies. They are also used as search algorithms based on mechanics of natural genetics that operates on a set of individual elements (the population) and a set of biologically inspired operators which can change these individuals. It maps strings of numbers to each potential solution and then each string becomes a representation of an individual. Then the most promising in its search is manipulated for improved solution [33]. The model developed by GARP is composed of a set of rules. These set of rules is developed through evolutionary refinement, testing and selecting rules on random subsets of training data sets. Application of a rule set is more complicated as the prediction system must choose which rule of a number of applicable rules to apply. GARP maximises the significance and predictive accuracy of rules without overfitting. Significance is established through a χ^2 test on the difference in the probability of the predicted value before and after application of the rule. GARP uses envelope rules, GARP rules, atomic and logit rules. In envelope rule, the conjunction of ranges for all of the variables is a climatic envelope or profile, indicating geographical regions where the climate is suitable for that entity, enclosing values for each parameter. A GARP rule is similar to an envelope rule, except that variables can be irrelevant. An irrelevant variable is one where points may fall within the whole range. An atomic rule is a conjunction of categories or single values of some variables. Logit rules are an adaptation of logistic regression models to rules. A logistic regression is a form of regression equation where the output is transformed into a probability [34].

Support Vector Machine (SVM): SVM are supervised learning algorithms based on statistical learning theory, which are considered to be heuristic algorithms [35]. SVM map input vectors to a higher dimensional space where a maximal separating hyper plane is constructed. Two parallel hyper planes are constructed on each side of the hyper plane that separates the data. The separating hyper plane maximises the distance between the two parallel hyper planes. An assumption is made that the larger the margin or distance between these parallel hyper planes, the better the generalisation error of the classifier will be. The model produced by support vector classification only depends on a subset of the training data, because the cost function for building the model does not take into account training points that lie beyond the margin [35].

In order to classify *n*-dimensional data sets, *n-1* dimensional hyper plane is produced with SVMs. As it seen from Fig. 1 [35], there are various hyper planes separating two classes of data. However, there is only one hyper plane that provides maximum margin between the two classes [35] (Fig. 2), which is the optimum hyper plane. The points that constrain the width of the margin are the support vectors.

In the binary case, SVMs locates a hyper plane that maximises the distance from the members of each class to the optimal hyper plane. If there is a training data set containing *m* number of samples represented by $\{x_i, y_i\}$ $(i = 1, \ldots, m)$, where $x \varepsilon R^N$, is an N-dimensional space, and $y \varepsilon \{-1, +1\}$ is class label, then the optimum hyper plane maximises the margin between the classes. As in Fig. 3, the hyper plane is defined as $(w.x_i + b = 0)$ [35], where x is a point lying on the hyper plane, parameter w determines the orientation of the hyper plane in space, b is the bias that the distance of hyper plane from the origin. For the linearly separable case, a separating hyper plane can be defined for two classes as:

$$w \,.\, x_i + b \geq +1 \text{ for all } y = +1 \qquad (1)$$

$w \cdot x_i + b \leq -1$ for all $y = -1$ (2)

These inequalities can be combined into a single inequality:

$y_i (w \cdot x_i + b) - 1 \geq 0$ (3)

The training data points on these two hyper planes, which are parallel to the optimum hyper plane and defined by the functions $w \cdot x_i + b = \pm 1$, are the support vectors [36]. If a hyper plane exists that satisfies (3), the classes are linearly separable. Therefore, the margin between these planes is equal to $2/\|w\|$ [37]. As the distance to the closest point is $2/\|w\|$, the optimum separating hyper plane can be found by minimizing $\|w\|^2$ under the constraint (3).

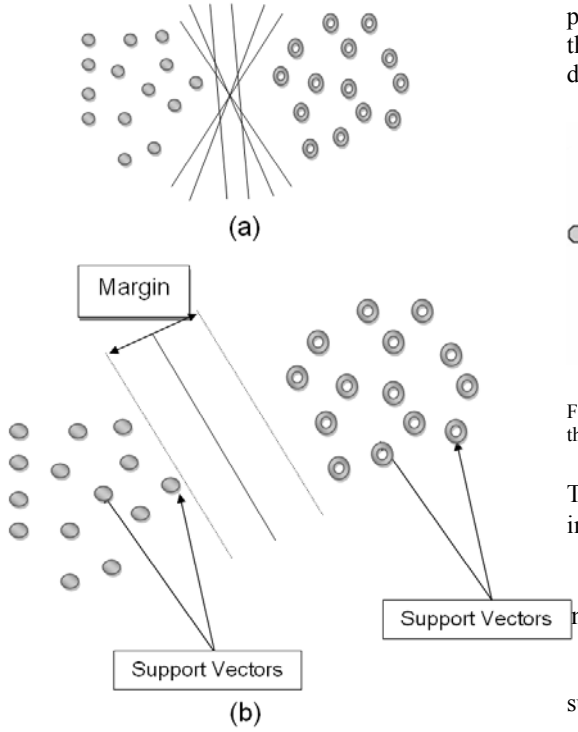

Fig. 1. (a) Hyper planes for linearly separable data, (b) Optimum hyper plane and support vectors [35].

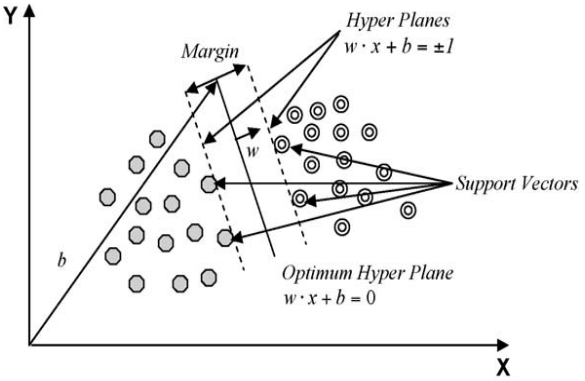

Fig. 2. Support vectors and optimum hyper plane for the binary case of linearly separable data sets [35].

Thus, determination of optimum hyper plane is required to solve optimisation problem given by:

$$\min(0.5 * \|w\|^2) \quad (4)$$

subject to constraints,

$$y_i (w \cdot x_i + b) \geq -1 \quad \text{and } y_i \in \{+1, -1\} \quad (5)$$

As illustrated in Fig. 3 (a) [35], nonlinearly separable data is the case in various classification problems as in the classification of remotely sensed images using pixel samples. In such cases, data sets cannot be classified into two classes with a linear function in input space. Where it is not possible to have a hyper plane defined by linear equations on the training data, the technique can be extended to allow for nonlinear decision surfaces [38, 39].

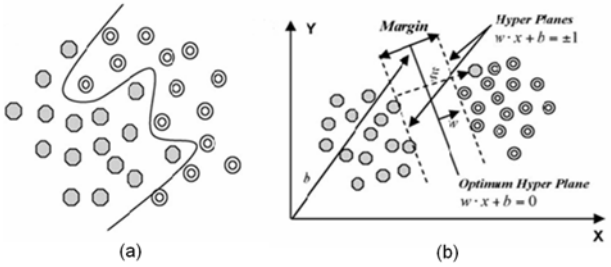

Fig. 3. (a) Separation of nonlinear data sets, (b) Generalisation of the solution by introducing slack variable for nonlinear data [35].

Thus, the optimisation problem is replaced by introducing ξ slack variable (Fig. 3(b)).

$$\min\left[\frac{\|w\|^2}{2} + C\sum_{i=1}^{r}\xi_i\right] \quad (6)$$

subject to constraints,

$$y_i(w.x_i + b) \geq 1 - \xi_i, \xi_i \geq 0, i = 1, \ldots, N \quad (7)$$

where C is a regularisation constant or penalty parameter. This parameter allows striking a balance between the two competing criteria of margin maximisation and error minimisation, whereas the slack variables ξ_i indicates the distance of the incorrectly classified points from the optimal hyper plane [40]. The larger the C value, the higher the penalty associated to misclassified samples [41].

When it is not possible to define the hyper plane by linear equations, the data can be mapped into a higher dimensional space (H) through some nonlinear mapping functions *(Φ)*. An input data point x is represented as Φ(x) in the high-dimensional space. The expensive computation of $(\Phi(x).\Phi(x_i))$ is reduced

by using a kernel function [36]. Thus, the classification decision function becomes:

$$f(x) = \text{sign}\left(\sum_{i}^{r} \alpha_i y_i K(x, x_i) + b\right) \qquad (8)$$

where for each of *r* training cases there is a vector (x_i) that represents the spectral response of the case together with a definition of class membership (y_i).α_i (i = 1,….., *r*) are Lagrange multipliers and K(x, x_i) is the kernel function. The magnitude of α_i is determined by the parameter C [42]. The kernel function enables the data points to spread in such a way that a linear hyper plane can be fitted [43]. Kernel functions commonly used in SVMs can be generally aggregated into four groups; namely, linear, polynomial, radial basis function and sigmoid kernels. The performance of SVMs varies depending on the choice of the kernel function and its parameters. A free and open source software – openModeller [44] was used for predicting the probable landslide areas. openModeller (http://openmodeller.sourceforge.net/) is a flexible, user friendly, cross-platform environment where the entire process of conducting a fundamental niche modeling experiment can be carried out. It includes facilities for reading landslide occurrence and environmental data, selection of environmental layers on which the model should be based, creating a fundamental niche model and projecting the model into an environmental scenario using a number of algorithms as shown in Fig. 4.

STUDY AREA AND DATA

The Uttara Kannada district lies 74°9′ to 75°10′ east longitude and 13°55′ to 15°31′ north latitude, extending over an area of 10, 291 km^2 in the mid-western part of Karnataka state (Fig. 5). It accounts for 5.37 % of the total area of the state with a population above 1.2 million [45]. This region has gentle undulating hills, rising steeply from a narrow coastal strip bordering the Arabian sea to a plateau at an altitude of 500 m with occasional hills rising above 600–860 m. This district with 11 taluks, can be broadly categorised into three distinct regions — coastal lands (Karwar, Ankola, Kumta, Honnavar and Bhatkal taluks), mostly forested Sahyadrian interior (Supa, Yellapur, Sirsi and Siddapur taluks) and the eastern margin where the table land begins (Haliyal, Yellapur and Mundgod taluks). Climatic conditions range from arid to humid due to physiographic conditions ranging from plains, mountains to coast.

Survey of India (SOI) toposheets of 1:50000 and 1:250000 scales were used to generate base layers – district and taluk boundaries, water bodies, drainage network, etc. Field data were collected with a handheld GPS. Environmental data such as precipitation of wettest month and precipitation in the wettest quarter were downloaded from WorldClim – Global Climate Data [http://www.worldclim.org/bioclim].

Precipitation (atmospheric water phenomena) is any product of the condensation of atmospheric water vapor that is pulled down by gravity and deposited on the Earth's surface such as rain.

Other environmental layers used in the model were obtained from USGS Earth Resources Observation and Science (EROS) Center based Hydro1Kdatabase [http://eros.usgs.gov/#/Find_Data/Products_and_Data_Available/gtopo30/hydro/asia] which are as follows:

Aspect - describes the direction of maximum rate of change in the elevations or the slope direction. It is measured in positive integer degrees from 0 to 360, clockwise from north. Aspects of cells (pixels) of zero slope (flat areas) are assigned values of -1.

DEM – is a digital representation of ground surface topography or terrain represented as a raster (a grid of squares) or as a triangular irregular network. DEMs are commonly built using remote sensing techniques or from land surveying.

Flow accumulation (FA) - defines the number of pixels which flow into each downslope pixel. Since the pixel size of the HYDRO1k data set is 1 km, the flow accumulation value translates directly into upstream drainage areas in square kilometers. Values range from 0 at topographic highs to very large numbers (on the order of millions of square kilometers) at the mouths of large rivers.

Flow direction (FD) - defines the direction of flow from each cell to its steepest down-slope neighbor derived from the hydrologically correct DEM. Values of flow direction vary from 1 to 255.

Slope - describes the maximum change in the elevations between each pixel and its eight neighbors expressed in integer degrees of slope between 0 and 90.

Compound Topographic Index (CTI) - commonly referred to as the Wetness Index, is a function of the upstream contributing area and the slope of the landscape. It is calculated using the flow accumulation (FA) layer along with the slope as:

$$\text{CTI} = \ln\left(\frac{\text{FA}}{\tan(\text{slope})}\right) \qquad \textbf{(9)}$$

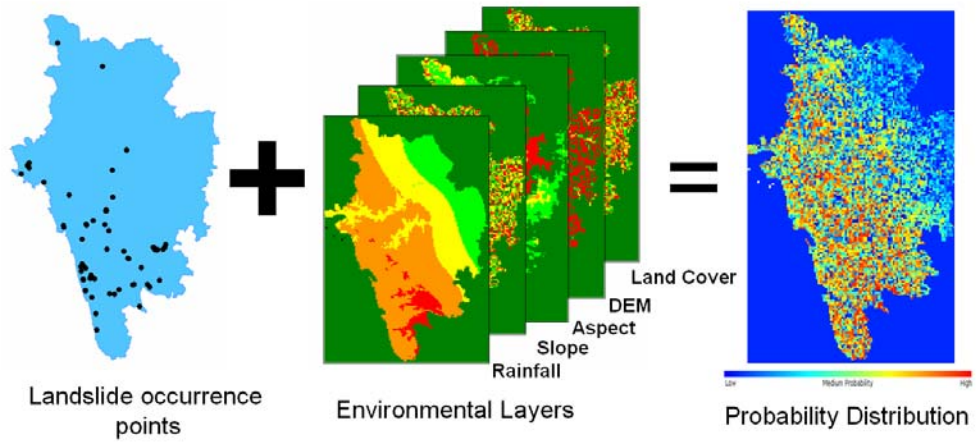

Fig. 4. Methodology used for landslide prediction in openModeller.

Fig. 5. Uttara Kannada district, Karnataka, India

In areas of no slope, a CTI value is obtained by substituting a slope of 0.001. This value is smaller than the smallest slope obtainable from a 1000 m data set with a 1 m vertical resolution.

8.) The global land cover change maps were obtained from Global Land Cover Facility, Land Cover Change [http://glcf.umiacs.umd.edu/services/landcoverchange/landcover.shtml; http://www.landcover.org/services/landcoverchange/landcover.shtml].

The spatial resolution of all the data were 1 km. Google Earth data (http://earth.google.com) served in pre and post classification process and validation of the results. 125 landslide occurrence points of low, medium and high intensity were recorded using GPS from the field and published reports.

RESULTS AND DISCUSSION

Two different precipitation layers were used to predict landslides – precipitation of wettest month and precipitation in the wettest quarter of the year along with the seven other layers as mentioned in section III. Figure 6 (a) and (b) are the landslide probability maps using GARP and SVM on precipitation of wettest month. The landslide occurrence points were overlaid on the probability maps to validate the prediction as shown in Fig. 7. The GARP map had an accuracy of 92% and SVM map was 96% accurate with respect to the ground and Kappa values 0.8733 and 0.9083 respectively. The corresponding ROC curves are shown in Fig. 8 (a) and (b). Total area under curve (AUC) for Fig. 8 (a) is 0.87 and for Fig. 8 (b) is 0.93. Figure 6 (c) and (d) are the landslide probability maps using GARP and SVM on precipitation of wettest quarter with accuracy of 91% and 94% and Kappa values of 0.9014 and 0.9387 respectively.

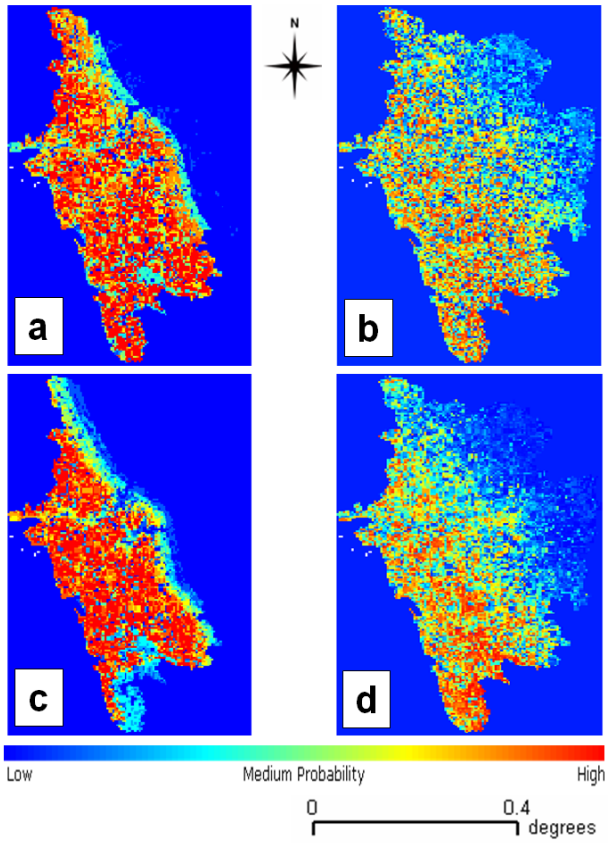

Fig. 6. Probability distribution of the landslide prone areas.

ROC curves in figure 8 (c) and (d) show AUC as 0.90 and 0.94. Various measures of accuracy were used as per [46] to assess the outputs. Table I presents the confusion matrix structure indicating true positives, false positives, false negatives and true negatives.

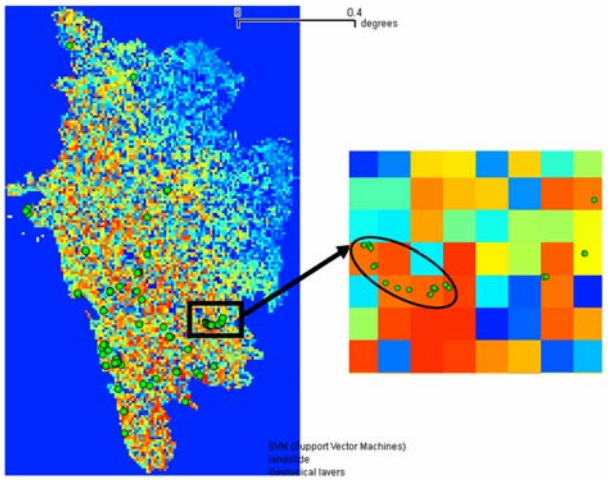

Fig. 7. Validation of the probability distribution of the landslide prone areas by overlaying landslide occurrence points.

Confusion matrices were generated for each of the 4 outputs (Table II) and different measures of accuracy such as prevalence, global diagnostic power, correct classification

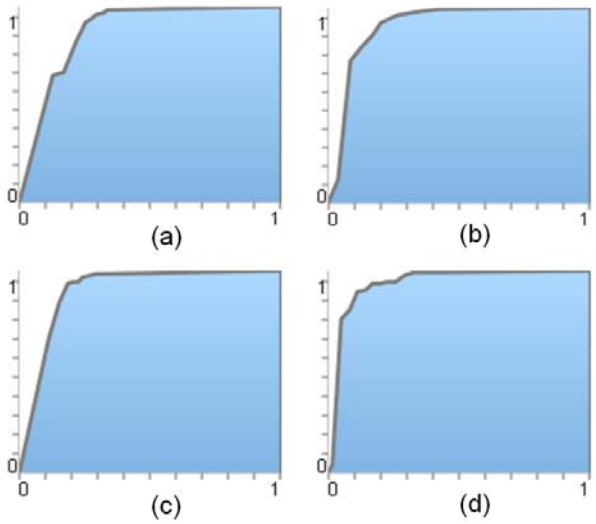

Fig. 8. ROC curves for landslide prone maps (a) GARP (b) SVM on precipitation of wettest month; (c) GARP and (d) SVM on precipitation of wettest quarter.

rate, sensitivity, specificity, omission and commission error were computed as listed in Table III.

The results indicate that the output obtained from SVM using precipitation of the wettest month was best among the 4 scenarios. It maybe noted that the outputs from GARP for both the wettest precipitation month and quarter are close to the SVM in term of accuracy. One reason is that, most of the areas have been predicted as probable landslide prone zones (indicated in red in Fig. 6 (a) and (c)) and the terrain is highly undulating with steep slopes that are frequently exposed to landslides induced by rainfall. Obviously, the maximum number of landslide points occurring in the undulating terrain, collected from the ground will fall in those areas indicating that they are more susceptible to landslides compared to north-eastern part of the district which has relatively flat terrain.

Another case study of Kerala state, India was carried out with the same environmental layers along with 10 landslide occurrence points as shown in Fig. 9. The predicted output for precipitation in the wettest month is shown in Fig. 10 and precipitation in the wettest quarter is shown in Fig. 11 with an overall accuracy of 60%. The Kappa values for two cases were 0.966335 and 0.96532. The ROC curves are shown in Fig. 12 (a) and (b) with 0.97 AUC for both the cases respectively. The confusion matrix and statistics are presented in Table IV and V. The reason for low accuracy is the presence of only 10 occurrence points throughout the state. Also, the coarse resolution of the pixel may be attributed for poor accuracy. However, the Kappa value and the AUC are high which indicate that the probability distribution of the predicted points fall well within the occurrence points. It is another matter that the intensity of these landslide points may vary from low to medium to high. One potential limitation of the above data is their spatial resolution – 1 km. It is highly unlikely that landslides of this magnitude can occur in the study area. However,

TABLE I
CONFUSION MATRIX STRUCTURE

	TRUE PRESENCE	TRUE ABSENCE
PREDICTED PRESENCE	A	B
PREDICTED ABSENCE	C	D

Key: A – True Positive, B – False Positive, C – False Negative, D – True Negative.

given the environmental layers along with the occurrence points, the probable areas of occurrence can be mapped with great certainty.

The movement of a slope is complex and it is induced or perturbed by many other factors besides rainfall such as groundwater data, soil moisture information, etc. which were not used in the prediction. It is known that there are accelerations of slope movements after intense rainfall, however, to what extent rainfall affects the slope movement remains unknown and the correlation between rainfall and the slope movement could be ambiguous in absence of detailed observations. Timely rainfall, soil moisture, grain-size, lithology, geological structure, seismological observations and the longer time intervals for which data are available can improve the accuracy of the model. Beyond their key role in identifying and mapping the landslides, the choice of the variables (environmental layers) used for the prediction are also closely involved. Some limitations of the data set cannot be overcome. In this study for example, no hydrological field data were available. However, significant results were obtained in the study because the variables most influential on landslide were used.

Natural disasters have drastically increased over the last decades. National, state and local government including NGOs are concerned with the loss of human life and damage to property caused by natural disasters. The trend of increasing incidences of landslides occurrence is expected to continue in the next decades due to urbanisation, continued anthropogenic activities, deforestation in the name of development and increased regional precipitation in landslide-prone areas due to changing climatic patterns [47]. The application of modern technologies required to control the effects of natural hazards including landslides must consider three significant factors - prediction, monitoring and conservation. In fact, the promotion of accessibility to urban facilities, such as homes and new roads in mountainous areas is difficult to achieve without considering geological and geotechnical factors to ensure that the development is pleasant and safe. Therefore, it is desired to have a notion about the main factors controlling the slope instability, assessing its severity, discriminating areas with presence/absence of landslides, updating and interpreting landslide data and determining areas that are prone to landslides. In this regard, the present work may be a contribution to the beginning of such disaster and mitigation studies.

Fig. 9. Landslide occurrence points in Kerala.

TABLE II
CONFUSION MATRIX FOR GARP AND SVM OUTPUTS FOR UTTARA KANNADA

UTTARA KANNADA		TRUE PRESENCE	TRUE ABSENCE	NUMBER OF USABLE PRESENCE	NUMBER OF USABLE ABSENCE
GARP WITH PRECIPITATION OF WETTEST MONTH	PREDICTED PRESENCE	120	0	125	0
	PREDICTED ABSENCE	5	0		
SVM WITH PRECIPITATION OF WETTEST MONTH	PREDICTED PRESENCE	118	0	125	0
	PREDICTED PRESENCE	7	0		

GARP WITH PRECIPITATION OF WETTEST QUARTER	**PREDICTED PRESENCE**	118	0	125	0
	PREDICTED PRESENCE	7	0		
SVM WITH PRECIPITATION OF WETTEST QUARTER	**PREDICTED PRESENCE**	117	0	125	0
	PREDICTED PRESENCE	8	0		

TABLE III
STATISTICS OF GARP AND SVM OUTPUTS FOR UTTARA KANNADA

UTTARA KANNADA	**PREVALENCE** (A+C)/N	**GLOBAL DIAGNOSTIC POWER** (B+D)/N	**CORRECT CLASSIFICATION RATE** (A+D)/N	**SENSITIVITY** A/(A+C)	**SPECIFICITY** D/(B+D)	**OMISSION ERROR** C/(A+C)	**COMMISION ERROR** B/(B+D)
GARP WITH PRECIPITATION OF WETTEST MONTH	-	-	0.96	0.96	-	0.04	-
SVM WITH PRECIPITATION OF WETTEST MONTH	-	-	0.94	0.94	-	0.06	-
GARP WITH PRECIPITATION OF WETTEST QUARTER	-	-	0.94	0.94	-	0.06	-
SVM WITH PRECIPITATION OF WETTEST QUARTER	-	-	0.94	0.94	-	0.06	-

* Key: A – True Positive, B – False Positive, C – False Negative, D – True Negative, N – Number of Samples.

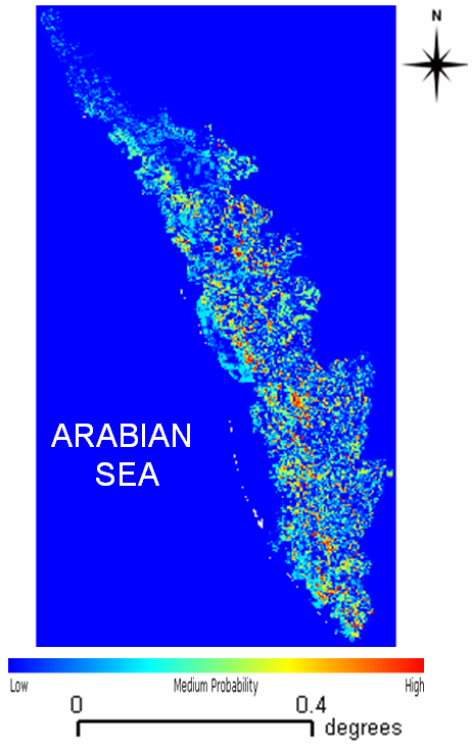

Fig. 10. Probability distribution of the landslide prone areas in Kerala using precipitation in the wettest month data.

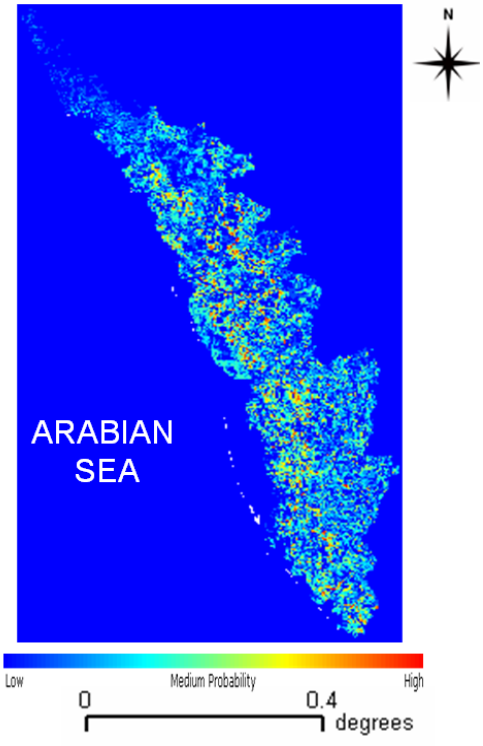

Fig. 11. Probability distribution of the landslide prone areas in Kerala using precipitation in the wettest quarter data.

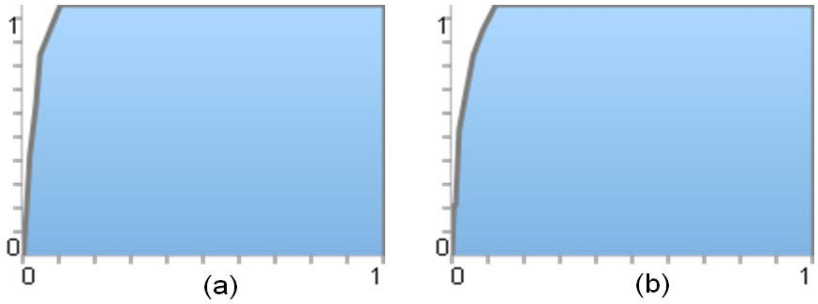

Fig. 12. ROC curves for the predicted landslide prone maps of Kerala.
(a) using precipitation of the wettest month, (b) using precipitation of the wettest quarter.

TABLE IV
CONFUSION MATRIX FOR GARP OUTPUTS FOR KERALA

KERALA		TRUE PRESENCE	TRUE ABSENCE	NUMBER OF USABLE PRESENCE	NUMBER OF USABLE ABSENCE
GARP WITH PRECIPITATION OF WETTEST MONTH	PREDICTED PRESENCE	6	0	10	0
	PREDICTED ABSENCE	4	0		
GARP WITH PRECIPITATION OF WETTEST QUARTER	PREDICTED PRESENCE	6	0	10	0
	PREDICTED PRESENCE	4	0		

TABLE V
STATISTICS OF GARP OUTPUTS FOR KERALA

KERALA	PREVALENCE (A+C)/N	GLOBAL DIAGNOSTIC POWER (B+D)/N	CORRECT CLASSIFICATION RATE (A+D)/N	SENSITIVITY A/(A+C)	SPECIFICITY D/(B+D)	OMISSION ERROR C/(A+C)	COMMISION ERROR B/(B+D)
GARP WITH PRECIPITATION OF WETTEST MONTH	-	-	0.6	0.6	-	0.4	-
GARP WITH PRECIPITATION OF WETTEST QUARTER	-	-	0.6	0.6	-	0.4	-

* Key: A – True Positive, B – False Positive, C – False Negative, D – True Negative, N – Number of Samples.

CONCLUSION

Landslides occur when masses of rock, earth or debris move down a slope. Mudslides, debris flows or mudflows, are common type of fast-moving landslides that tend to flow in channels. These are caused by disturbances in the natural stability of a slope, which are triggered by high intensity rains. Mudslides usually begin on steep slopes and develop when water rapidly collects in the ground and results in a surge of water-soaked rock, earth and debris. Causes may be of two kinds: 1. Preparatory causes & 2: Triggering causes. Preparatory causes are factors which have made the slope potentially unstable. The triggering cause is the single event that finally initiated the landslide. Thus, causes combine to make a slope vulnerable to failure, and the trigger finally initiates the movement. Thus a landslide is a complex dynamic system. An individual 'landslide' characteristically involves many different processes operating together, often with differing intensity during successive years.

The primary criteria that influence landslides are precipitation intensity, slope, soil type, elevation, vegetation, and land cover type. The present study demonstrated the effectiveness of two pattern recognition techniques: Genetic Algorithm for Rule-set Prediction and Support Vector Machine. The landslide hazard prediction study conducted in Uttara Kannada and Kerala have shown that small datasets can yield landslide susceptibility maps of significant predictive power. The efficiency of the model has been demonstrated by the successful validation. However, when the predicted features may have different immediate causes, one should carefully avoid including triggering factors among the predictor variables since they restrict the scope of the prediction map and convey often a poorly constrained time dimension. Beyond the sample size, the reliability of the susceptibility map fundamentally depends on a good knowledge of which environmental variables act to determine landslides, and on the availability and the quality of the data. To be reliable or simply useful, the prediction map must also be appropriately validated. The
analysis showed that SVM applied on precipitation data of the wettest month with 96% accuracy was close to reality for Uttara Kannada district and GARP applied on precipitation data of the wettest quarter was more successful in identifying the landslide prone areas in Kerala.

VI. ACKNOWLEDGMENT

The environmental layers were obtained from WorldClim - Global Climate Data. NRSA, Hyderabad provided the LISS IV data used for land cover analysis. We thank USGS Earth Resources Observation and Science (EROS) Center for providing the environmental layers and Global Land Cover Facility (GLCF) for facilitating the Land Cover Change product.

REFERENCES

[21] S. Monia, G. Salvatore, N. Fernando, P. Andrea and R. C. Maria , "Pre-processing algorithms and landslide modelling on remotely sensed DEMs," Geomorphology, vol. 113, pp. 110–125, 2009.

[22] J. N. Hutchinson, "Morphological and geotechnical parameters of landslides in relation to geology and hydrology," *Proc. 5th Int. Symp. on Landslides,* Lausanne, pp. 3–36, 1988.

[23] R. H. Campbell, "Soil slips, debris flow, and rainstorms in the Santa Monica Mountain and vicinity Southern California," *US Geological Survey Professional Paper 851*, 1975.

[24] S. D. Ellen, G. K Wieczorek, "Landslides, floods and marine effects of the storm of January 3-5, 1982, in the San Francisco Bay Region, California," *United States Geological Survey Profession Paper*, pp. 1434, 1988.

[25] N. Caine, "The rainfall intensity–duration control of shallow landslides and debris flows," *Geografiska Annaler,* vol. 62, pp. 23–27, 1980.

[26] S. H. Cannon, and S. Ellen, "Rainfall conditions for abundant debris avalanches. San Francisco Bay Region, California," *California Geology*, vol. 38, pp. 267–272, 1985.

[27] G. F. Wieczorek, "Effect of rainfall intensity and duration on the debris flows in central Santa Cruz Mountains, California," *Geological Society of America Reviews in Engineering Geology*, vol. 7, pp. 93–104, 1987.

[28] D. K. Keefer, R. C. Wilson, R. K. Mark, E. E. Brabb, W. M. Brown, S. D. Ellen, E. L. Harp, G. F. Wieczorek, C. S. Alger, R. S. Zatkin, "Real time landslide warning during heavy rainfall," *Science*, col. 238, pp 921–925, 1987.

[29] D. R. Montgomery, W. E. Dietrich, "A physically based model for the topographic control on shallow landsliding," *Water Resources Research*, vol. 30 (4), pp. 1153–1171, 1994.

[30] D. R. Montgomery, K. Sullivan, and H. M. Greenberg, "Regional test of a model for shallow landsliding," *Hydrological Processes*, vol. 12, pp. 943–955, 1998.

[31] R. M. Iverson, "Landslide triggering by rain infiltration," *Water Resources Research*, vol. 36(7), 1910.

[32] Y. Hong, R. Adler, G. Huffman, "Evaluation of the potential of NASA multisatellite precipitation analysis in global landslide hazard assessment," *Geophysics Research Letter*, vol. 33, L22402, 2006.

[33] R. Rosso, M. C. Rulli, G. Vannucchi, "A physically based model for the hydrologic control on shallow landsliding," *Water Resources Research,* 42, W06410, 2006.

[34] G. B. Crosta, and P. Frattini, "Rainfall-induced Landslides and debris flows," *Hydrological Processes*, 22, pp. 473-477, 2008.

[35] W. Wu, R. Sidle, "A distributed slope stability model for steep forested basins," *Water Resources Research*, vol. 31(8), pp. 2097–2110, 1995.

[36] M. Casadei, W. E. Dietrich and N. L. Miller, "Testing a model for predicting the time and location of shallow

landslide initiation in soil-mantled landscapes," *Earth Surface Processed and Landforms*, 28, pp. 925–950, 2003.

[37] T. L. Kwan, and H. Jui-Yi, "Prediction of landslide occurrence based on slope-instability analysis and hydrological model simulation," *Journal of Hydrology*, vol. 375, pp. 489–497, 2009.

[38] M. Borga, G. Dalla Fontana, D. Da Ros, and L. Marchi, "Shallow landslide hazard assessment using a physically based model and digital elevation data," *Environmental Geology*, vol. 35, pp. 81–88, 1998.

[39] A. Burton, and J. C. Bathurst, "Physically based modelling of shallow landslide sediment yield at a catchment scale," *Environmental Geology*, vol. 35, pp. 89–99, 1998.

[40] R. Romeo, "Seismically induced landslide displacements: a predictive model," *Engineering Geology*, vol. 58, pp. 337–351, 2000.

[41] K. J. Shou, and C. F. Wang, "Analysis of the Chiufengershan landslide triggered by the 1999 Chi-Chi earthquake in Taiwan," *Engineering Geology*, vol. 68, pp. 237–250, 2003.

[42] W. R. Lambe, R. V. Whitman, Soil Mechanics, 2nd ed. Wiley, New York, 1979.

[43] R. D. Barling, I. D. Moore, and R. B. Grayson, "A quasi-dynamic wetness index for characterizing the spatial distribution of zones of surface saturation and soil water content," *Water Resources Research*, vol. 30, pp. 1029–1044, 1994.

[44] W. E. Dietrich, R. Reiss, M. Hsu, D. R. Montgomery, "A process-based model for colluvial soil depth and shallow landsliding using digital elevation data," *Hydrological Processes*, vol. 9, pp. 383–400,1995.

[45] M. Casadei, W. E. Dietrich, N. L. Miller, "Testing a model for predicting the timing and location of shallow landslide initiation in soil-mantled landscapes," *Earth Surface Processes and Landforms*, vol. 28, pp. 925–950, 2003.

[46] D. R. Montgomery, W. E. Dietrich, "A physically based model for the topographic control on shallow landsliding," *Water Resources Research*, vol. 30, pp. 1153–1171, 1998.

[47] J. DeGraff, H. Romesburg, "Regional landslide-susceptibility assessment for wildland management: a matrix approach" In: Coates, D., Vitek, J. (Eds.), George Allen and Unwin, "Thresholds in Geomorphology," London, pp. 401–414, 1980.

[48] A. Carrara, "Multivariate models for landslide hazard evaluation," *Mathematical Geology*, vol. 15(3), pp. 403–426,1983.

[49] A. K. Pachauri, and M. Pant, "Landslide hazard mapping based on geological attributes," *Engineering Geology*, vol. 32(1–2), pp. 81– 100, 1992.

[50] P. M. Atkinson, and R. Massari, "Generalised linear modelling of susceptibility to landsliding in the central Appennines, Italy," *Computer and Geosciences*, 24(4), pp. 371–383, 1998.

[51] K. Turner, and G. Jayaprakash, Introduction. In: Turner, A. K., Schuster, R.L. (Eds.), Landslides: Investigation and Mitigation,

[52] Special Report, vol. 247. National Academic Press, Washington, DC, pp. 3– 12, 1992.

[53] T. Ward, L. Ruh-Ming, and D. Simons, "Mapping landslide hazard in forest watershed," *Journal of Geotechnical Engineering Division*, 108(GT2), pp. 319–324, 1988.

[54] A. K. Pujari, Data Mining Techniques, University Press, Hyderabad, 2006.

[55] D. R B. Stockwell, and D. P. Peters, "The GARB modeling system; Problems and solutions to automated spatial prediction," *International Journal of Geographic Information Systems*, vol. 13, pp. 143-158, 1999.

[56] T. Kavzoglu , I. Colkesen, "A kernel functions analysis for support vector machines for land cover classification", *International Journal of Applied Earth Observation and Geoinformation*, vol 11, pp. 352-359, 2009

[57] A. Mathur, and G. M. Foody, "Multiclass and binary SVM classification: Implications for training and classification users," *IEEE Geoscience and Remote Sensing Letters*, vol. 5, pp. 241–245, 2008a.

[58] A. Mathur, and G. M. Foody, "A relative evaluation of multiclass image classification by support vector machines," *IEEE Transactions on Geoscience and Remote Sensing*, vol. 42, pp. 1335–1343, 2004.

[59] C. Cortes, and V. Vapnik, "Support-vector network," Machine Learning 20, pp 273–297, 1995.

[60] M. Pal, P. M. Mather, "Support vector machines for classification in remote Sensing," *International Journal of Remote Sensing*, vol. 26, pp. 1007–1011, 2003.

[61] T. Oommen, D. Misra, N. K. C. Twarakavi, A. Prakash, B. Sahoo, and S. Bandopadhyay, "An objective analysis of support vector machine based classification for remote sensing," *Mathematical Geosciences*, vol. 40, pp. 409–424, 2008.

[62] F. Melgani, and L. Bruzzone, "Classification of hyperspectral remote sensing images with support vector machines," *IEEE Transactions on Geoscience and Remote Sensing*, vol. 42, pp. 1778–1790, 2004.

[63] A. Mathur, and G. M. Foody, "Crop classification by support vector machine with intelligently selected training data for an operational application," *International Journal of Remote Sensing*, vol. 29, pp. 2227–2240, 2008b.

[64] B. Dixon, and N. Candade, "Multispectral land use classification using neural networks and support vectormachines: one or the other, or both?," *International Journal of Remote Sensing*, vol. 29, pp. 1185–1206, 2008.

[65] M. E. S Munoz, R. Giovanni, M. F Siqueira, T. Sutton, P. Brewer, R. S. Pereira, D. A. L. Canhos, and V. P Canhos, "openModeller- a generic approach to species' potential distribution modeling," *Geoinformatica*. DOI: 10.1007/s10707-009-0090-7.

[66] T. V. Ramachandra and A. V. Nagarathna, "Energetics in paddy cultivation in Uttara Kannada district," *Energy Conservation and Management*, vol. 42(2), pp. 131-155, 2001.

[67] A. H. Fielding, and J. F. Bell, "A review of methods for the assessment of prediction errors in conservation presence/absence models," *Environmental Conservation*, vol. 24, pp. 38-49, 1997.

[68] T V Ramachandra, M D Subashchandran and Anant Hegde Ashisar,. Landslides at Karwar, October 2009: Causes and Remedial Measures, ENVIS Technical Report: 32, Environmental Information System, Centre for Ecological Sciences, Bangalore, 2009.

LANDSLIDES IN COASTAL UTTARA KANNADA: MANAGEMENT TOWARDS RISK REDUCTION

Abstract: The hilly coast of Uttara Kannada, interrupted with backwaters and river mouths, had no notable history of landslides until multiple slides struck Karwar during the rain-soaked early days of October 2009 causing live burial of 19 persons. That the proneness of the region to landslides has increased due to rising human impacts can be assumed considering the collapse of a hillside along Kumta coast during the peak rainy days of 2010 and in yet another incident near Karwar, boulders rolling down a steep hill hit a running train causing one death and injuries to others.

A combination of factors may be blamed for the landslides that happened and likely to repeat, especially during days of excessive rains which are on the rise. Low lateritic coastal hills are formed of eroded and re-deposited materials from the Western Ghats through geological ages. Vegetation flourished on these hills until pressures from rising population and developmental activities erased bulk of it. The exposed soils of denuded hills got laterised through surface erosion, fine clay materials seeping down into the lower horizons leaving honey-combed iron rich, indurated surface laterite, a poor terrain for plant growth. The indurated surface laterite is an effective shield against landslides, except when deep vertical cuts are made exposing the soft clayey soil horizon beneath.

The vulnerability of deposited lateritic hills to landslides increases if such deposits have taken place along the river courses or estuarine regions, causing capillary rise of water from beneath and descend of rain water through fissures and holes formed by rotten tree stumps. Rainy spells can soak up the soft soils in the interior triggering mudslides due to rupture of the hills, as is the case with the killer landslide at Kadwad in Karwar. Quarrying, pediment cutting, soil removal and stripping of vegetation increase risks.

The granitic hills of Karwar coast are also posing potential landslide problems. The rocks here are of fractured type with ample pockets and cracks with trapped soils. Good forest cover could minimize risks. Deforestation in these is at its peak, caused erosion of top soil and water seepage into the interior of hills. Whereas the soils soak up and expand the granite rocks do not, unlike the laterite. Heavy rainfall acts as triggering cause for landslide hazards in such hills. Pediment cutting and quarrying add to the risk factor.

Probable landslide prone areas in Uttara Kannada district and also in Kerala were predicted using algorithms – GARP (Genetic Algorithm for Rule-set Prediction) and Support Vector Machine (SVM) in a free and open source software package - openModeller. Several environmental layers such as aspect, digital elevation data,

flow accumulation, flow direction, slope, land cover, compound topographic index, and precipitation data were used in modelling. A comparison of the simulated outputs, validated by overlaying the actual landslide occurrence points showed 92% accuracy with GARP and 96% accuracy with SVM in predicting landslide prone areas considering precipitation in the wettest month whereas 91% and 94% accuracy were obtained from GARP and SVM considering precipitation in the wettest quarter of the year.

To prevent landslide hazards, there should be accepted norms for each region, based on composition of soil and rocks, rainfall, quality and biomass of vegetation etc. Reduction of risk factor lies in providing appropriate vegetation cover, and any interference with the hills should be strictly adhering to norms of geology and ecology of the region.

Introduction:

Landslides, around the world, take a heavy toll on life and property every year. Indeed, they are one of the most significant contributors to loss of life and aggregate national losses caused by natural disasters associated with earthquakes, severe storms and heavy rainfall in mountainous terrain **(**Lundgren, 1986; Swiss Reinsurance Co., 2000). Sediment disasters by debris flows, mud flows, and landslides occur almost every year during the rainy and typhoon period of July to October in Japan. In July 1982, a heavy rainfall of 488 mm in a day caused 4300 debris flows in Kyushu Island killing 299 people. Many debris flows caused by intensive rainfall during July 1983, in Honshu Island killed 199 people. Both created also enormous loss of property (Abe and Ziemer, 1990). Considered some of the worst ever natural disasters in Brazil, 806 people were killed and hundreds were yet to be traced killed as cloud-burst triggered avalanches of mud and water ripped through already water-soaked mountainsides in January, 2011 (*Geology & Earth Sciences,* 2011; *Scientific American.com*, 2011). The month also saw such disasters worldwide as floods and landslides caused devastation in Australia, China and Sri Lanka.

Types of landslides: Landslides are classified by causal factors and conditions, and include falls, slides and flows. There are many attributes and criteria for identification and classification including rate of movement, type of material and nature of movement (Ramachandra et al., 2009).

a. ***Falls:*** Falls move through the air and land at the base of a slope. Material is detached from a steep slope or cliff and descends through the air by free fall or by bouncing or rolling down slope. Rock fall, the most common type, is a fall of detached rock from an area of in tact bedrock.
b. ***Slide:*** Slides move in contact with the underlying surface. They include rockslides - the down slope movement of a rock mass along a plane surface; and slumps - the sliding of material along a curved (rotational slide) or flat

(translational slide) surface. Slow moving landslides can occur on relatively gentle slopes, and can cause significant property damage, but are less likely to result in serious injuries.

c. ***Flows:*** Flows are plastic or liquid movements in which mass (e.g. soil and rock) breaks up and flows during movement. Debris flows normally occur when a landslide moves down slope as a semi-fluid mass scouring, or partially scouring soils from the slope along its path. Flows are typically rapidly moving and also tend to increase in volume as they scour out the channel.

Causes of Landslides: A landslide is a complex dynamic system. An individual landslide characteristically involves many complex processes operating together. These are classified into intrinsic and extrinsic variables.

a. ***Intrinsic variables:*** Geology, slope gradient, slope aspect, elevation, soil geotechnical properties, vegetation cover, and long term drainage patterns are intrinsic variables that contribute to landslide susceptibility. The steeping of the slope, water content of the stratum and mineralogical composition and structural features, which tend to reduce the shearing strength of the rocks, are also vital factors.
b. ***Extrinsic variables:*** A slight variation or jerk to the mass, or a tremor would greatly add up against frictional resistance and the mass would become unstable. The heavy traffic in a hilly terrain could be a contributing factor towards causing the imbalance of the masses. The extrinsic variables may change over a very short time span, and are thus very difficult to estimate.

The main causal factors for slope failures can be divided into preparatory and triggering causal factors.

a. ***Preparatory factors:*** These are factors which make slopes susceptible to movement over time without actually initiating it – e.g. deforestation caused reduction in material strength; loose soil, rock and fragmented materials, bedding lineaments, faults, erosion of the slope toe due to streams or human activities, dam construction, loading of the slope at its crest such as construction on the top slope, soil of clayey or clayey loam which absorb considerable quantity of water etc.
b. ***Triggering factors:*** These are external stimuli responsible for the actual initiation of mass movements – e.g. earthquake, intense rainfall for a short duration on a weak plane or prolonged high precipitation, inconsiderate irrigation etc. (Knapen et al., 2006; Ramachandra et al., 2009).

KARWAR LANDSLIDES

On 2nd October, 2009, on an exceptionally high rainy day (423.6 mm recorded on 3rd morning) 21 landslides of varied intensities struck the coastal hills of Karwar towards

the centre of Indian west coast. Karwar is a taluk in the Uttara Kannada district (formerly North Kanara) of coastal Karnataka and also the district headquarters (Figures 1 & 2 for topography and important landslide locations). Flanked by the Arabian Sea to the west, most of Uttara Kannada's low altitude (seldom exceeding 600 m) hilly terrain receives heavy monsoon downpour from 3000-5000 mm, confined to six or seven months. Waters rush down the rugged terrain and streams and rivers swell during the peak rainy period of June to September. Exceptionally October might get cloudbursts as well, otherwise receiving lesser rains seldom ever associated with floods. The district's north-eastern region, in the taluks of Mundgod and Haliyal, which merge with the drier Deccan receive rains less than 1600 mm, and are characterized by less rugged undulating terrain. Whereas tropical evergreen-semi-evergreen forests characterize the heavy rainfall region, moist to dry deciduous forests are natural to the lower rainfall areas. The coast itself, unlike rest of the South Indian west coast, is hilly in many places and interrupted by the mouths of five rivers and several small creeks. Steep rising hills, promontories of the Western Ghats, are notable of the physiography of the coastal Karwar town and its neighbourhood, that witnessed unprecedented floods and landslides in early October, 2009. The sprawling Kali River estuary with its several ramifications is notable feature of landscape between Karwar town and Goa territory border about 10 km to the north.

Horticultural gardens with arecanut, coconut, banana, pepper, cardamom, cocoa, vanilla etc. characterize partially shaded narrow valleys having perennial water supply. Rice, sugarcane, groundnut, vegetables etc. are grown in wider valleys and plains of the north-east and the coast. Fields of rice, jowar, sugarcane, chillies etc and mango orchards characterize the otherwise wooded landscape of Mundgod and Haliyal. Unlike anywhere else along the South Indian coast the Western Ghats come too close to the coast in Karwar, some of its promontories entering into the sea itself. The steep escarpments of the Western Ghats form almost a semi-circle to the south, west, and far north of Karwar, closer to the Goa border. The National Highway-17 winds its way through the foothills and coastal alluvium, before entering the Karwar town, from where it passes northwards parallel to the beach. The Karwar port is situated towards the immediate south-west of the main town in the Karwar Bay. The fisheries port at Baitkol is close to the main port on the east of a 210 m high promontory of the Western Ghats. The INS Kadamba Naval Base occupies the narrow stretch of coastal strip from north of Ankola taluk to the south of the Karwar port. Many hills of heights from 300 to 500 m are present within few kilometers of Karwar town.

Locations of landslides: The 21 landslides of different magnitudes happened in the hills, most of them along the NH-17 and other roads (Figures-1& 2 for important landslide locations). The densely populated town itself was lucky to have escaped from the damages of landslides but not from the flood fury. Some of the low hills that suffered landslides are in the villages bordering the south of the estuary in the villages of Kadwad, Makkeri and Mandralli. Habitations have sprung up along the toes of these low hills in these villages. But human casualties (19 deaths) happened only in

Jariwada site (Kadwad-2). The locations of the landslides are given in the Table-1. The NH-17 was blocked in several places due to the landslides in Arga and Binaga. Some of these slides destroyed the compound wall of the Naval base to the west of the highway. The Baithkol fisheries port and main port areas together suffered 5 landslides; as all these happened just outside the densely populated hillsides the people had providential escape. Shirwad hill of 81 m, bordering the marshes had a landslide and roughly 100,000 cum material came out of it.

Jariwada (Kadwad-2) had the worst landslide in the history of Uttara Kannada district which buried alive 19 people, and destroyed several houses and property. The slide happened on a mound of 65 m, to the south of Kali estuary. The slide material volume of approximately 750,000 cu.m, traveled a distance of 300 m, burying people and destroying houses and entering the estuary, its further advance stopped by the Konkan Raliway embankment (Figures 3-5). Kadwad -1 slide happened in another mound of 78 m. About 400,000 cu.m of debris and soil travelled a distance of 300m from the slide, crossing a road there wwas no human casualty from this slide (Mishra, 2009). Interaction of a variety of factors caused the landslides. Of these important are geological factors, excessive rainfall and anthropogenic pressures.

Table-1: Landslide locations in Karwar taluk

Slide location	**Lat –Long**	**No. of slides**	**Approx. volume of slide material**
Kadwad-1 (near Forest naka)	14°49’59.2”N -74°10’39.8”E	01	400,000 cu.m
Kadwad-2	14°52’40.2”N -74°10’47.6”E	01	750,000 cu.m
Arga (near NH-17)	14°46’51.2”N - 14º46’58.9”N 74°08’29.2”E - 74°08’47.3”E	04	70,000 cu.m
Baithkol (near port)	14°48’07.4”N - 14°48’16.5”N 74°06’47.9”E - 74°06’50.8”E	05	14°48’38.7”N - 74°10’47.6”E 88,000 cum
Shirwad	14°48’38.7”N - 74°10’47.6”E	01	100,000 cu.m
Mandralli	14°50’50.2”N - 74°09’22.7”E	01	45,000 cu.m
Makeri	14°49’15.3”N - 14°50’50.2”N 74°10’17.5”E - 74°10’17.6”E	03	13,300 cu.m
Baad	14°48’14.5”N -	02	8,000 cu.m

	14°48’25.1”N 74°08’13.2”E - 74°08’22.4”E		
Binaga	14°46’53.9”N - 14°47’27.9”N 74°06’53.5”E - 74°08’10.0”E	03	37,000 cu.m

GEOLOGICAL FACTORS

Landslides on lateritic hills: Coastal hills of Uttara Kannada broadly come under two categories. Hills which rise precipitously, most of them exceeding 200 m high, have granite as the main rock type. These hills characterize northern coastal stretches from Ankola to Karwar. Low lateritic, flat-topped hills and plateaus, not exceeding 100 m are feature of the southern coast of Kumta, Honavar and Bhatkal taluks. The main rock type of landslide hills in Karwar is granitic. However, some of the low hills bordering the Kali estuary are nothing but mounds of soil with laterised tops. The Kadwad hills (Kadwad-1 and 2) fall in this category. Such hills are not true hills of the Western Ghats but constituted of sedimentary soils deposited by archaic water courses that rushed down from the hills of Ghats. Forests of evergreen nature flourished once on these soil mounds, as their vestiges in a sacred grove at Kadwad-2 site indicate. Similar was the case with most other laterite topped low hills and plateaus of coastal Uttara Kannada. Shifting cultivation through ages and savannization for cattle grazing created much denudation of the coastal hills (Chandran, 1997).

An understanding of laterite formation is required to explain some of the Karwar landslides, especially of Kadwad hills. Laterites are formed by the decomposition of rock, removal of the bases and silica and formation of oxides of iron and aluminium at the top of the soil profile. They are soft when wet but harden with age. Laterites are of two types. Primary laterite is found *in situ*. The original rock structures, joints and quartz material are in tact and the laterite deposit overlies the bedrock. Primary laterite is found at higher altitudes. The Indian south-west coast laterites are considered to be of secondary nature, being formed from sedimentary deposits such as gravels and pebbles by sesquioxide impregnation and cementation. They are pellet type and quite different from the underlying soil or bedrock. These laterites have a continuous softening effect with depth. The laterites are normally subjected to alternate wet and dry climates (Ranjan and Rao, 1991). Leaching down of soluble materials during rains and cementation of accumulated detritus, especially iron and aluminium, on exposure makes secondary laterites dry and hard. Denuded hills and plateaus covered with hardened and eroded surface laterite, with characteristic honey-combed structure, are characteristic of southern coast of Uttara Kannada. These hills are very stable, being covered with natural shields of iron rich laterite. The two hills at Kadwad, (Kadwad-1 of 78 m & Jariwada-Kadwad-2 of 65 m) exhibit only partial laterite formation towards the exposed top. Exposed indurated boulders with typical honey comb structure, characteristic of the southern hills of Uttara Kannada coast are

scanty in the Kadwad hills. Laterisation process is incomplete iniside the hill also (Figure-6) mainly due to insufficient soil drainage due to the closeness of the estuary and the hills themselves being formed on palaeo river courses as springs exist in these hills to this day. 'Jariwada' in local language means hamlet situated on 'jari' or spring. Water table is high in the Kadwad village and it is expected also for the water to rise through the soil by capillary force from below. Soil samples from the bottom of Kadwad-2 showed 88.3% sand revealing its weak foundation. Such dampness in the interior of these clayey soils with high mix of sand especially towards the base would have been considerably aggravated by the heavy rains of late September and the first two days October. Water would have percolated through the thin mantle of laterite as well as through crown cracks developed on the hills, understandably due to swelling of the clayey soil in the interior.

The natural proneness of the weak structured Kadwad hills to landslides would have been aggravated by deforestation due to past shifting cultivation, hacking for biomass by the locals, ever-increasing toe cutting by locals for expansion of holdings, soil removal by some local contractors etc. The situation got worsened when the remaining natural vegetation was cleared some years ago by the Cashew Corporation for raising plantations, unaware of the fact that cashew would be a poor choice for covering fragile, landslide prone hills of soft clayey, water-logged soils. The stumps of the earlier trees, expectedly, underwent deterioration making hollows on hill surface facilitating increased rain water seepage into the interior of the hills and soil expansion probably causing the formation of crown cracks. The heavy rains ultimately triggered the disastrous slope failures during early October 2, 2009. Indeed, any coastal hills, with their bases moored in estuarine shores, if they are inadequately covered with natural vegetation and/or their sides cut for expansion of holdings or for soil, landslides are likely to happen. Such a slide occurred in the Holegadde village of Kumta taluk during the rainy season of 2010, but fortunately without any casualties.

Landslides on granitic hills: Granite is the main rock type in the slides that happened in 12 locations. Eight of these slides were along the hills adjoining the NH-17, viz. Arga (4 slides), Binaga (3 slides) and one opposite the Karwar commercial port. The entire western portion of these villages fall under the high security INS Kadamba Naval Base, the NH side wall of which was badly breached by landslides and storm waters, for which the wall acted like a dam that could not stand the force of the storm water. The debris in all these slides included granite boulders, cobbles and overburden of soil and weathered granite (figure-8). Five slides happened in the hills towards the south and south-west of Karwar Port at Baithkol. In a slide that took place along the vertical slope of the hill (DC's residence hill) huge granite boulders came crashing down on the NH-17 and even crossed over it towards the Arabian Sea. Approximately 10,000 cu.m of debris moved down the slope and blocked the road. In the rest of the Baithkol slides, close to the fisheries port, the material consisted of boulders, cobbles of weathered granite and mafic dyke, laterite and lateritic soil (Mishra, 2009).

Shearing forces: On steep granitic slopes, inadequately covered with vegetation, heavy rains would have soaked up the overburden of soil and fractured rocks activating shearing forces. Cutting deep swathes in the hills for expansion of holdings, highways and other roads as well as for soil removal would have also activated shear forces. In the words of Dikshit (2009): "The underlying rock is almost everywhere granite which is non-porous to water. Though the hills look monolithic …. There were many deep cracks in the granite rocks that were draining rainwater that fell on the hill surfaces. Over this granite hill is the soil …. Of varying thickness bound and staying in place primarily due to cohesive and adhesive biding forces. It is plastic but rock like hard in dry summers, but becomes a viscid mass capable of moving under sufficient shearing force in the form of a semi-solid mass having great momentum along slopes. At many landslide affected places the original forests were degraded and replaced by shrubs. Owing to high rainfall, low porosity of the granites, and moderate jointing percolated water flow laterally as subsurface flow. Since laterite is missing at many places, there is no continuity between rocks and soil, and hence water lubricates the contact between rocks and soil/weathered debris thereby increasing shearing forces (Hegde, 2009).

TRIGGERING FACTORS

Rainfall: Slope instability due to rainfall is a common geotechnical problem in tropical and subtropical areas. Infiltration of rain water into a slope decreases slope stability. When water starts to infiltrate the unsaturated soil the negative pore-water pressure builds up turning into the mechanism that causes slope failures (Gasmo et al; 2000; Tsaparas et al., 2001). Slope failures in the tropical regions like Malaysia are commonly triggered by frequent rainfall (Lee et al., 2009). Deforestation on steep slopes by logging or fires have increased debris-flow frequency (DeGraff, 1991; Guthrie, 2002). Analysis by Dahal and Hasegawa (2008) of 193 landslides in the Himalayan locations showed that when the daily precipitation exceeded 144 mm, the risk of landslides was high. All the 21 landslides in Karwar occurred on 2nd October, 2009, the most fatal of them at Jariwada in Kadwad, between 4-4.30 pm. By the morning of October 2, Karwar had already received 3,370 mm of rainfall for the season. That fateful day, when all the slides are stated to have happened, Karwar experienced a very heavy spell of rains exceeding 400 mm (423.06 mm recorded in the morning of October, 3rd).

Recurrence of heavy rainfall: As the hill slopes of coastal Karwar remain heavily deforested slope failures could happen on any day of incessant rains, the threshold for this important triggering factor will depend on the previous rainfall during the season, the state of tree cover in the hills and the degree of slope. A look at the daily rainfall history of Karwar for the 1994-2009 period (Figure-7) shows that heavy rainfall (> 200 mm a day) events happen periodically. If the site-specific threshold value is crossed the landslides could happen on any day in vulnerable slopes. October 2, 2009 episodes of 21 landslides indicate that on the recurrence of similar events slope failures are likely to return.

Deforestation and landslides: The heavy annual rainfall of over 3,000 mm at Karwar is sufficient to create an evergreen forest of high biomass. Given moderate amount of human pressures happening today as in many of slightly more interior parts of Karwar taluk, in rest of the forests, even on more precipitous slopes, hardly had any landslides taken place in the past. These inner coastal forests normally have denser tree growth and basal area of 30-40 sq.m/ha. Same is the situation in most of Uttara Kannada which has hardly any history of fatal landslides. It is well known fact that good forest cover on hills is some kind of security from landslides and flash floods. Abe and Ziemer (1990) state that forest vegetation, especially tree roots can extend into joints and fractures in the bedrock or into a weathered transitional layer between the soil and bedrock. The stabilization of slopes by vegetation depends on the depth to which the roots grow. The more the roots penetrate a potential shear plane, the greater is the chance that the vegetation will increase slope stability. Rooting strength is important factor in cohesion of substratum. Forest vegetation can potentially attenuate downstream effects of landslides. If the slope vegetation is clear-felled the probability of landslides occurring will increase, particularly after a few years when the roots are decomposed and loose their stabilizing force. According to Bruijnzeel (2004), whereas a well developed tree cover can prevent shallow landslides up to about 1 m depth, deep landslides of >3 m are not appreciably affected by forest cover. In cases of extreme climate events such as hurricanes, trees may actually increase slope instability due to the tree weight and the susceptibility of particularly high trees to uprooting due to extreme storms, damaging the soil matrix. Thousands of landslides occur in the Himalayas every year. On an average, nearly 200 earthquakes of smaller magnitude, most of them undetected by local communities, occur every year in the Uttarakhand region alone. According to V.C. Thakur, former Director of Wadia Institute of Himalayan Geology, the uncontrolled downhill flow of water after heavy rains, particularly along barren slopes, was an important causative factor in these landslides. A study conducted in 1984 on the relationship between the building of the Mussoorie-Tehri road and landslides revealed that landslides caused more devastation in deforested rather than forested areas (Kazmi, 1998).

Too poor and human impacted vegetation: We selected three localities for vegetational study in the coastal hills of Karwar, two of them in the landslide affected hills (Kadwad and Arga) and the third one in Amdalli, on a steep rising coastal granitic hill, of over 300 m abutting on the NH-17, which has somewhat lesser human pressure, and where landslides have not happened, despite having experienced almost similar rainfall conditions as the rest of coastal Karwar. All the hills had, presumably, a history of shifting cultivation during the pre and early colonial period, at least towards the latter half of the 19^{th} century, as per ecological history of the region and as revealed by nature of the present day vegetation and eroded soil surfaces. Some of the elderly residents of Kadwad-2 site also referred to the hill as bearing the name *kumri-jaga* (shifting cultivation locality), and Kunbis (former shifting cultivators) once resided in the village. The passage of over one century after last of shifting cultivation episodes would have facilitated forest succession leading towards

reasonably good semi-evergreen forests in all the hills. However, due to increased pressure from growing population, for meeting their biomass needs the British declared the forests of most coastal hills as 'minor forests' which eventually suffered from over-exploitation of resources. Remains of a sacred grove towards the base of the hill has few large forest trees such as *Mammea suriga, Mimusops elengi, Mangifera indica* and *Sterculia guttata.* The vegetation analysis of the three sample sites is given in the Table 2

Study locality	**Estimated trees/ha**	**Estimated basal area/ha (sq.m)**	**% evergreen trees**	**Mean ht (m)**
Kadwad-2	76	2.356	3	3.8
Arga hill	44	5.92	20	5.9
Amdalli hill	435	26.84	87	10

Table 2: Vegetation composition

Some decades ago the Kadwad hills (the sites of two major landslides) were stripped of natural vegetation; in Kadwad-2, 20 hectares were planted with cashew. Uncared for subsequently the hill has neither good cashew trees nor any other native species. The trees were sparse and stunted with a density of just 76/ha; it could have been at least 350/ha, more of evergreen nature, and the basal area maintained at a minimum of 30 sq.m/ha, considering the fragile geology. The present basal area of 3.8 sq.m/ha, is too low to offer any slope stability. The cashew is a shallow rooted tree to offer any slope stability. The Arga hill was having dense growth of weeds and scrub and trees were sparse and the basal area too low at 5.9 sq.m/ha. Amdalli hill, which did not undergo any landslide, and considered a control, had much higher tree number at 435/ha. The basal area of 26.84 sq.m/ha is still short of the desired 30 sq.m/ha. Moreover the trees were mostly undersized in height and girth as they were subjected to constant hacking. Most of the species were of secondary nature; yet basically multi-strata evergreen vegetation, ideal for soil and slope persisted. Most of the landslide hills had impenetrable tangle of weeds and creepers and thorny bushes, all shallow rooted. The entire coastal hillscape of coastal Karwar is fragile and calls for urgent attention as to the restoration of ideal ecological conditions leading to greater stability in the region.

Alterations in slope angle: According to Mishra (2009) the original slope angle of Jariwada hill of Kadwad was very low at ~20º, prior to human interference. The modification of the slope by cutting 15-20 m vertical slope (as observed in the right and left flanks of the slide zone of 60 m width and 30 m depth) for human settlement and plantation increased instability. In Kadwad-1, which had a 100 m width slide, of 15-20m depth, there was a vertical cut of 10 m height near the toe. The slope was cut for road formation. There was also excavation at the mid-slope to flatten the slope. The toe cutting and removal of material from the site has increased the driving force. As the slope forming material is mostly lateritic soil, clayey soil and overburden, the over-saturation of the slope material decreased the resisting force. Similar toe cutting,

mostly for road making, happened almost in all the studied landslide locations. The original slope angles were gentle with a very low relief.

Land use changes: The clearances of natural vegetation for planting cashew apparently became an important cause for landslide in the Kadwad hills, so too expansion of household gardens into the hill by slope cutting. Slope cutting for road formation was common cause wherever landslides happened. There has been heavy colonization of humans in the Baithkol fisheries port area, causing rampant toe cutting of the isolated, steep sided 210 m tall hill protruding into the Arabian Sea from the south of the Karwar Bay.

Improper drainage: Natural drainage of rainwater has been affected in the slide areas due to different reasons. In the Kadwad hills the water table is high due to the nearness of the estuary and the hills being ancient mounds of soil in the way of a palaeo-river course descending from the Western Ghats. Over-saturation of soils during heavy rains is a constant factor here.

Blockage of natural drainage, increasing the overburden saturation during heavy rains has been considered a potent reason for the landslides in Arga and Binaga hills. The high rising compound wall of INS Kadamba Naval Base acted like a dam impeding storm water drainage; the wall itself crumbled in few places due to the rush of storm water and slide material of stones and soil.

Stone quarrying and soil removal: In Zariwada there was reported excavation of soil in front of the slope that failed for the construction of the Konkan Railway embankment, increasing vertical slope height, inducing slope instability due to the volume and weight of material above the toe (Mishra, 2009). Granite quarries in the hills adjoining NH-17 would have also destabilized the hill sides as rocks came tumbling down from near a quarry site towards the highway and damaging the wall of the naval base.

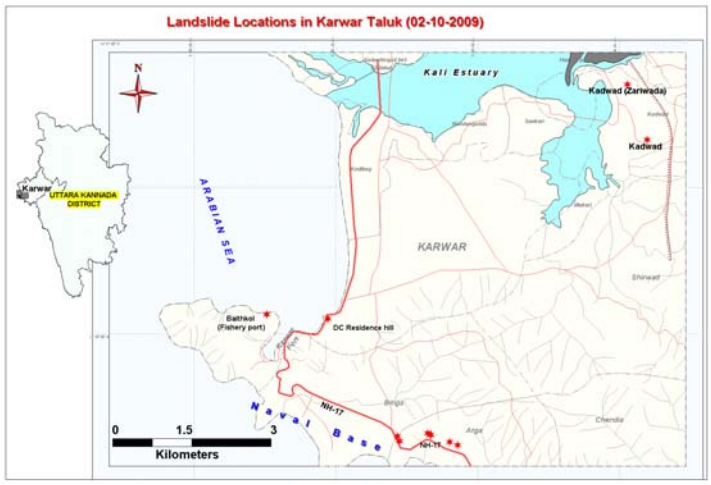

Figure-1: Important landslide locations in Karwar

Figure 2: Google Earth image of Karwar showing landslide areas

Figure 3: Kadwad village on the bank of Kali estuary

Figure-4: Kadawd – 2 (Jariwada landslide)

Figure-5: A house that was drifted and destroyed in the Kadwad-2 landslide

Figure 6: Incompletely formed laterite due to water logging in Kadwad-2 landslde

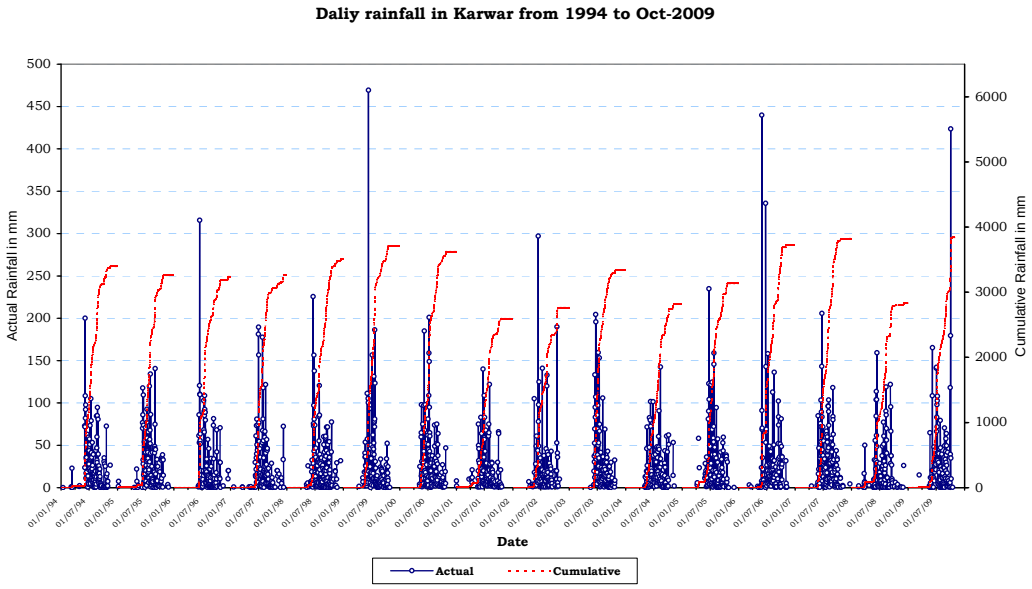

Figure 7: Sixteen years (1994-2009) of daily rainfall records for Karwar showing frequent recurrence of heavy rainfall events (>20 cm a day)

Figure 8: Landslide along NH-17, the slide material entering INS Kadamba Naval Base breaking through the compound wall

LANDSLIDE SUSCEPTIBLE LOCATIONS PREDICTION THROUGH OPENMODELLER

This study use pattern recognition techniques such as Genetic Algorithm for Rule-set Prediction and Support Vector Machine based models to predict the probable distribution of landslide occurrence points based on several environmental layers along with the known points of occurrence of landslides. The model utilises precipitation and six site factors including aspect, DEM, flow accumulation, flow direction, slope, land cover, compound topographic index and historical landslide occurrence points. Both precipitation in the wettest month and precipitation in the wettest quarter of the year were considered separately to analyse the effect of rainfall on hill slope failure for generating scenarios to predict landslides (Ramachandra et al., 2010).

A free and open source software – openModeller was used for predicting the probable landslide areas. openModeller (http://openmodeller.sourceforge.net/) is a flexible, user friendly, cross-platform environment where the entire process of conducting a fundamental niche modeling experiment can be carried out. It includes facilities for reading landslide occurrence and environmental data, selection of environmental layers on which the model should be based, creating a fundamental niche model and projecting the model into an environmental scenario using a number of algorithms as shown in Fig. 9.

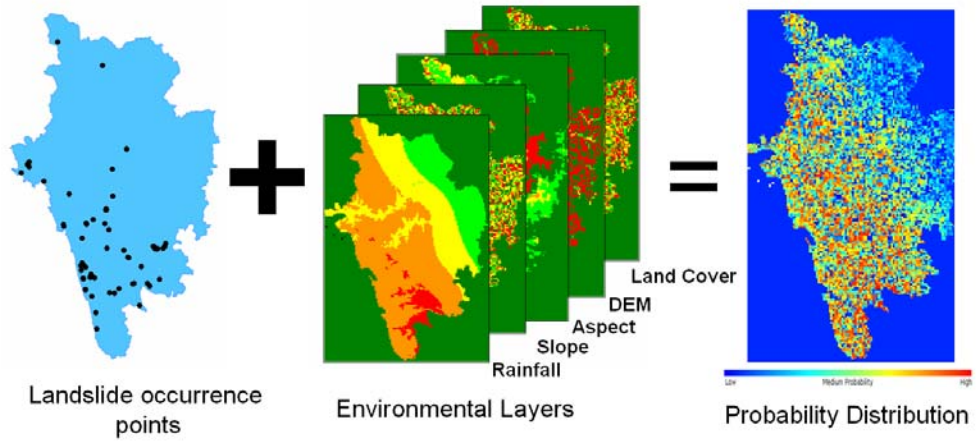

Figure 9. Methodology used for landslide prediction in openModeller.

Two different precipitation layers were used to predict landslides – precipitation of wettest month and precipitation in the wettest quarter of the year along with the seven other layers. Figure 10 (a) and (b) are the landslide probability maps using GARP and SVM on precipitation of wettest month. The landslide occurrence points were overlaid on the probability maps to validate the prediction as shown in Fig. 11. The GARP map had an accuracy of 92% and SVM map was 96% accurate with respect to the ground and Kappa values 0.8733 and 0.9083 respectively. The corresponding ROC curves are shown in Fig. 3 (a) and (b). Total area under curve (AUC) for Fig. 12 (a) is 0.87 and for Fig. 12 (b) is 0.93. Figure 12 (c) and (d) are the landslide probability maps using GARP and SVM on precipitation of wettest quarter with accuracy of 91% and 94% and Kappa values of 0.9014 and 0.9387 respectively.

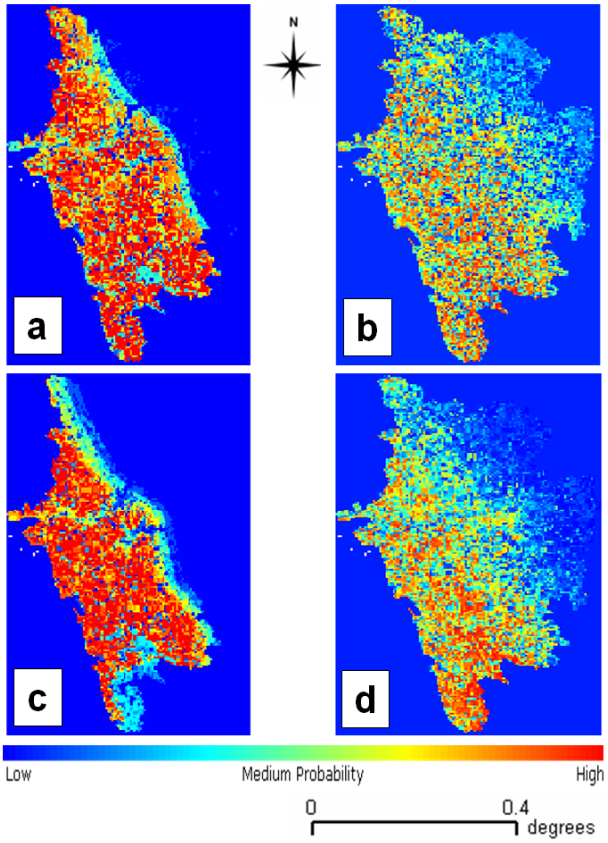

Figure 10. Probability distribution of the landslide prone areas.

ROC curves in figure 12 (c) and (d) show AUC as 0.90 and 0.94. Various measures of accuracy were used to assess the outputs. Table 3 presents the confusion matrix structure indicating true positives, false positives, false negatives and true negatives.

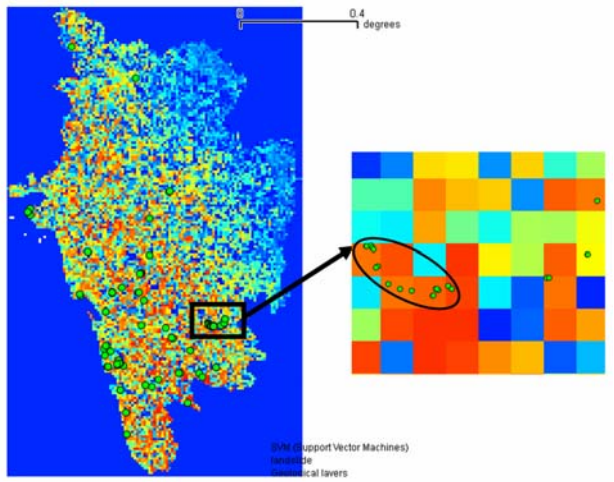

Figure. 11. Validation of the probability distribution of the landslide prone areas by overlaying landslide occurrence points.

Confusion matrices were generated for each of the 4 outputs (Table 4) and different measures of accuracy such as prevalence, global diagnostic power, correct classification rate, sensitivity, specificity, omission and commission error were computed as listed in Table 5. The results indicate that the output obtained from SVM using precipitation of the wettest month was best among the 4 scenarios. It maybe noted that the outputs from GARP for both the wettest precipitation month and

quarter are close to the SVM in term of accuracy. One reason is that, most of the areas have been predicted as probable landslide prone zones (indicated in red in Fig. 2 (a) and (c)) and the terrain is highly undulating with steep slopes that are frequently exposed to landslides induced by rainfall. Obviously, the maximum number of landslide points occurring in the undulating terrain, collected from the ground will fall in those areas indicating that they are more susceptible to landslides compared to north-eastern part of the district which has relatively flat terrain.

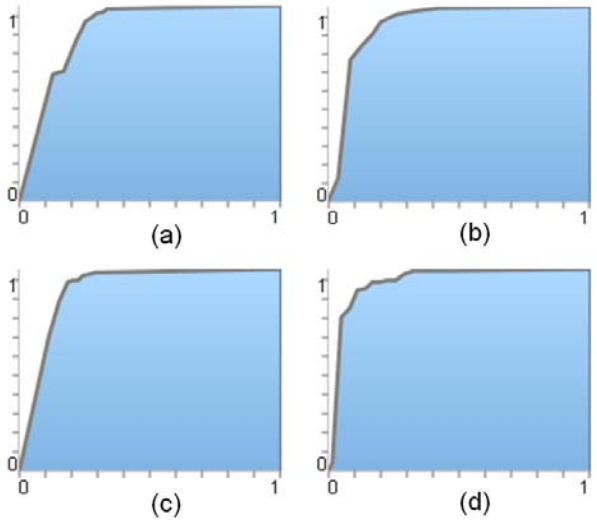

Fig.ure 12. ROC curves for landslide prone maps (a) GARP (b) SVM on precipitation of wettest month; (c) GARP and (d) SVM on precipitation of wettest quarter.

TABLE 3 : CONFUSION MATRIX STRUCTURE

	TRUE PRESENCE	**TRUE ABSENCE**
PREDICTED PRESENCE	A	B
PREDICTED ABSENCE	C	D

Key: A – True Positive, B – False Positive, C – False Negative, D – True Negative.

TABLE 4: CONFUSION MATRIX FOR GARP AND SVM OUTPUTS FOR UTTARA KANNADA

UTTARA KANNADA		**TRUE PRESENCE**	**TRUE ABSENCE**	**NUMBER OF USABLE PRESENCE**	**NUMBER OF USABLE ABSENCE**
GARP WITH PRECIPITATION OF WETTEST MONTH	**PREDICTED PRESENCE**	120	0	125	0
	PREDICTED ABSENCE	5	0		
SVM WITH PRECIPITATION OF WETTEST MONTH	**PREDICTED PRESENCE**	118	0	125	0
	PREDICTED PRESENCE	7	0		
GARP WITH PRECIPITATION OF WETTEST QUARTER	**PREDICTED PRESENCE**	118	0	125	0
	PREDICTED PRESENCE	7	0		
SVM WITH PRECIPITATION OF WETTEST QUARTER	**PREDICTED PRESENCE**	117	0	125	0
	PREDICTED PRESENCE	8	0		

TABLE 5: STATISTICS OF GARP AND SVM OUTPUTS FOR UTTARA KANNADA

UTTARA KANNADA	PREVALENCE (A+C)/N	GLOBAL DIAGNOSTIC POWER (B+D)/N	CORRECT CLASSIFICATION RATE (A+D)/N	SENSITIVITY A/(A+C)	SPECIFICITY D/(B+D)	OMISSION ERROR C/(A+C)	COMMISION ERROR B/(B+D)
GARP WITH PRECIPITATION OF WETTEST MONTH	-	-	0.96	0.96	-	0.04	-
SVM WITH PRECIPITATION OF WETTEST MONTH	-	-	0.94	0.94	-	0.06	-
GARP WITH PRECIPITATION OF WETTEST QUARTER	-	-	0.94	0.94	-	0.06	-
SVM WITH PRECIPITATION OF WETTEST QUARTER	-	-	0.94	0.94	-	0.06	-

* Key: A – True Positive, B – False Positive, C – False Negative, D – True Negative, N – Number of Samples.

PREVENTION AND MANAGEMENT

Several ways of prevention and management, many with general applicability and the others of site specific nature, are employed worldwide. Here only ecologically compatible non-engineering measures have been dealt with.

Identification of landslide prone areas: Based on soil and rock structure, rainfall patterns, slope and vegetation characteristics (evergreen, deciduous, scrub, plantations, fields, gardens etc.) and human impacts, preparation of landslide hazard zonation maps at 1:1000 scale are essential. The methodology has been already evolved by the Department of Science and Technology, Government of India, under the Natural Resources Data Management System.

Drainage correction: In the hilly areas natural drainage patterns should be studied and maintained properly without any blockage. Characteristic stream-side species are to be promoted for stream-bank protection and ecology.

Restoration of vegetation cover: A replanting programme should be undertaken giving priority for strong and deep rooted species which check erosion and withstand water-logging. *Pongamia pinnata, Calophyllum inophyllum, Ficus racemes, Thespesia populnea, Barringtonia* spp., *Terminalia arjuna* etc. may be considered for lower slopes bordering the estuarine areas. Middle and upper slopes in landslide prone areas should be planted with tree having lower biomass but stronger and deeper root networks. High biomass trees are likely to cause the weight of the overburden precipitating slope failures in future. Minimum of 350 trees/ha would be ideal number for the hills. Locality-specific members of the natural vegetation of any given

area may be given priority. The general practice of monoculturing of trees has to be discontinued in all hazard zones

Enhancing the scope of VFCs: The scope of the already existing village forest committees may be expanded to landslide/natural resource management as well. Necessary awareness and training programmes may be arranged for them in landslide prevention and management.

Regulations on slope cutting and quarrying: Indiscriminate slope cuttings have to be strictly regulated and engineering solutions such as protective walls/embankments to be made where they are essential. Bio-protection is by far most important. Quarrying for stones and soils to be strictly limited to specified localities which pose no threat of landslides.

Development to be limited to carrying capacity: Karwar with several major projects such as India's largest naval base, Kaiga Atomic Plant, commercial port and a fisheries port, offices and several more establishments appears to be transgressing its ecological carrying capacity. The authors are presently engaged in a project estimating the ecological carrying capacity of Uttara Kannada district, and are expected to formulate specific measures for safeguarding ecological stability of the region as well as recommend developmental projects that are compatible with the rich biodiversity and ecological fragility of the region.

ACKNOWLEDGMENT: The environmental layers were obtained from worldclim - Global Climate Data. NRSA, Hyderabad provided the LISS IV data used for land cover analysis. We thank USGS Earth Resources Observation and Science (EROS) Center for providing the environmental layers and Global Land Cover Facility (GLCF) for facilitating the Land Cover Change product.

REFERENCS

1) Abe, K. and Ziemer, R.R. 1990. Effect of tree roots on shallow-seated landslides. Paper presented at the Technical Session on Geomorphic Hazards in Managed forests, XIX World Congress, IUFRO, August 5-11, 1990, Montreal, Canada.
2) Bruijnzeel, L.A. 2004. Hydrological functions of tropical forests: Not seeing the soil for the trees? *Agriculture, Ecosystems and Environment* 104: 185-228.
3) Chandran, M.D.S. 1997. On the ecological history of the Western Ghats. *Current Science* 73, 148-155.
4) Dahal, R.K. and Hasegawa, S. 2008. Representative rainfall thresholds for landslides in the Nepal Himalaya. *Geomorphology* 100(3-4) 429-443.

5) DeGraff, J.V. 1991. Increased debris flow activity due to vegetative changes. In: Bell (ed) *6th International Symposium on Landslides* Christchurch **vol. 2**, A.A. Balkema, Rotterdam (1991), pp. 1365–1373.
6) Dikshit, B.K. 2009. Report of Forest Department in the matter of mud slide incidence in Madibagh, Jarivadi village on 01 October 2009. In: Ramachandra, T.V., Chandran, M.D.S. & Ashishar, A.H. (eds.) *Landslides at Karwar, October 2009: Causes and Remedial Measures. ENVIS Technical Report-33,* CES, Indian Institute of Science, Bangalore, pp. 101.
7) Gasmo, J.M., Rahardjo, H. and Leong, E.C. 2000. Infiltration effects into the stability of a residual soil slope. *Computers and Geotechnics*, 26(2), 145-165.
8) *Geology & Earth Science*, 18.1.2011. http://all.go.org
9) Guthrie, R.H. 2002. The effects of logging on frequency and distribution of landslides in three watershed on Vancouver Island, British Columbia, *Geomorphology* **43**, pp. 273–292.
10) Hegde, V.S. 2009. Report on the site investigations of the landslides at Karwar. In: Ramachandra, T.V., Chandran, M.D.S. & Ashishar, A.H. (eds.) *Landslides at Karwar, October 2009: Causes and Remedial Measures. ENVIS Technical Report-33,* CES, Indian Institute of Science, Bangalore, pp. 91-96.
11) Kazmi, S. 1998. Danger: landslide zone. *Indian Express*, August 23.
12) Knapen, A. *et al*., 2006. Landslides in a densely populated county at the footslopes of Mount Elgon (Uganda): Characteristics and causal factors. *Geomorphology* **73(1-2)**, 149-165.
13) Lee, L.M., Gofar, N. and Rahardjo, H. 2009. A simple model for rainfall induced slope instability. *Engineering Geology*, 108, (3-4), 272-285.
14) Lundgren, L. 1986. *Environmental Geology*, Prentice-Hall, New Jersey, p. 576.
15) Mishra, A.K. 2009. A note on the preliminary post disaster investigation of landslides occurred during October 2009 in Karwar taluk, Uttara Kannada district, Karnataka (Lateral priority Item-1, FS 2009-10). In: Ramachandra, T.V., Chandran, M.D.S. & Ashishar, A.H. (eds.) *Landslides at Karwar, October 2009: Causes and Remedial Measures. ENVIS Technical Report-33,* CES, Indian Institute of Science, Bangalore, pp. 73-90.
16) Ranjan, G. and Rao, A.S.R. 1991. *Basic and Applied Soil Mechanics.* New Age International Publishers, Delhi.
17) Ramachandra, T.V., Chandran, M.D.S. & Ashishar, A.H. 2009. *Landslides at Karwar, October 2009: Causes and Remedial Measures. ENVIS Technical Report-33,* CES, Indian Institute of Science, Bangalore.
18) Ramachandra T V, Uttam Kumar, Bharath H Aithal, Diwakar P G, Joshi N V, 2010. Landslide susceptible locations in Western Ghats: Prediction through Open Modeller, In proceedings of the 25th Annual In-House Symposium on Space Science and Technology, 28-29th January 2010, Organised by ISRO-IISc Space Technology Cell, IISc, pp 65-74.

19) *ScientificAmerican.com* 23.1.2011. *http://www.sciam.com*. Report on Brazil mudlslides
20) Swiss Reinsurance Company 2000. Natural catastrophes and man-made disasters in 1999, Economic Research and Consulting. Zurich, Sigma No. 2/2000, 35 p.
21) SRC, 2000. Natural catastrophes and man-made disasters in 1999. Economic Research and Consulting; Swiss Reinsurance Company, Zurich, Sigma No. 2/2000, 35 p.
22) Tsaparas, I., Rahardjo, H., Toll D.G. and Leong, E.C. 2002. Controlling parameters for rainfall-induced landslides. *Computers and Geotechniques*, 29(1), 1-27.